Research Institute of Molecular Pathology
IMP Group leader: Prof. Dr. med. Johannes Zuber

Identifying modulators of TNFα mediated cytotoxicity using genome-wide CRISPR screens

Master Thesis

University of Veterinary Medicine, Vienna

Submitted by
Stefanie Ruhland, B.Sc.

Vienna, January 2020

External supervision

Prof. Dr. med. Johannes Zuber

Markus Schäfer, PhD

Internal supervision

Univ.- Prof. Dr.med. univ. Veronika Sexl

Table of contents

1. Introduction

1.1. Antigen-specific adaptive immunity

The adaptive immunity is activated by the exposure to pathogens leading to immune response by antigen recognition. Antigens are presented by major histocompatibility complexes (MHC). There exist two different main types of MHCs: Class I and class II. MHC class I is present on all cells with a nucleus and presents degraded cytosolic proteins to effector $CD8^+$ T cells, which leads to cell death. MHC class II can present extracellular proteins after endocytosis to $CD4^+$ T cells. Both T cell populations induce an immune response against antigens, stimulate B cells for antibody production and generate memory T cells (K. Murphy and Weaver 2017).

1.1.1. Antigen presentation via MHC-I

MHC class I is the analogue to the most frequent human leukocyte antigen (HLA)-A*0201. They are heterodimers formed by dimerization of the α-chain and the β2-microglobulin. Three domains, α1, α2 and α3, belong to the polymorphic α-chain, also called heavy chain. This α-chain is anchored to the membrane and is responsible for the unique characteristic of MHC molecules. The groove for the peptide binding is between α1 and α2 and bind unique peptides with a length of eight to ten amino acids. The fourth domain is the β2-microglobulin, also called the light chain, which is not polymorph. This shorter chain is only non-covalent attached to the α-chain, especially to α3 (K. Murphy and Weaver 2017).

Before a peptide can be bound, the MHC class I complex is folded and stabilized with the help of chaperones, namely calnexin, calreticulin and ERp57. For this purpose, the transporter associated with antigen processing (TAP) act together with the TAP-associated glycoprotein (tapasin) as an assembly platform and form the peptide-loading complex. TAP, persisting out of TAP1 and 2, is a peptide transporter and transports degraded peptide fragments from the proteasome complex in the cytosol to the MHC in the ER. Through the correct binding of the peptide into the groove, the folding of the MHC finishes to the closed and stable conformation. After dissociation of the chaperons, it is transported to the cell membrane. Now the peptide can be recognized by cytotoxic T lymphocytes (CTLs) (Neefjes et al. 2011).

1.1.2. Generation and activation of CD8$^+$ T cells

For the generation of CD8$^+$ T cells out of naive T cells three key signals are needed. The antigen presentation via MHC, primarily through dendritic cells (DCs), is recognized via the T cell receptor (TCR) of a CD8$^+$ T cell specific for the epitope:MHC-complex. In addition, the CD8 coreceptor binds to the MHC. The cytoplasmic tail of the TCR interacts with the cytoplasmic tail of the CD3, whereas the CD8 cytoplasmic tail interact with LCK, a protein tyrosine kinase. Next, LCK leads to the phosphorylation of the immunoreceptor tyrosine-based activation motifs (ITAMs). The phosphorylated ITAMs recruited and activate Zap-70, another protein tyrosine kinase initiating a phosphorylation cascade. This whole process initiated by antigen recognition is known as "first signal". Co-stimulatory signals are needed as a "second signal" for the activation, survival and expansion of naive T cells. One example for this co-stimulatory signal is the attachment of B7 (CD80, CD86) to CD28. For differentiation into the subsets of effector T cells a third signal through inflammatory cytokine mediators is needed, like interleucine-12 (IL-12), which is important for the cytotoxic activity (Andersen et al. 2006; Malissen and Bongrand 2015).

The activation of CTLs can then eliminate cells in an antigen-specific manner through mediating cytotoxicity. This can be achieved via one of three main pathways. A direct cell-cell contact between the CD8$^+$ T cell and the antigen presenting target cell can induce apoptosis of the target cell either via triggering the death receptor or via granzyme B and perforin release of the CTL. Another indirect killing mechanism can occur through the release of the tumor necrosis factor α (TNFα) and interferon γ (IFNγ) (Andersen et al. 2006).

1.1.3. The human cytomegalovirus

The human cytomegalovirus (HCMV) is categorized as a β-herpesvirus and is the largest of the *herpesviridae* family with around 230,000 bp (Britt and Boppana 2004). The majority of the worldwide population (60-80 %) is infected by this virus and it leads to many different immune responses, including CD4$^+$ and CD8$^+$ T cell responses, induction of natural killer (NK) cells and inflammatory cytokines. Once infected, HCMV results in a lifelong persistence (Khan et al. 2002; Jackson, Mason, and Wills 2011). Normally naive T cells become effector T cells after priming and are maintained in the long-term antigen-independent memory pool as central

memory T cells. The HCMV instead leads to an effector memory T cell pool. This pool still has the effector function. No indication of T cell exhaustion could be detected so far. In healthy adults up to 30 % of total $CD8^+$ T cells can be HCMV responsive and they keep their functionality *ex vivo* alive (Klenerman and Oxenius 2016). The 65kDa phosphoprotein (pp65) and 55kDa immediate-early protein 1 (IE1) induce dominant responses due to their HCMV derived epitopes. The pp65contains the HLA-A*0201 restricted NLVPMVATV (NLV) epitope (Khan et al. 2002).

1.2. Tumor immune evasion

Cancer development is a multistep process and evolves by accumulation of several capabilities. Hanahan and Weinberg (2011) defined these as the hallmarks of cancer, which in summary lead to ongoing proliferation by deregulating key cellular regulatory processes, including e. g. sustaining proliferative signaling and evading growth suppressors. The deregulation is mostly the result of mutations and these mutations also lead to neoantigens (Hanahan and Weinberg 2011). These neoantigens are released by dying cancer cells and can subsequently be taken up by antigen presenting cells (APCs) such as DCs. These cells traffic to the lymph node where they present the received tumor antigen via a human HLA complex to naive T cells (Chen and Mellman 2013). The antigen is recognized via the TCR of a $CD8^+$ T cell specific for the peptide:HLA complex resulting in activation. The activated tumor antigen specific effector T cells can traffic to the tumor beds via the blood vessels and infiltrate these. Following successful infiltration, they can bind specifically to the HLA-presented neoantigens of the tumor cells via their specific TCR. This recognition initiates the killing of cancer cells via distinct killing mechanisms, which are accompanied by the release of new tumor specific antigens. This process is called the cancer immunity cycle (Figure 1) (Chen and Mellman 2013). Besides $CD8^+$ T cells, NK cells are important mediators of anti-cancer immunity. NK cells are activated though a misbalance of inhibitory signals and activation cues. One such inhibitory signal are HLA complexes on target cells. Consequentially, cells with low or absent HLA on the cell surface that are undetectable for T cells, can be eliminated by NK cells. Even though the modes of target cell detection are different between T and NK cells, the killing mechanisms are very similar. These include the release of cytotoxic molecules like granzymes and perforin and the secretion of inflammatory cytokines like TNFα and IFNγ (Cifaldi et al. 2017; Isaacson

and Mandelboim 2018; Freeman et al. 2019). However, the cancer cells are able to adapt to the cancer immunity cycle and develop mechanisms to evade attacks by effector lymphocytes to avoid immune destruction, which is another hallmark of cancer (Hanahan and Weinberg 2011).

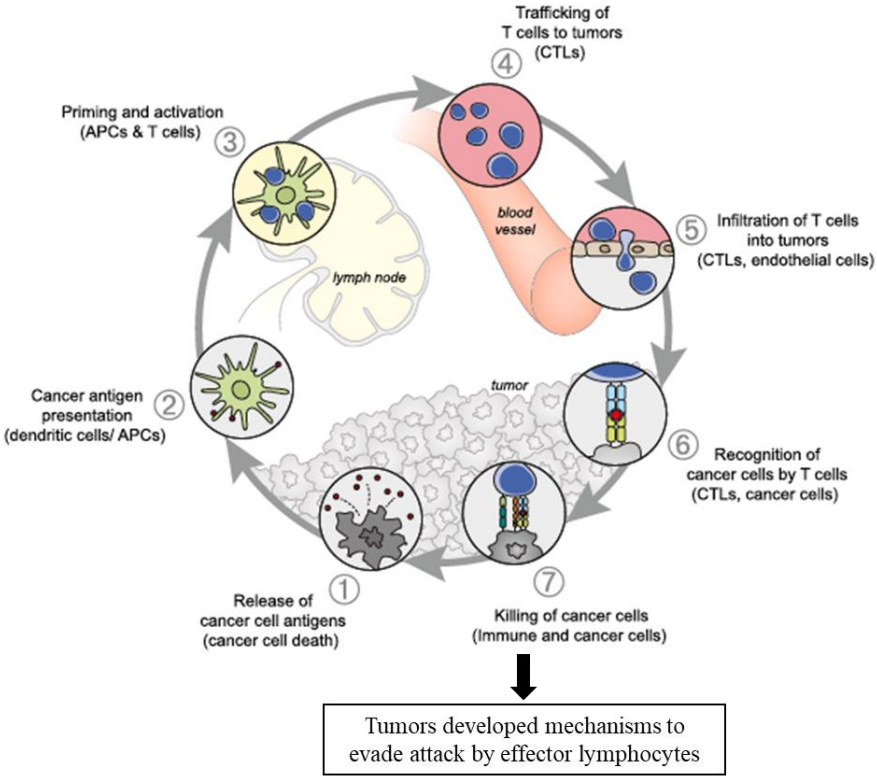

Figure 1: The Cancer-Immunity Cycle (adapted from Chen and Mellman 2013)
The diagram depicts the process of how the immune system can recognize and kill cancer cells. Starting with the uptake of neoantigens and presentation via epitope:HLA complexes to T cells. Primed and activated T cells can travel to the tumors via blood vessels. After infiltration into the tumor, they can specifically recognize cancer cells via antigen presentation and kill the cancerous cells. However, the cancer cell can develop mechanisms to evade killing via effector lymphocytes.

There are many ways of how cancer can avoid getting killed by the immune system (Dunn et al. 2002; Khong and Restifo 2002; Prendergast 2008; Stewart and Abrams 2008). A recent study demonstrated that tumor immune evasion from cytotoxic lymphocytes can arise through the deletion of genes that can be grouped into three main pathways: the suppression of antigen presentation and becoming resistant to the IFNγ as well as the TNFα signaling pathway. They obtained these results by conducting a series of whole-genome clustered regularly interspaced short palindromic repeat (CRISPR)-based *in vivo* and *in vitro* screens. Some cell lines were co-cultured with either T cells or NK cells up to three times during the *in vitro* screen revealing genes important for tumor immune evasion from NK cells as well as T cells. This

demonstrated that TNFα is very important for T and NK cell mediated killing (Kearney et al. 2018).

1.3. The TNFα signaling pathway

TNFα is an inflammatory cytokine mainly produced by activated macrophages, T cells and NK cells. The TNF superfamily consists of 19 cytokines with high structural homology. Each one of them can exist in two different TNF forms. One is the 26 kDa membrane bound ligand (mTNF), which contains a transmembrane domain with a signal peptide, directing the synthesized protein directly to the membrane. MTNF can be cleaved by the metalloprotease TNFα converting enzyme (TACE) into the soluble protein (sTNF) with a molecular weight of 17 kDa. Both, the mTNF and the sTNF can exist as mono-, di- or trimeric ligands via non-covalent interactions with only the homotrimeric structure being active (H. Wajant, Pfizenmaier, and Scheurich 2003; Vanamee and Faustman 2018; Cabal-Hierro and Lazo 2012). The active trimers are formed by a self-assembly process mediated by the TNF homology domain (THD), which is conserved at the C-terminus for all 19 different TNF superfamily members (Harald Wajant and Beilhack 2019). Both TNF forms can bind to TNF receptors (TNFR) to activated downstream signaling pathways. The TNFR superfamily consists of 29 different receptors, which can be grouped into three different subfamilies: (i) the death receptors containing a death domain (DD), (ii) the activating receptors containing no DD and (iii) the pleiotropic receptors, which have a DD but can also trigger the cell proliferation pathway. Examples for (i) are Fas and TRAIL-R, for (ii) TNFR2 and OX40 and for (iii) the pleiotropic receptors TNFR1 and DR3. Whereas TNFR1 is expressed in nearly all cell types, TNFR2 is only expressed in oligodendrocytes, astrocytes, T cells, myocytes, thymocytes, endothelial cells and human mesenchymal stem cells. Both receptors, TNFR1 and TNFR2 can bind the mTNFα, while sTNFα can only activate downstream signaling via TNFR1 (Yi et al. 2018; Cabal-Hierro and Lazo 2012; Vanamee and Faustman 2018). The receptors themselves are transmembrane proteins, which consist of a cysteine-rich extracellular domain to which the ligands bind and an intracellular domain that activates the downstream signaling modules. Like the TNF superfamily, the receptors can also exist in a mono-, di- or trimeric form and need to form homotrimers in order to be able to bind the ligand. This interaction originates through the contact of each receptor chain with the interface between two promotor regions of

the TNF trimer. The membrane bound TNFR (mTNFR) can also be cleaved via TACE, resulting in soluble TNFR (sTNFR). They can regulate TNF activity in two ways: (i) by decreased mTNFR, which leads to reduced downstream signaling or (ii) by acting as an intrinsic TNF inhibitor and quenching of sTNF (Harald Wajant and Beilhack 2019; Ribeiro et al. 2019). TNF signaling can mainly lead to two different outcomes: cell survival mainly via transcriptional induction of anti-apoptotic genes or cell death including apoptosis and necrosis. The outcome depends on the TNF receptor and the recruiting cytokines.

1.3.1. TNFα mediated cell proliferation pathway

The activating receptors lacking a DD have specific peptide motifs in their intercellular tails, which directly recruit TNFR-associated factor 1/2/3 (TRAF1/2/3). In contrast, the pleiotropic receptors like TNFR1 contain a DD domain, they first recruit the TNFR1 associated DD (TRADD). It serves as an interacting platform for TRAF2, for the serine-threonine receptor interacting kinase 1 (RIP1) and for the cellular inhibitors of apoptosis protein 1 and 2 (cIAP1/2). Together, all these proteins create the complex I (Figure 4) (Z. G. Liu 2005; Yi et al. 2018; Karin and Lin 2002). Within this complex, RIP1 is ubiquitylated at Lys63 via TRAF2 and cIAP1/2, resulting in the recruitment of the TAK1 complex members: transforming growth factor beta-activated kinase 1 (TAK1), also known as mitogen-activated protein kinase kinase kinase 7 (MAP3K7), and its three TAK1 binding proteins 1/2/3 (TAB1/2/3). Subsequently, TAK1 can either phosphorylate the IκB kinase (IKK) complex directly or via phosphorylation of Mitogen-Activated Protein Kinase Kinase Kinase 3 (MEKK3) (Festjens et al. 2007). In addition, complex I can recruit the linear ubiquitin assembly complex (LUBAC) consisting of its catalytic subunit HOIL-1 interacting protein (HOIP) and two accessory proteins, the heme-oxidized IRP2 ubiquitin ligase 1 (HOIL-1) and SHANK-interacting protein like 1 (SHARPIN). The binding of the two accessory proteins to HOIP activate the Met1-poly ubiquitination of RIP1 and inhibitor of nuclear factor kappa B kinase regulatory subunit gamma (IKKγ, also called NEMO). NEMO is the regulatory subunit of the IKK complex, formed together with two catalytic subunits IKKα and IKKβ. OTULIN counteracts LUBAC through deubiquitinating of the specific Met1-poly-Ub chain. The linear ubiquitination of NEMO and RIP1 bring these two proteins into spatial proximity which is advantageous for the IKK activation (Aksentijevich and Zhou 2017; Keusekotten et al. 2013; Haas et al. 2009; Cabal-Hierro and Lazo 2012).

From here onwards, one can distinguish between the canonical and the non-canonical or alternative nuclear factor kappa-light-chain-enhancer of activated B cells (NFκB) pathway. To be able to understand the differences between these pathways, it is important to know that NFκB or also called Rel family, consists of five different members which can be divide into two groups. All members contain a conserved amino-terminal Rel homology domain (RHD) which is essential for the hetero- or homo-dimerization of the different NFκB family members (Figure 2) (Dixit and Mak 2002; Lawrence 2009; T. Liu et al. 2017).

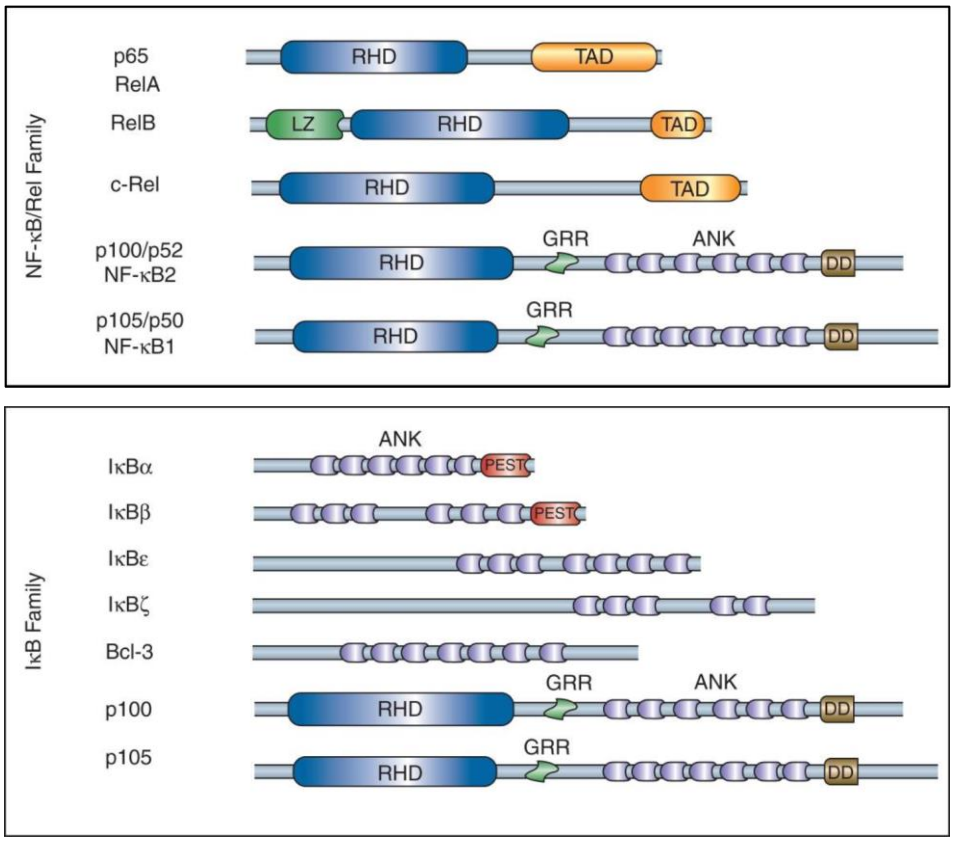

Figure 2: Structural elements of NFκB/Rel and IκB family members (Oeckinghaus and Ghosh 2009)
The RHD domain is specific for the NF**κ**B family, whereas the ANKs are characteristic for the I**κ**B family.

In the first group, RelA, RelB and c-Rel are already mature synthesized proteins containing a carboxyl-terminal transactivation domain (TAD) in addition to the RHD (Figure 2). However, the NFκB dimers can be inhibited by NFκB specific inhibitors, the IκBs, which render them inactive in the cytoplasm (Karin and Lin 2002; Ghosh and Karin 2002). These can be degraded by the canonical pathway, resulting in the activation of the NFκB proteins. For this purpose, phosphorylated IKKβ via TAK1 enables the phosphorylation of two specific serine residues in

the IκBs. These are recognized by β-TrCP, marking them for proteasomal degradation via the SCF polyubiquitin ligase complex. The NFκB dimer is released and translocates to the nucleus, where it undergoes conformational change to interact with the DNA as a transcription factor (Dixit and Mak 2002; Lawrence 2009; T. Liu et al. 2017).

The second group contains the long, inhibited precursors p105 and p100. These contain a glycine rich region (GRR) followed by multiple ankyrin repeats (ANK), similar to NFκB specific inhibitors, the IκBs (Figure 2) (Oeckinghaus and Ghosh 2009). The inhibitory components of the two precursors p105 and p100 are catalytically cleaved resulting in the mature p50 and p52. In contrast, in the non-canonical pathway the NFκB-inducting kinase (NIK) enables IKKα activation through phosphorylation. This pathway is activated via TNF family cytokines like RANKL, however not by TNFα itself (Dixit and Mak 2002; Lawrence 2009; T. Liu et al. 2017).

Both pathways, the canonical and the non-canonical cause transcriptional activation of a broad range of genes. These include NFκB regulatory genes, resulting in an auto-regulatory feedback loop. Other NFκB target genes are important for cell proliferation, like growth factors, or for anti-apoptotic factors, like IAPs. In addition, NFκB is involved in transcription of immunoregulatory proteins, like components of immune receptors, and in the production of proinflammatory cytokines, like TNFα (Figure 3) (Dixit and Mak 2002; Lawrence 2009; T. Liu et al. 2017; Oeckinghaus and Ghosh 2009).

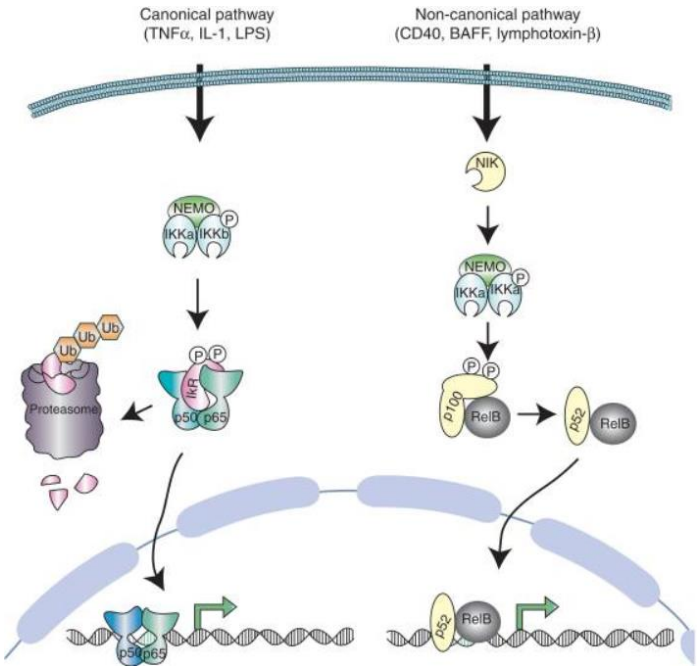

Figure 3: Canonical and non-canonical NFκB signaling pathway (Oeckinghaus and Ghosh 2009)
The canonical pathway can be induced e.g. via TNFα or different adaptor proteins causing IKK complex activation through the phosphorylation of IKKβ. In the next step, the inhibitors of NFκB are phosphorylated and marked for proteasomal degradation resulting in active NFκB dimers. The non-canonical pathway can be induced e. g. through CD40 leading to IKK complex activation via phosphorylation of IKKα through NIK. This results in processing of the p100-RelB dimer to its mature form p52-RelB dimer.

1.3.2. Cell death pathways

Usually, the cell death pathway induces apoptosis. To trigger cell death, a ligand of the TNF superfamily needs to bind to its corresponding TNFR with a DD like a trimeric FasL to a trimeric FasR. This leads to the dissociation of the silencer of DD (SODD) and a conformational change of the receptor, which is then able to recruit an adaptor protein like Fas associated DD (FADD). This protein binds to the unbound DD of the receptor itself via its DD. If another TNF ligand like TNFα binds to its corresponding receptor like TNFR1, then TRADD will interact with the receptor first and recruit FADD in the following step. Both processes lead to the exposure of the death effector domain (DED) of FADD, which recruits the initiator procaspase-8. This complex of TNFR, FADD and procaspase-8 is called complex IIa or death inducing signaling complex (DISC) (Figure 4). Due to the trimeric nature of TNFR, one receptor can recruit up to three FADDs with each of them creating a platform for caspase-8/-10 recruitment. Caspases are proteases with a cysteine in their catalytic center being specific for substrates with aspartic acid residues. There exist two different groups of caspases: (i) the initiator caspases and (ii) the effector or executioner caspases. Both have a small and a large

subunit, with the large subunit containing the catalytic center. While the effector caspases are mainly found as inactivated dimers, the initiator caspases exist as inactive monomers, which are activated when they are in close proximity to each other. The pro-domains of initiator caspases mediate the interaction with adaptor proteins via either a DED or a caspase recruiting domain (CARD) domain. Only the DED containing caspases, namely caspase-8 and -10 can be recruited and interact with FADD leading to the formation of the DISC. The close proximity of several caspases to one another leads to dimerization of two initiator caspases, which are processed into a tetrameric complex consisting of one large and two small subunits. This activated initiator caspases can then cleave and thus activate dimeric effector caspases like caspase-3, -6 and -7. Next, theses can cleave multiple substrates leading to activation of apoptosis (Hu and Kavanagh 2003; Green and Llambi 2015; H. Wajant, Pfizenmaier, and Scheurich 2003).

This type of apoptosis activation is called the extrinsic pathway due to the external stimulus via a death receptor. The intrinsic apoptosis pathway is another type of apoptosis and is activated via an intrinsic stimulus. It is a mitochondrial pathway in which proteins from the BCL2 family containing both pro-apoptotic and anti-apoptotic members play an important role. There is a link between the extrinsic and the intrinsic pathway through caspase cleavage of apoptosis promoting factors belonging to the BH3-only activator protein subfamily like BCL-2-interacting mediator of cell death (BIM), BH3-interacting domain death agonist (BID) and p53-upregulated modulator of apoptosis (PUMA). These can subsequently activate BCL-2-associated X protein (BAX) and BCL-2 antagonist/killer (BAK). Being attached to the mitochondrial surface, BAX and BAK are responsible for creating pores through oligomerization in the outer membrane, also referred to as mitochondrial outer membrane permeabilization (MOMP) (Singh, Letai, and Sarosiek 2019; Zhou and Yuan 2014; Hu and Kavanagh 2003). This results in the release of e.g. cytochrome c from the intermembrane space into the cytosol, enabling the formation of an apoptosome, a caspase activating complex made up of cytochrome c, the CARD-domain containing apoptotic protease-activating factor-1 Apaf1 and the CARD-domain containing initiator caspases (either caspase-2 or -9). This platform further causes the activation of executioner caspases, leading to the same outcome as activation of the extrinsic pathway (Fadeel, Ottosson, and Pervaiz 2008; Singh, Letai, and Sarosiek 2019).

Beside apoptosis, TNF can also trigger necroptosis, a programmed cell death form of necrosis. Several factors must coincide for this cell death pathway to materialize (note that there may be differences between different cell types). The kinase activity of RIP1 is key to the necroptosis activation. As previously mentioned, the ubiquitination of RIP1 results in the activation of the NFκB survival pathway. In order to trigger cell death, RIP1 ubiquitination needs to either be stopped by cIAP1/2 and LUBAC or deubiquitinated through CYLD, a Lys63 deubiquitinase. Following this, the autophosphorylation, e.g. triggered via reactive oxygen species (ROS), of RIP1 leads to the recruitment and phosphorylation of RIP3, which subsequently causes the activation of the mixed lineage kinase domain like (MLKL) protein. RIP1, RIP3 and MLKL form the necrosome complex (complex IIb) (Figure 4). While the C-terminus of MLKL is activated via phosphorylation, the N-terminus is important for oligomerization and membrane translocation to either the plasma or the intracellular membrane, resulting in membrane permeabilization. Necroptosis is a programmed cell death. However, it still leads to the same outcome as necrosis: swelling until membrane rupture causes the release of pro-inflammatory cytokines and thus initiates inflammatory responses (Zhou and Yuan 2014; Green and Llambi 2015). The caspase-8 need to stay inactive in order to enable necroptosis (Fritsch et al. 2019). Otherwise extrinsic apoptosis is activated resulting in caspase activation and the cleavage of RIP1, RIP3 or MLKL, the three components of the necrosome complex. This can e.g. be achieved through the NFκB activated expression of antiapoptotic proteins like c-FLIP, a catalytic inactive homolog to caspase-8 resulting in heterodimers with caspase-8. These heterodimers are unable to trigger apoptosis (Cabal-Hierro and Lazo 2012; Newton and Dixit 2012; Green and Llambi 2015).

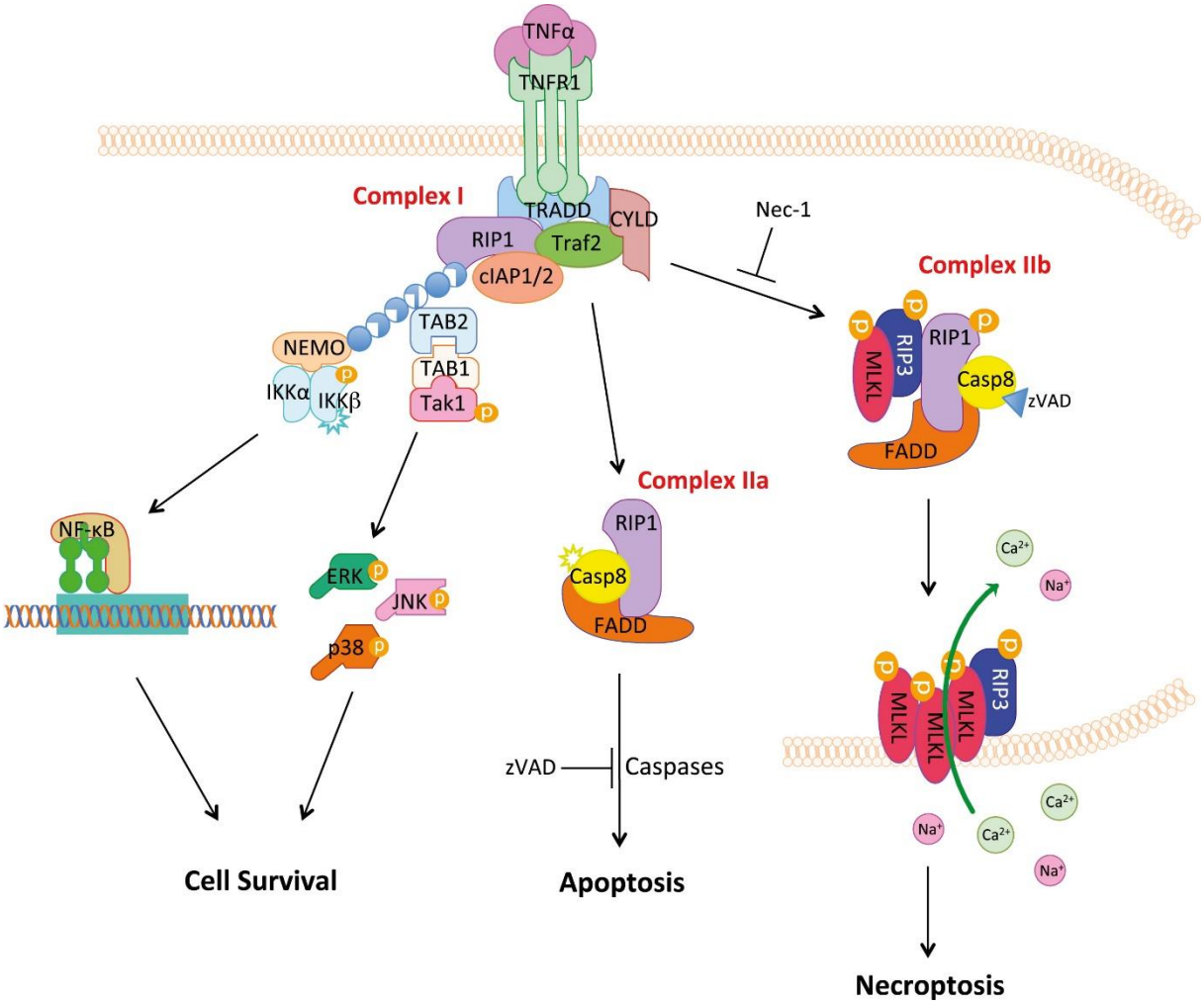

Figure 4: Cell survival and cell death (apoptosis or necroptosis) induced via TNFα binding to the pleiotropic TNFR1 (Zhou and Yuan 2014)
The recognition of TNFα by TNFR1 can either lead to complex I formation and thus trigger cells survival via either NFκB or ERK/JNK, or lead to complex II formation. Complex IIa leads to apoptosis, whereas complex IIb results in necroptosis.

Its ability to trigger cell death makes TNFα is an interesting treatment to be utilized for cancer therapy. Brouckaert et al. (1986) and Balkwill et al. (1986) demonstrated that treatment of different mouse tumor models with recombinant TNFα resulted in tumor necrosis. Based on this success, first clinical trials of TNFα in advanced cancers were conducted (Kimura et al. 1987; Feinberg et al. 1988). However, the first excitement was derailed when it became apparent that TNFα therapy could cause a cytokine storm, resulting in an endotoxic shock. In addition, researchers found evidence that TNF may increase cancer growth and spread (F. Balkwill 2009). Thus, the ability to switch between cell survival and cell death pathways triggered by TNFα is a major goal for cancer therapies. Recently, Vredevoogd et al. (2019)

identified a critical mediator to TNFα-mediated killing of tumor cells via a CRISPR screen. They showed that the deletion of TRAF2 sensitizes tumors to cell death with an even greater effect upon simultaneous inhibition of cIAPs. This suggests that TNF signaling and its complex factors leading to either pro- or anti-survival signals are not entirely understood, yet. CRISPR screens are a powerful tool to search for them systematically and recognize new effective targets for cancer therapy.

1.4. CRISPR screens

CRISPR's natural function is the adaptive immune system in prokaryotes protecting themselves from viral infections (Barrangou et al. 2007). The adaption of this system has enabled targeted genome modification in both prokaryotic and eukaryotic cells. Single guide RNAs (sgRNA) recognize target sequences in the DNA, bind to it and recruit the CRISPR associated protein Cas9. This complex can then recognize foreign DNA via the G-rich, 2-5bp long protospacer adjacent motive (PAM) upstream of the target site. This initiates the endonuclease activity of Cas9 resulting in a blunt end double strand break (Figure 5). This DNA damage then stimulates different DNA repair mechanisms. The most frequent one is the non-homologous end joining (NHEJ) pathway. Since this pathway is error-prone, it can lead to deletions as well as insertions also called indels. If they are not a multiple of three, they will cause a frameshift mutation most commonly followed by mRNA translation of a non-functional protein, thus causing a knockout (KO) of the gene. The frameshift mutation can also result in a premature stop codon. If two double strand breaks occur in close proximity to each other it can either lead to a deletion of the intermediate section or its reverse or correct orientated insertion. Another DNA repair mechanism is the homology directed repair (HDR) pathway, which occurs with a lower frequency. In contrast to NHEJ, HDR is error-free and can incorporate an externally delivered homologous DNA template leading to a knock-in (Pickar-Oliver and Gersbach 2019; Barman, Deb, and Chakraborty 2019).

In combination with lentiviral whole-genome sgRNA libraries and next generation sequencing, a pooled loss-of function screen can be conducted. For this purpose, a pooled KO cell population is generated by sgRNA infection. The sgRNAs target different coding regions of genes and induce gene KO together with Cas9 expression. A single KO per cell is ensured by a low infection rate. Transduced cells are selected afterwards and cultured for a specific period

of time to ensure the drop-out of cells with a proliferative disadvantage upon KO. The sgRNA composition is quantified by next-generation sequencing (Hinterndorfer and Zuber 2019).
During the screen the cells can be positively or negatively selected depending on either survival or selection of another phenotype e.g. using cell sorting. CRISPR screens were also shown to be a powerful tool to decipher mode of action of drugs. In so called drug modifier screens a Cas9 expressing cell population containing a sgRNA library is exposed to drugs during the screening time. For example, Fang et al. (2019) showed that TIGAR is a modifier of PRARP inhibitor sensitivity.
However, it is not only drugs the cells can be exposed to, they can also be cultured with innate immune system stimuli like lipopolysaccharide (Aregger, Hart, and Moffat 2015) or they can be cultured with cytokines like IFNγ (Ohainle et al. 2018).
Afterwards, one can identify which gene alterations are necessary for the mechanism of action of e.g. a specific drug. Increased sgRNA occurrence demonstrates a proliferative advantage of cells containing this KO. This implies resistance towards the co-cultured drug. Whereas, cells harboring a KO leading to sgRNA deletion emphasize resistance towards the drug. Cells containing a KO which is unaffected by the treatment remain constant in the sgRNA pool (Hinterndorfer and Zuber 2019).
The various applications make CRISPR screens a powerful tool for the identification of genes that increase cells resistance or sensitivity to a specific treatment.

1.5. Aims of the project

Besides IFNγ, TNFα is one of the key cytokines mediating cytotoxic activity and anti-tumor immunity. However, in certain cancers types resistance to TNFα mediated killing mechanism was observed, which resulted in rapid cancer progression (Kearney et al. 2018). Consequently, strategies to make cells more sensitive to TNFα mediated cytotoxicity are commonly believed to hold great promise for cancer treatment. Furthermore, both sensitization and resistance to TNFα on the molecular level are incompletely understood.
In recent years, CRISPR/Cas9 loss-of-function screens have proven to be a powerful tool to study biological processes on a genome wide level. I want to adapt this technology to identify genetic dependencies that render a human cancer cell line resistant or more sensitive to TNFα treatment. For this purpose, I will utilize the colon carcinoma cell line RKO which is sensitive

to TNFα treatment. This cell line was adapted in the Zuber lab for CRISPR/Cas9 screening by 1) engineering it to express an inducible Cas9 allele and 2) infecting it with the sgRNA library. Thus, Cas9 expression can be induced at the starting time point of the screen, resulting in gene editing and generation of KO clones. The analysis of the screen data will be performed with the model-based analysis of genome-wide CRISPR/Cas9 knockout (MAGeCK) algorithm to determine differential sgRNA abundances at various time points and TNFα conditions of the screen. One goal is to find highly reduced or increased sgRNA levels in the end time point with TNFα treatment compared to the untreated culture. Reduced sgRNA counts would suggest sensitization to TNFα, whereas increased sgRNA abundances indicate resistance to TNFα.

Another aim was to establish a human co-culture system to test $CD8^+$ T cell mediated killing of tumor cells. This system together with conducting a single sgRNA competition assay should be used for further hit validations.

Taken together, the aim of the thesis is to utilize the CRISPR/Cas9 loss-of function screen system to identify genetic dependencies that render a human cancer cell line resistant or sensitive to TNFα treatment. These genetic dependencies will improve the understanding of the basic mechanisms of resistance and sensitization to TNFα mediated cytotoxicity and might allow to exploit these dependencies to improve cancer immunotherapy strategies.

2. Material and Methods

2.1. Material

Table 1: Material utilized for this thesis

Fluorophores	**Source**	**Clone**
Zombie Aqua™ Fixable Viability Kit	BioLegend	
CD8 - SB780	eBioscience	Okt-8
Fixable Viability Dye – eF780	eBioscience	
HLA-A2 – BV785	BioLegend	BB7.2
Restiction enzymes & Buffers	**Source**	**Catalogue #**
AscI	NEB	R0558S
BamHI-HF	New England Biolabs	R3136L
CutSmart (10x)	NEB	B7200S
CIP	New England Biolabs	M0290S
NsiI-HF	NEB	R3127S
BsiWI	New England Biolabs	R0553L
Gibson mix (2x)	Media Kitchen VBC	
Chemicals & Pept. & Prot.	**Source**	**Catalogue #**
Recombinant human TNFα	PeproTech	300-01A
Doxycycline (dox)	Sigma-Aldrich	D9891
Agarose	Sigma-Aldrich	A9539
Ampicillin	Sigma-Aldrich	A0166-25G
Elution buffer (EB)	Media Kitchen VBC	
Ethylenediaminetetraacetic acid (EDTA)	VWR International	97061-406
EtOH	VWR International	
Isopropanol	VWR International	
Sodium Acetate (NaAc)	VWR International	
Sodium chloride (NaCl)	VWR International	

Pellet Paint Co-Precipitant	VWR International	69049-3
Phenol solution	Sigma-Aldrich	P4557
Polyethylenimine (PEI)	PolyScience	23966-2
Proteinase K	New Englans Biolabs	P8107S
RNAse DNAse free	Sigma-Aldrich	11119915001
Tris(hydroxymethyl)aminomethane (Tis-HCl)	Sigma-Aldrich	
HCMV pp65 peptide NLVPMVATV	IBA	6-7001-901
Ligation buffer (10x)	NEB	
High concentration ligase	NEB	
NaCL (5 M)	VWR International	
FuGENE HD Transfection Reagent	Promega	E2311
Dynabeads™ Human T-Activator CD3/CD28 for T Cell Expansion and Activation	Thermo Fisher Scientific	11131D
RetroNectin	TaKaRa	T202
HCMV-sepcific TCR	Ton Schuhmacher	
Kits & Lab. Material	**Source**	**Catalogue #**
AmpliTaq Gold DNA polymerase	Thermo Fisher Scientific	43-118-20
Magnetic beads	Media Kitchen VBC	
Mini-Prep kit	Media Kitchen VBC	
Phase-Lock Gel Light	VWR International	10847-800
Platinum (R) Pfx DNA Polymeras	Invitrogen	11708021
Cell lines & Bacteria	**Source**	**Characteristics**
Lenti-X	ATCC	
MIA Paca-2 BFP2	Zuber	Cas9-BFP

NEB stabl3 bacteria		Zuber	
RKO wt		ATCC	
RKO c16		Zuber	Cas9-BFP
RKO c20		Zuber	Cas9-GFP
Plate-GP		ATAC	
human $CD8^+$ T cells		STEMCELL	
Media & Supplements		**Source**	**Catalogue #**
Dimethylsulfoxide (DMSO)		Sigma-Aldrich	276855
DMEM high Glucose		Media Kitchen VBC	
Fetal bovine Serum (FCS)		Sigma-Aldrich	F7525
Human Serum (HS)		Sigma-Aldrich	H3667
LB medium		Media Kitchen VBC	
L-Glutamine 200 mM		Thermo fisher scientific	25030024
PBS		Media Kitchen VBC	
Penicillin-Streptomycin solution		Sigma-Aldrich	P0781
RPMI-1640		Invitrogen	21875091
Sodium pyruvate solution		Sigma-Aldrich	10519979001
Trypsine EDTA 10x		Thermo fisher scientific	15400-054
Trypsine EDTA 1x		Thermo fisher scientific	25200056
IL-15		BioLegend	570302
IL-7		PeproTech	200-07-50ug
Oligonucleotides		**Sequence**	
PCR_1	HLA-A*0201_fwd	TCACTCGGCGCGCCAGTC	
PCR_2	HLA-A*0201_rev	GTGCGGCCGCGGATCCTTAC	
PCR_3	IRFP720_fwd	atgataatatggccacaaccATGGCTGAGGGCAGCGTT	
PCR_4	IRFP720_rev	agacgcgtttcgaagtcgacTCACTCCTCCATGACACCTATTTG	
PCR_5	IRFP720 w/o stop codon_rev	cacctgagccCTCCTCCATGACACCTATTTGCC	
PCR_6	P2A pp65 & presenter_fwd	catggaggagGGCTCAGGTGCCACCAAC	

PCR_7	P2A pp65_rev	agacgcgtttcgaagtcgacTCATCCCCGATGTTTCTTCGG
PCR_8	P2A presenter_rev	agacgcgtttcgaagtcgacTTACACGGTGGCCACCATG
Sanger-Seq_1	HLA_fwd	GGAGGTACCTGGAAAACGGT
Sanger-Seq_2	HLA_rev	ACTTGGAACGACTACAGCCG
Sanger-Seq_3	pp65_fwd	GCGCAAACATAGACACCTGC
Sanger-Seq_4	pp65_rev	CAGCCTTCAATCTCCCTCGT
Sanger-Seq_5	P2A_fwd	GTGCCACCAACTTCAGCTTG
Sanger-Seq_6	P2A_rev	CCCAGCCTGTTTCAACAAGC
Sanger-Seq_7	IRFP720_fwd	CAGGCCTGTCCCTGTTACAC
Sanger-Seq_8	IRFP720_rev	AGCCACTGGCAGGTGTCTAT
Sanger-Seq_9	IRES_fwd	CGGCCCGAGGCCAAGAACAG
Sanger-Seq_10	IRES_rev	CCTCACATTGCCAAAAGACG
Sanger-Seq_11	sgRNA_fwd	TTTCTTGGGTAGTTTGCAGTTTT
Sanger-Seq_12	sgRNA_rev	ACGGTTCTCCCCCACCCTCG
sgRNA_1	AAVS1(2)_fwd	caccGCTCCGGAAAGAGCATCCT
sgRNA_2	AAVS1(2)_rev	aaacAGGATGCTCTTTCCGGAGC
sgRNA_3	AAVS1(3)_fwd	caccGCTGTGCCCCGATGCACAC
sgRNA_4	AAVS1(3)_rev	aaacGTGTGCATCGGGGCACAGC
sgRNA_5	CAB39_fwd	caccGCCATACAGAATTTCTTTCA
sgRNA_6	CAB39_rev	aaacTGAAAGAAATTCTGTATGGC
sgRNA_7	CDK6_fwd	caccGACCTTCGAGCACCCCAACG
sgRNA_8	CDK6_rev	aaacCGTTGGGGTGCTCGAAGGTC
sgRNA_9	DUSP5_fwd	caccGCCAGTGTGGAAAACCAG
sgRNA_10	DUSP5_rev	aaacCTGGTTTTCCACACTGGC
sgRNA_11	EGR1_fwd	caccGCACCTTCAACCCTCAGG
sgRNA_12	EGR1_rev	aaacCCTGAGGGTTGAAGGTGC
sgRNA_13	ETV6_fwd	caccGTGTATAGAGTTTCCAGGG
sgRNA_14	ETV6_rev	aaacCCCTGGAAACTCTATACAC
sgRNA_15	GTF2I_fwd	caccGCTTTTGTCAATACCAGAA
sgRNA_16	GTF2I_rev	aaacTTCTGGTATTGACAAAAGC
sgRNA_17	MRGBP(1)_fwd	caccGGTCCCAGATGACCTTGGAT
sgRNA_18	MRGBP(1)_rev	aaacATCCAAGGTCATCTGGGACC
sgRNA_19	MRGBP(2)_fwd	aaacAGGTGGAGGTGTGCCTCTTC
sgRNA_20	MRGBP(2)_rev	caccGAAGAGGCACACCTCCACCT
sgRNA_21	PBRM1_fwd	caccGGCCCAAGCAGGAAAAGG

sgRNA_22	PBRM1_rev	aaacCCTTTTCCTGCTTGGGCC
sgRNA_23	PEA15(2)_fwd	caccGAGCTGTTCTAGATCTTCA
sgRNA_24	PEA15(2)_fwd	caccGTTGGTCAGGTCTTGCAGGA
sgRNA_25	PEA15(2)_rev	aaacTGAAGATCTAGAACAGCTC
sgRNA_26	PEA15(2)_rev	aaacTCCTGCAAGACCTGACCAAC
sgRNA_27	PIH1D1_fwd	caccGTGATCACCATCGCCAGGG
sgRNA_28	PIH1D1_rev	aaacCCCTGGCGATGGTGATCAC
sgRNA_29	PPP6R3_fwd	caccGACCTTATTATAAAGCACAT
sgRNA_30	PPP6R3_rev	aaacATGTGCTTTATAATAAGGTC
sgRNA_31	STAU1_fwd	caccGCTGCTGCCAAAGCGTTG
sgRNA_32	STAU1_rev	aaacCAACGCTTTGGCAGCAGC
sgRNA_33	TRIB1_fwd	caccGGCCTATGTCTTCTTTGAGA
sgRNA_34	TRIB1_rev	aaacTCTCAAAGAAGACATAGGCC
sgRNA_35	UBE2D3_fwd	caccGAATACACCGCCTTGATA
sgRNA_36	UBE2D3_rev	aaacTATCAAGGCGGTGTATTC
gBlock_1	HLA-A*0201	Supplemental Table 15
gBlock_2	pp65	Supplemental Table 15
gBlock_3	presenter	Supplemental Table 15

Plasmids	**Abbreviation**
pRRL-SFFV-rtTA3-IRES-EcoReceptor-PGK-Puro	RIEP
pRRL-U6-filler-improved tracer-EF1a-mCherry-P2A-Neo	ECPN
pLentiV2-U6-IT-sgRNA-PGK-IRFP720	
pVSV-G	

Scientific Software
FlowJo
ForeCyt
MAGeCK
Spotfire

2.2. Methods

2.2.1. Cell culture

For this study two different adherent cell lines, RKOs and MIA PaCa-2, were utilized. For both of them inducible Cas9 clones exist. In addition, two packaging cell lines were used for virus production. A human co-culture system to test tumor cell killing was established with human $CD8^+$ T cells.

2.2.1.1. Cell lines and their cultivation

The colon carcinoma cell line RKO was obtained from ATCC, henceforward referred to as RKO wild-type (wt) population. This cancer cell line is driven by two activating mutations, namely the B-Raf Proto-Oncogene $BRAF^{V600E}$ and $PIK3CA^{H1047R}$. It still comprises the wt gene of KRAS, PTEN and TP53 (Ahmed et al. 2013).

The pancreas cell line MIA PaCa-2 was obtained from ATCC. This cell line is driven by an activating $KRAS^{G12C}$ mutation, an inactivation $TP53^{R248W}$ mutation and the loss of the $CDKN2A/p16^{INK4A}$ gene (Gradiz et al. 2016).

Aa packaging cells for lenti-virus production Lenti-X were used and for retro-virus production Plate-GP.

The RKOs were cultivated in RPMI medium supplemented with FCS [10 % v/v], Pen/Strep [1x], GlutaMAX [1x], sodium pyruvate [1mM], non-essential amino acids [1x], 2-mecaptoethanol [50 µM], HEPES [20 mM]. The MIA PaCa-2, Lenti-X and Plate-GP were cultivated in DMEM medium containing the same supplements as the RPMI medium except HEPES.

Human $CD8^+$ T cells were ordered from STEMCELL and cultivated in RPMI medium supplemented with HS [5 % v/v], Pen/Strep [1x], GlutaMAX [1x], sodium pyruvate [1mM], non-essential amino acids [1x], 2-mecaptoethanol [50 µM], HEPES [20 mM].

All cells were cultured at 37 °C with a 5 % CO_2 atmosphere.

2.2.1.2. Generation of inducible Cas9 clones

Inducible Cas9 clones for RKO and MIA PaCa-2 were generated in the Zuber group by using the tetracycline-controlled transcriptional regulation (tet-on) system.

For this purpose, the RKO wt population was successively transduced with two different lentiviral vectors. First, the gene for the reverse tetracycline transactivator was stably integrated into the genome in combination with a Puromycin or Hygromycin antibiotic resistance cassette (SFFV-rtTA3-IRIS-EcoR-PuroR or SFFV-rtTA3-IRIS-EcoR-Hygro respectively). In a second step, the selected cells were transduced with a lentiviral plasmid encoding the Cas9 protein of S. pyogenes (SpCas9) (TRE3G-Cas9-P2A-GFP for RKO c20 and TRE3G-Cas9-P2A -BFP for c16). Infected cells were sorted into single cell clones.

The MIA PaCa-2 BFP2 clone was generated by the same experimental strategy as for the RKO cell line with the exception that it was transduced with both rtTA3 plasmids, the one containing EcoR and the one containing HygroR. The transduced Cas9 plasmid was coupled to BFP.

2.2.2. Molecular cloning

sgRNAs were cloned into an established sgRNA delivery plasmid for conducting competition assays of sensitization hits identified by CRISPR screens. Additionally, three HLA-A*0201 constructs were cloned for the establishment of an antigen specific human co-culture system to test tumor cell killing via $CD8^+$ T cells.

2.2.2.1. sgRNA cloning for CRISPR screen validation

To validate the CRISPR screen results two sgRNAs, targeting top hit of the screen, were cloned into a guide delivery plasmid. Neutral controls, targeting the adeno-associated virus integration site 1 (AAVS1) locus, were included.

The two sgRNAs of the top hits were selected based on their performance during the screen. Ideally, they should exhibit neutral behavior in the control condition and have a significant effect in the treatment condition.

The respective forward and reverse sgRNA were annealed via the following protocol and PCR program:

Table 2: Protocol for annealing of the forward and reverse oligos of the sgRNAs

Reagent	Amount [µL]
Oligo 1 (Fwd) [100µM]	1.00
Oligo 2 (Rev) [100µM]	1.00
T4 Ligase buffer (10x)	1.00
T4 PNKinase	1.00
ddH_2O	to 10.00

Table 3: PCR program for oligonucleotide annealing

Temperature [°C]	Time [s]
37	2100
95	300
95 (-5 °C increase)	60 (14 times)
4	∞

The annealed sgRNAs were diluted at a ratio of 1:250 and cloned in the filler region of the pRRL-U6-filler-improved tracer-EF1a-mCherry-P2A-Neo (ECPN) vector. This plasmid was enzymatically digested using the restriction enzyme BsmBI via the following protocol:

Table 4: Protocol for BsmBI restriction digest of the plasmid ECPN

Reagent	Amount
Plasmid	5.00 µg
NEB Buffer 3.1 (**10**x)	5.00 µL
BsmBI	1.00 µL
dd**H2O**	to 50.00 µL

After an incubation period at 55 °C for 5 h the annealed oligos were dephosphorylated by adding 2 µL of the calf-intestinal-phosphatase (CIP) and then additionally incubated at 37 °C for 30 min. Afterwards the phosphorylated oligonucleotides were ligated into the ECPN plasmid via the following protocol:

Table 5: Ligation of sgRNA into an ECPN plasmid

Reagent	Amount
Processed plasmid (ECPN)	0.50 µg
Annealed and phosphorylated oligos (1:250 diluted)	1.00 µL
T4 ligase buffer (10x)	1.00 µL
T4 ligase	1.00 µL
ddH_2O	to 10.00 µL

The ligation was incubated at RT for 1 h and then transformed into competent bacteria. Therefore, 3 µL of the ligation were incubated with 10 µL of the NEB stabl3 bacteria for 30 min on ice followed by a heat shock at 42 °C for 42 s. After recovery on ice for 5 min, the bacteria were plated on ampicillin containing LB agar plates and incubated overnight at 37 °C. Transformed colonies were picked the next day and cultured in 8mL LB medium containing ampicillin [100 µg/mL] overnight at 37 °C on a shaker.

Plasmid purification was performed with an in-house Mini-Prep kit according to the manufacturer's protocol.

The purified plasmids were sequenced via Sanger sequencing at the Molecular Biology Service at the Vienna Biocentre.

*2.2.2.2. Cloning of HCMV specific HLA-A*0201^{+} constructs*

Three different HLA-A*0201 constructs were generated (Figure 5). The pRRL-SFFV-rtTA3-IRES-EcoReceptor-PGK-Puro (RIEP) vector was used as a backbone. The sequence of the HLA-A*0201 itself was integrated downstream of the SFFV promotor and replaced the rtTA3 gene, whereas the three different epitope containing constructs replaced the EcoReceptor-PGK-Puro cassette. All constructs contained the fluorophore IRFP720 which was either followed by a stop codon, referred to as the empty construct, or by the P2A linked to an epitope expressing gene cassette. The NLV-epitope was either present as a full length pp65 sequence or as a nonpeptide sequence itself, which was linked to an ER-signaling peptide, referred to as the presenter construct (Gejman et al. 2019).

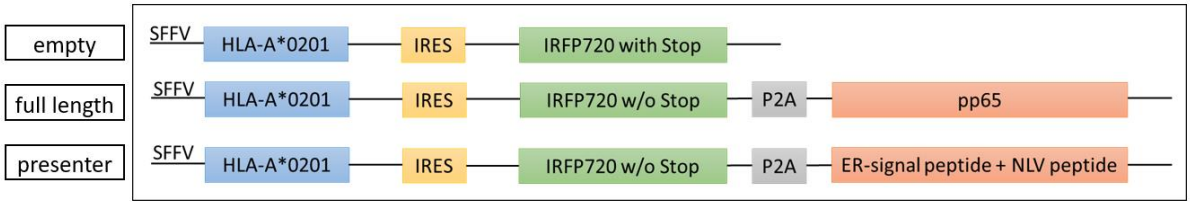

Figure 5: The three different HLA-A*0201 constructs
All three constructs contained the HLA-A2*0201 sequence linked to the IRFP720 fluorophore via IRES. The empty construct had a stop codon at the end of the IRFP720 element, while the two other constructs did not. The full-length construct contained the full sequence of pp65 after a P2A and the presenter contained an ER signal peptide linked to the NLV nonamer itself.

2.2.2.2.1. Amplification of the different inserts

The HLA-A*0201, P2A-pp65 and P2A-ER signal peptide-NLV sequences were ordered as gBlocks from IDT and first amplified according to the following PCR protocol:

Table 6: PCR reaction for amplification of the gBlocks

Reagent	Amount [µL]
Pfx buffer (10x)	5.00
dNTP [10 mM]	1.50
$MgSO_4$ [50 mM]	1.00
Fwd primer [10 µM]	1.00
Rev primer [10 µM]	1.00
DNA template [0.01-200.00 ng]	1.00
Platinum DNA polymerase	1.00
ddH_2O	to 50.00

Table 7: PCR protocol for amplification of the gBlocks

PCR steps	Temperature [°C]	Time [s]
1. Initial Denaturation	95	600
2. Denaturation	95	30
3. Primer Annealing	52	45
4. Extension	72	180
Cycle replication	GOTO 2	27x
5. Final extension	72	420
Storage	4	∞

The PCR amplicons were loaded on a 2 % agarose gel and purified using gel extraction.

The IRFP720 sequence was amplified from the pLentiV2-U6-IT-sgRNA-PGK-IRFP720 plasmid either with or without a stop codon. The following PCR reaction was performed and the stop codon was added for the empty construct by a different revers primer:

Table 8: PCR reaction for IRFP720 amplification

Reagent	Amount [µL]
Pfx buffer (10x)	5.00
dNTP [10 mM]	1.50
$MgSO_4$ [50 mM]	1.00
Fwd primer [10 µM]	1.00
Rev primer [10 µM]	1.00
DNA template [0.01-200.00 ng]	1.00
Platinum DNA polymerase	1.00
ddH2O	to 50.00

Table 9: PCR program for IRFP720 amplification

PCR steps	Temperature [°C]	Time [s]
1. Initial Denaturation	95	600
2. Denaturation	95	30
3. Primer Annealing	52	45
4. Extension	72	180
Cycle replication	GOTO 2	27x
5. Final extension	72	420
Storage	4	∞

The PCR amplicon was loaded on a 1 % agarose gel for verification of successful amplification and column purified.

*2.2.2.2.2. Cloning of HLA-A*0201 constructs into the backbone vector*

In order to clone the three HLA-A*0201 containing constructs, two ligations had to be performed. The first approach replaced the rtT3A cassette with the HLA-A*0201 sequence. Therefore, both the backbone vector and the HLA-A*0201 gBlock were digested with the restriction enzymes AscI and BamHI-HF according to the following protocol:

Table 10: Restriction digest of the RIEP backbone vector and the HLA-A*0201 gBlock

RIEP backbone vector	
Reagent	**Amount**
Backbone vector	17.60 µg
CutSmart (10x)	5.00 µL
AscI	3.00 µL
BamHI-HF	3.00 µL
ddH2O	to 50.00 µL
HLA-A*0201 gBlock	
Reagent	**Amount**
DNA	0.02-3.00 µg
CutSmart (10x)	5.00 µL
AscI	3.00 µL
BamHI-HF	3.00 µL
ddH2O	to 50.00 µL

The digest was incubated at 37 °C for 45 min, dephosphorylated by adding 2 µL of the CIP and then additionally incubated at 37 °C for 30 min. Again, the product was checked on a 2 % agarose gel and column purified.

Next, the digested products were ligated in a vector:insert ratio of 1:3 with ligation buffer (10x), 1 µL high concentration ligase (NEB) and distilled water of up to 20 µL in total.

Afterwards, the bacterial transformation and Mini-Prep was done. The plasmids were subsequently sequenced.

*2.2.2.2.3. Gibson assembly of the antigen-specific inserts into the HLA-A*0201 containing backbone*

The second ligation inserted the IRFP720 constructs together with the HCMV-specific constructs and removed the EcoReceptor-PGK-Puro cassette. Therefore, the vector containing the HLA-A*0201 sequence was digested with the restriction enzymes Nsil-HF and BsiWI according to the following protocol:

Table 11: Restriction digest of the HLA-A*0201 containing vector and the IRFP720 HCMV-specific constructs

Reagent	Amount
HLA-A*0201 containing vector	15.00 µg
CutSmart (10x)	5.00 µL
NsiI-HF	3.00 µL
ddH_2O	to 50.00 µL
Incubation at 37 °C for 45 min	
NaCL [5 M]	1.00 µL
BsiWI	3.00 µL
Incubation at 55 ° for 45 min	

Afterwards, it was again checked on a 1 % agarose gel to ensure digestion and the product was purified via column purification.

Finally, the Gibson assembly of the HLA-A*0201 containing vector and the different inserts was done with an in-house Gibson mix (2x). The backbone and the inserts were mixed in a molar ratio of 1:1, with the total DNA amount not exceeding 0.15 µg. The different constellations are depicted in table 16. The Gibson assembly mix was incubated at 50 °C for 15 min and afterwards, bacterial transformation and Mini-Prep was done. Next, the product was sequenced.

Table 12: Gibson cloning of the three different HLA-A*0201 constructs

Empty construct		
Backbone	**Insert 1**	**Insert 2**
HLA-A*0201 containing vector	IRFP720 w/ stop codon	/
Full length construct		
Backbone	**Insert 1**	**Insert 2**
HLA-A*0201 containing vector	IRFP720 w/o stop codon	P2A-pp65
Presenter construct		
Backbone	**Insert 1**	**Insert 2**
HLA-A*0201 containing vector	IRFP720 w/o stop codon	P2A-ER signal peptide-NLV

2.2.3. Virus production

Lenti-virus was produced for the sgRNA validation and HLA-construct infection, whereas for the TCR infection retro-virus was produced.

2.2.3.1. Lenti-virus production

To transduce the target cells, lenti-virus of the plasmids containing the sgRNA was produced. For this purpose, the plasmid of interest, the helper plasmid pHCMVR8.74 and the Eco envelope gene were mixed at a ratio of 4:2:1, with a maximum total amount of 4.00 µg DNA, and diluted with 200 µl DMEM. To increase the transfection efficiency, 12 µL of polyethylenimine (PEI) were added and directly mixed. After an incubation period at RT for 20 min, the transfection mixture was carefully dropped onto Lenti-X cells cultured in DMEM in a 6-well plate, which were grown to 80 % confluency. 24 h after the transfection, the medium was changed to 2 mL target medium, in this case RPMI. The virus was harvested 72 h after transfection. In order to remove remaining Lenti-X cells from the virus solution, it was centrifuged for 10 min at 500 g and the supernatant was transferred to a new tube. Virus transduction was performed afterwards in combination with polybrene [10 µg/mL] which supports the infection.

Additionally, lenti-virus was produced for the HLA-construct infection in a similar way, but with the exception that a VSV-G expressing virus instead of an EcoR one was produced in a 10 cm dish this time.

2.2.3.2. Retro-virus production

Therefore, retro-virus containing the HCMV-specific TCR construct had to be produced. To prepare the transfection medium 200 µL of RPMI medium without any supplements was

incubated with 5 µL Fugene at RT for 5 min. Then, the HCMV-specific TCR construct and the pVSV-G were added in a 4:1 ratio and again incubated at RT for 15min. Afterwards, the transfection medium was carefully dropped onto Plate-GP cells cultured in the target medium hRPMI in a 6-well plate, which were grown to 70 % confluency. After 48 h the virus containing medium was harvested and centrifuged for 10 min at 500 g to remove remaining Plate-GP cells from the virus solution.

2.2.4. TNFα modulator screen

A CRISPR/Cas9 screen was conducted in the Cas9 inducible RKO c16 clone to detect TNFα dependent modulators.

2.2.4.1. TNFα titration on cell lines

In order to identify the optimal concentration to induce TNFα mediated killing, I first titrated the amount of TNFα on RKO an MIA PaCa-2 cells.

Two independent TNFα titration experiments were conducted in duplicates, respectively. Cells were cultivated in 3 mL RPMI per well for 20 days. Every 2nd or 3rd day the cells were split according to their density and IntelliCyt® iQue Screener was used for cell counting. To determine the cumulative cell number of viable cells, they were stained with Zombie Aqua (1:1000 in PBS) prior to counting.

To estimate a suitable range, TNFα sensitivity was first tested on RKO c20 (1 Mio cells/well) and MIA Paca-2 BFP2 (0.5 Mio cells/well) at the six different concentrations of TNFα 0 ng/mL, 0.1 ng/mL, 1 ng/mL, 10 ng/mL, 100 ng/mL, 1000 ng/mL.

In order to identify the exact concentration needed for each cell line, a second TNFα titration experiment was conducted on RKO c20, RKO c16 and the RKO wt population (0.5 Mio cells/well) with the narrow concentration range of 0 ng/mL, 0.25 ng/mL, 0.5 ng/mL, 0.75 ng/mL, 1 ng/mL, 10 ng/mL TNFα.

2.2.4.2. Whole-genome TNFα modulator CRISPR/Cas9 screen

The whole-genome CRISPR/Cas9 screen was performed in the RKO colon carcinoma cell line (clone c16) in the Zuber lab. In brief, cells were transduced with a lentiviral packaged customized genome-wide sgRNA library (123,00 sgRNAs/6 per gene, including 1000 non-targeting control sgRNAs) at a representation of 1000x with a low multiplicity of

infection (MOI) to guarantee a singular infection per cell. The sgRNAs were delivered utilizing the vector U6-sgRNA-EF1as-Thy1.1-P2A-NeoR. This allows to determine the infection rate through fluorescence activated cell sorting (FACS) analysis and to select sgRNA expressing cells using neomycin. After complete selection, cells were either frozen (TP-A) in several multiplicities of the library representation or Cas9 expression was induced via addition of doxycycline (dox) in a concentration of 0.10 µg/mL to the cell culture media. Dox was continually added to the media throughout the first week of the screen to achieve full editing. Cells were split every second day according to the cell density for a period of 12 cell duplications to ensure robust and clean dropout of sgRNAs targeting essential genes. At the end of this screen (day 18) cells were harvested for deep sequencing and again large quantity of cells were frozen (TP-B) to ensure complete representation of the library (Figure 7).

To identify regulators of TNFα mediated killing in RKO cells, I made use of the frozen cells of this screen (Figure 7).

For the pre dropout screen (preDOS), 150 Mio Neomycin selected cells from TP-A were thawed and expanded. Cells were then cultured either (i) without TNFα or with TNFα in a concentration of (ii) 0.5ng/mL, (iii) 2.0 ng/mL or (iv) 6.0 ng/mL. Cells were passaged every second or third day according to their density and a minimum of 65 Mio cells were reseeded in medium containing fresh TNFα to maintain the full library presentation throughout the screen. In addition, at each passage a sample of 120 Mio cells was stored at -80 °C for potential sequencing of the library. Cells were cultured for 20 cell duplications, counted in the non TNFα treated condition.

For the post dropout screen (postDOS) 150 Mio cells from the endpoint of the genome wide CRISPR screen (TP-B) were thawed and expanded. Cells were cultured either (i) without TNFα or (ii) with 2.0 ng/mL TNFα. Equivalent to the preDOS experiment, the cultures were passaged every second or third day according to their density. Again, a minimum amount of 65 Mio cells were reseeded and a sampel containing 120 Mio cells was stored at -80 °C for sequencing. This screen was ended once the condition without TNFα reached 13 duplications.

2.2.4.3. Preparation of the library for next generation sequencing

Frozen samples were analyzed using deep sequencing. This allows to identify the abundance of each sgRNA in every sample.

From preDOS the following time points were chosen for sequencing:

- TP-0 (time point 0)
- Without TNFα
    - Day 4 (3.34 duplications)
    - Day 10 (8.29 duplications)
    - Day 23 (20.04 duplications) = End point
- With 2 ng/mL TNFα
    - Day 4 (2.91 duplications)
    - Day 10 (6.49 duplications)
    - Day 23 (14.70 duplications) = End point

From postDOS the following time points were chosen for sequencing:

- TP-0 (already sequenced in the Zuber-lab)
- Without TNFα
    - Day 16 (13.49 duplications)
- With 2 ng/mL TNFα
    - Day 16 (9.98 duplications)
- With 6 ng/mL TNFα
    - Day 16 (9.90 duplications)

For library preparation, cells were first lysed to isolate the genomic DNA. Therefore, 120 Mio cells were resuspended in 6.4 mL extraction buffer (Tris-HCl [10mM], NaCl [150mM], and EDTA [10mM]). The cell suspension was transferred to 2mL tubes (15 Mio cells/tube) and 8 µL proteinase K and 8 µL of 10 % w/v SDS were added to each tube. The cell suspension was incubated at 55 °C and 1200 rpm for 24h. Thereafter, additional 8 µL proteinase K was added and cells were lysed for additional 24h. In order to digest all RNA in the sample, 8 µL of RNAse-DNAse free was added and cells were incubated at 37 °C for two hours.
In order to isolate the genomic DNA, a Phenol extraction was performed. Therefore, cells were mixed in a 1:1 ration with equilibrated Phenol and centrifuged at RT at maximum speed for 8 min. The procedure was repeated until the aqueous phase, which contains the gDNA, was clear.

In a next step, DNA precipitation was conducted by adding 0.1x volumes of NaAc [3M], 1 µL PelletPaint and 0.8x volumes of isopropanol. After vortexing, the tubes were incubated over night at -20 °C and the gDNA was pelleted via centrifugation at maximum speed and 4 °C for 60min. The gDNA was washed twice with 70 % EtOH, air-dried and resuspended in elution buffer (EB). The quality of the gDNA was analyzed on a 1 % agarose gel and gDNA was fragmented by ten cycles of freezing and thawing for the subsequent PCR amplification.

Next, two consecutive PCR reactions were performed. The first PCR reaction was run to amplify the sgRNA cassette, whereas the second reaction was used to add a 4 bp long sample barcode, a 6 bp cluster barcode and the solexa sequencing primer. This was introduced via an extended reverse primer. Additionally, primers in the second PCR added either the P7 adaptor (forward primer) or the P5 adaptor (reverse primer) for flow cell binding. Both PCR cycles were performed using the AmpliTaq Gold kit.

In order to maintain a 500x representation, 410 µg of DNA were amplified, assuming that every cell contains 3 pg of DNA, due to diploidy of the RKOs. The 410 independent reactions were pooled and the amplified product (367bp) was loaded on a 2 % agarose gel. The PCR reaction was carried out using the following ingredients and programs respectively.

Table 13: PCR reaction of the first PCR for U6-sgRNA-tracer amplification

Reagent	Amount [µL]	x410 [µL]
Template [1 µg/µL]	1.00	410.00
PCR buffer gold (10x)	5.00	2050.00
$MgCl_2$ [25 mM]	4.00	1640.00
dNTP [25 mM each]	0.40	164.00
Rev ALT 1 primer [100 µM]	0.15	61.50
Fwd ALT 1 primer [100 µM]	0.15	61.50
Amplitaq Gold	0.20	82.00
ddH_2O	to 50.00	to 20500.00

Table 14: PCR program of the first PCR for U6-sgRNA-tracer amplification

PCR steps	Temperature [°C]	Time [s]
1. Initial Denaturation	95	600
2. Denaturation	95	30
3. Primer Annealing	52	45
4. Extension	72	30
Cycle replication	GOTO 2	27x
5. Final extension	72	420
Storage	4	∞

In the last step, the PCR product was purified via size exclusion by customized magnetic beads 2 mL of the PCR product from one time point were transferred to two 2 mL tube containing 0.5 mL beads (resulting in a 2:1 ratio of PCR product to beads solution) and incubated for 5 min. At this ratio only the gDNA is binding to the beads due to the polyethylene glycol and salt concentration. The DNA-bead mix was placed on a magnet and the supernatant was transferred to a new tube containing 0.5 mL beads, resulting in a 1:1 ratio (PCR product:beads solution). At this ratio the amplicon is binding to the beads. Then the amplicon bound beads were washed twice with 70 % EtOH, air-dried and eluted using EB. To verify the amplicon size the respective eluted PCR fragment (376 bp) was loaded on a 1.5 % agarose gel. Then, the second PCR with 16 reactions per time point was performed:

Table 15: PCR reaction of the second PCR for adding sample barcodes, cluster barcodes, solexa sequencing primer and P5/P7 adaptors to the U6-sgRNA-tracer sequence

Reagent	Amount [µL]
Template [6-7ng/µL]	1.50
10x PCR buffer gold	5.00
MgCl2 [25mM]	4.00
dNTP [25mM each]	0.40
Rev ALT 1 primer [100uM]	0.15
Fwd ALT 1 primer [100uM]	0.15
Amplitaq Gold	0.20
H_2O	to 50.00

Table 16: PCR program of the second PCR for adding sample barcodes, cluster barcodes, solexa sequencing primer and P5/P7 adaptors to the U6-sgRNA-tracer sequence

Reagent	Temperature [°C]	Time [s]
1. Initial Denaturation	95	600
2. Denaturation	95	30
3. Primer Annealing	57	45
4. Extension	72	30
Cycle replication	GOTO 2	8x
5. Final extension	72	420
Storage	4	∞

The PCR fragment (448 bp) was again loaded on a 3 % agarose gel after the second PCR and the amplicon was purified via magnetic beads in a 1:1 ratio. If the purity was deemed unsatisfactory, gel purification followed by another bead purification was performed before sequencing.

Sequencing of the amplified sgRNAs was performed at the next generation sequencing facility at the Vienna Biocentre using the Illumina HiSeq ® 2500 Sequencing System. For this, 14 pM of the amplicons together with 8 % phiX DNA were loaded on the flowcell. The latter was necessary to maintain diversity on the flow cell due to sequence similarity of the tracer region.

2.2.4.4. Analysis of the CRISPR screen result

The analysis of the sequenced sgRNAs was carried out via MAGeCK method (Wei Li et al. 2014). This method first performs a read count normalization by using the median ratio method. It is necessary to adjust the read count distribution and the sequencing depth so that technical differences between the samples can be normalized. This allows for more precise detection of biological differences. Afterwards, mean-variance modeling is used to calculate the variance and mean of each sgRNA and thus determine the difference between the treatment and control conditions. The Poisson model suggests that the variance is equal to the mean and is used in combination with the negative binominal model which adjusts these values. In a third step, two-sided p-values are calculated to identify a significant difference, either in the form of a positive or negative selection, between the two conditions. In a last step, sgRNAs are ranked based on a significance score that is calculated with the modified robust rank aggregation (α-RRA). Further processing of the data was performed using the TIBICO spotfire software.

The following thresholds were used to filter for significant hits, which either sensitize or convey resistance toward TNFα treatment:

Table 17: Thresholds for filtering for either sensitization or resistance modulators

Genes of postdocs			
		Sensitization	**Resistance**
2 ng/mL TNFα vs. no TNFα	L2FC	≤ -1.0	≥ 1.0
2 ng/mL TNFα vs. no TNFα	-Log10 p-value	≥ 2.0	≥ 2.0
2 ng/mL TNFα vs. no TNFα	guides	> 2	> 2
2 ng/mL TNFα vs. no TNFα	ggratio	≥ 0.5	≥ 0.5
Essential genes of preDOS			
		Sensitization	**Resistance**
2 ng/mL TNFα vs. no TNFα	L2FC	≤ -1.0	≥ 1.0
2 ng/mL TNFα vs. no TNFα	-Log10 p-value	≥ 2.0	≥ 2.0
2 ng/mL TNFα vs. no TNFα	Guides	> 2	> 2
2 ng/mL TNFα vs. no TNFα	ggratio	≥ 0.5	≥ 0.5
no TNFα vs. TP-0	L2FC	≤ -1.0	≤ -1.0
no TNFα vs. TP-0	-Log10 p-value	≥ 2.0	≥ 2.0
no TNFα vs. TP-0	Guides	> 2	> 2
no TNFα vs. TP-0	ggratio	≥ 0.5	≥ 0.5
Non-essential genes of preDOS (were extracted after filtering)			
		Sensitization	**Resistance**
2 ng/mL TNFα vs. no TNFα	L2FC	≤ -1.0	≥ 1.0
2 ng/mL TNFα vs. no TNFα	-Log10 p-value	≥ 2.0	≥ 2.0
2 ng/mL TNFα vs. no TNFα	Guides	> 2	> 2
2 ng/mL TNFα vs. no TNFα	ggratio	≥ 0.5	≥ 0.5

2.2.5. Validation of CRISPR screen results

The validations were conducted in the RKO c16 cells, which were infected in duplicates with a lenti-virus delivering single sgRNAs. The sgRNA cassette stably integrates into the genome of the target cells. The infection rate was measured via FACS and varied between 40-70 %. The validation experiment was initiated at with dox treatment to induce Cas9 expression and ensure editing of the cells. Two days after, the culture was split into two parts, one cultured with and one without 2 ng/mL TNFα, referred to as day 0. The validation experiment was performed in 1 mL medium and cells were split every second or third day, according to their density. At every split, cells were counted with the iQue intellicyte. The cells were stained with ZomieAqua (1:1000) prior to the FACS analysis, to determine the cumulative cell number (CCN) of viable cells.

2.2.6. Establishment of a human co-culture system to test tumor cell killing via CD8$^+$ T cells

The aim was to establish a human co-culture system that could model antigen specific tumor cell killing via CD8$^+$ T cells. As an epitope the cytomegalovirus (HCMV) pp65$_{495\text{-}503}$ nonapeptide, also known as NLV, was used This peptide is known to be HLA-A*0201 restricted.

*2.2.6.1. Transduction of RKOs with the three different HLA-A*0201 constructs*

The RKO c20 cell lines were lentivirally transduced with the three different HLA-A*0201 constructs. The infected cells were stained for viability and HLA-A2*0201 and analyzed by FACS. The cells were sorted based on their IRFP720$^+$ and HLA-A*0201-SB780$^+$ levels and the infection rate was monitored over three weeks to see if a stable expression was achieved.

2.2.6.2. Generation of HCMV specific CD8$^+$ T cells

In order to generate human HCMV-specific CD8$^+$ T cells, human CD8$^+$ T cells were retrovirally transduced with an HCMV-specific TCR construct (obtained from Tom Schumacher's Lab).
Therefore, retro-virus containing the HCMV-specific TCR construct had to be produced. To prepare the transfection medium 200 µL of RPMI medium without any supplements was incubated with 5 µL Fugene at RT for 5 min. Then, the HCMV-specific TCR construct and the pVSV-G were added in a 4:1 ratio and again incubated at RT for 15min. Afterwards, the transfection medium was carefully dropped onto Plate-GP cells cultured in the target medium hRPMI in a 6-well plate, which were grown to 70 % confluency. After 48 h the virus containing medium was harvested and centrifuged for 10 min at 500 g to remove remaining Plate-GP cells from the virus solution.
Next, the human CD8$^+$ T cells were prepared for transduction with the HCMV-specific TCR. Therefore, the T cells were thawed in hRPMI with 20 % HS and activated with medium prewashed human T-activator dynabeads in a 1:2 ratio (cells:beads) in PBS containing 5 % HS. After incubation on a tumbler at RT for 30 min, the unbound cells were removed through magnetic attraction. The bound cells were resuspended in fresh medium with IL-7 [5 ng/mL] and L-15 [5 ng/mL] and plated at a density of 1 Mio/mL.
Transduction was performed using Retronectin [10 µg/mL] coated non tissue culture treated 24-well plates. These plates were coated for at least 2 h at RT with Retronectin and afterwards,

the PBS-RN solution was taken off, washed with blocking buffer (PBS containing 2 % BSA) and afterwards with PBS, and coated with 0.5 mL virus. The coating was performed at 2000 rpm for 90 min at 24 °C. Afterwards, the virus was removed and the human $CD8^+$ T cells were cultured at a density of 0.5 Mio/mL per 24-well. A second transduction was performed on the next day. The infection rate was analyzed via FACS by staining the transduced TCR with mTCR-PE.

3.2.4.4. Human co-culture system to test tumor cell killing via $CD8^+$ T cells

In order to test tumor cell killing via cytotoxic $CD8^+$ T cells, the antigen-presenting HLA-A*0201$^+$ RKO c20 cells were seeded at a density of 0.2 Mio cells per 24-well. The empty HLA-A*0201$^+$ RKO c20 cells were pulsed with either 10 µg/mL, 5 µg/mL, 1 µg/mL or no NLV peptide. The pulsing occurred in hRPMI with IL-7 [5 ng/mL] and IL-15 [5 ng/mL] overnight in the seeded 24-well plate. On the next day, the cells were adherent, the medium was taken off and the cells were washed with PBS to remove the peptide. Afterwards, fresh hRPMI with fresh cytokines containing the HCMV-infected $hCD8^+$ T cells was added in a ratio of 1:1. Three days after the start of the co-culture the samples were analyzed via FACS with staining for CD8 and viability. Based on the fluorophore staining it was possible to distinguish between T cells and the tumor cells in the FACS analysis. The percentage of remaining tumor cells among the viable population was calculated to compare the effectivity of the different constructs.

3. Results

3.1. TNFα titration on cell lines

In order to identify genetic dependencies that render a human cancer cell line resistant or more sensitive to TNFα treatment, inducible Cas9 expressing cell lines established in the Zuber lab were used to perform a whole-genome CRISPR/Cas9 screen. To determine a suitable TNFα concentration for the screens that allows for simultaneous observation of cancer cell killing and continued expansion, the long-term effects of different concentrations were tested in cell culture.

Previous research has emphasized the high TNFα serum concentration found in colon and pancreas cancer patients as well as in mouse models (Yako et al. 2016; Maier et al. 2010; Karayiannakis et al. 2001; Wenya Li et al. 2017; Zhou and Yuan 2014; F. Balkwill 2006). They state that TNFα can be secreted by cells in the tumor microenvironment (e.g. macrophages) or by the tumor cells themselves (Zins et al. 2007). To see what exact effect TNFα has on the tumor cells, I chose one colon and one pancreas cell line. Based on the expression data received form Ordino, I know that all relevant members of the TNFα signaling, including the TNFR1 are expressed in this the colon carcinoma cell line RKO and in the pancreas carcinoma cell line MIA PaCa-2. Thus, one different tetracycline-inducible Cas9 cell clones was tested, namely MIA PaCA-2 BFP2 and RKO c20, respectively.

The results indicate that the MIA PaCa-2 BFP2 clone does not respond to a TNFα concentration of up to 1000 ng/mL (Figure 6B), while the growth of RKO c20 is affected by TNFα killing starting at a concentration of 1 ng/mL from day three onwards (Figure 6A). Further experiments with a narrowed concentration range of TNFα from 0.1 ng/mL to 10 ng/mL and including the paternal wt RKO cells and a second tetracycline-inducible Cas9 expressing RKO clone (c16) were consistent with the results above (Figure 6C). Based on these results, RKO c16 was chosen for the CRISPR screen for two reasons: Firstly, its growth dynamics upon TNFα treatment are more similar to the wt RKO cells then the c20. Secondly, if the CRISPR screen was conducted with MIA Paca-2, I would only gain information on how I can again sensitize these cells towards TNFα. On the other hand, a CRISPR screen with the RKO cell line enabled the obtainment of information on genes leading to increased sensitivity as well as resistance. The concentration of 1 ng/mL TNFα demonstrated both, a well detectable response to the treatment

and continued expansion of the culture. Finally, after adjusting for a higher cell number:culture volume ratio during the screen compared to the TNFα titration setup, I choose a concentration of 2 ng/mL for the screen.

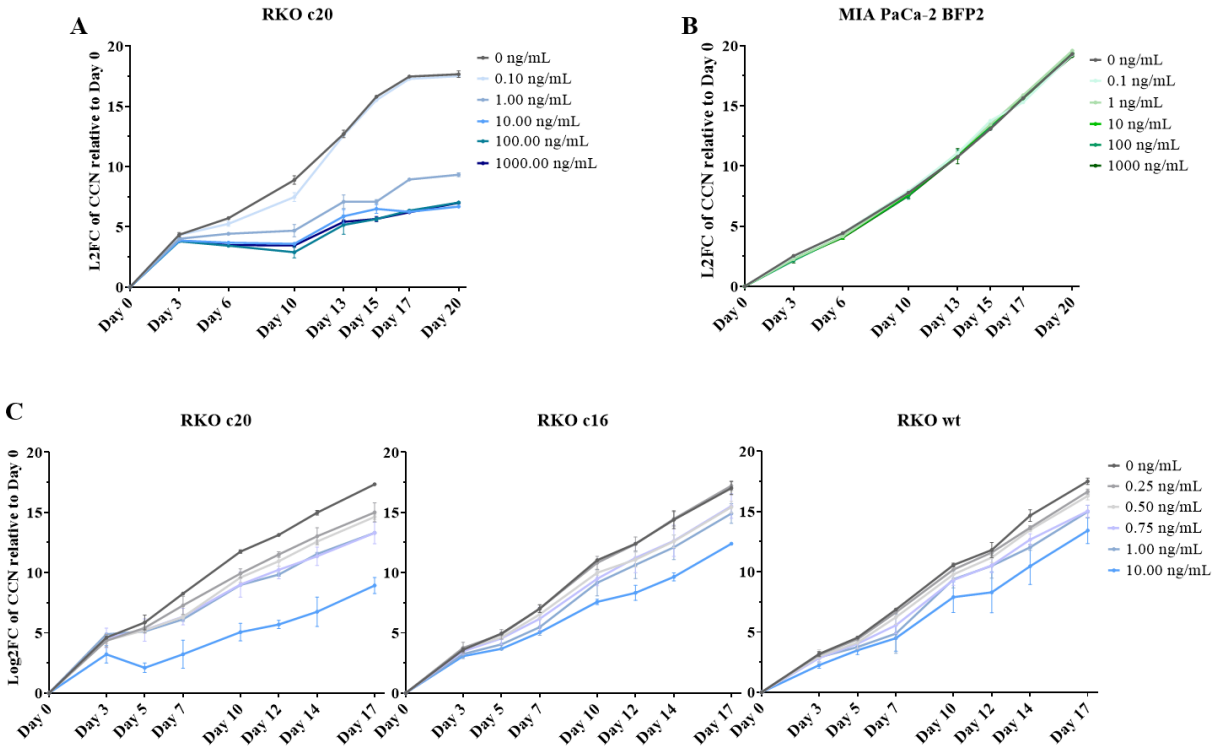

Figure 6: TNFα titration on Mia PaCa-2 and RKO cells
Growth curves of RKO c20 (A) and MIA PaCa-2 BFP2 clones (B) upon a broad range of TNFα concentrations. Y-axis shows the log2-fold change (L2FC) of the CCN which was calculated in relation to day 0 and the X-axis depicts the timeline of the experiment. While MIA PaCa-2 BFP2 did not respond to the treatment, RKO c20 growth reduction correlates with the increasing TNFα concentrations. (C) Growth curves of tetracycline-inducible Cas9 RKO clones c20 and c16 and parental wt RKO cells with a narrowed concentration range of up to 10 ng/mL.

3.2. Experimental setup of the CRISPR/Cas9 screen

For previous screening efforts in the Zuber lab, a genome-wide sgRNA library was already infected in the RKO c16 clone. The cells were cryo-preserved at two different time points: Time point-A (TP-A) is prior to Cas9 induction and thus gene editing. TP-B is a sample that was cryo-preserved after 18 days of culture, after which most sgRNAs targeting essential genes are depleted from the culture (Figure 7).

Of note, previous work in the Zuber lab has shown, that the freezing and thawing process of library-infected RKO cells has no influence on library composition (B.Moedl 2019; Zuberlab unpublished). Therefore, I was able to utilize cryo-preserved RKO c16 cells for my own study.

The TNFα signaling modulator screen was performed with two different starting populations, the preDOS and the postDOS. The preDOS enabled me to detect modulators that have an essential function. However, these essential genes could also be a noise Source and detection of no-essential modulators could become more difficult. Therefore, it was decided to additionally conduct a postDOS. If a gene is identified in both screens, its role in promoting sensitivity or resistance upon TNFα treatment can be assumed with higher confidence.

The preDOS as well as the postDOS were initiated by thawing the two different frozen RKO c16 library infected populations. For both screens an untreated population as well as a 2 ng/mL TNFα (referred to as medium) treated population were cultured. In the postDOS, two additional TNFα concentration were screened: One with a lower [0.5 ng/mL] and one with a higher TNFα concentration [6 ng/mL]. These were included to assess if the concentration difference is also reflected in the gene hit-list leading to a decreased or increased L2FC and p-value and may even lead to the loss or gain of new modulators.

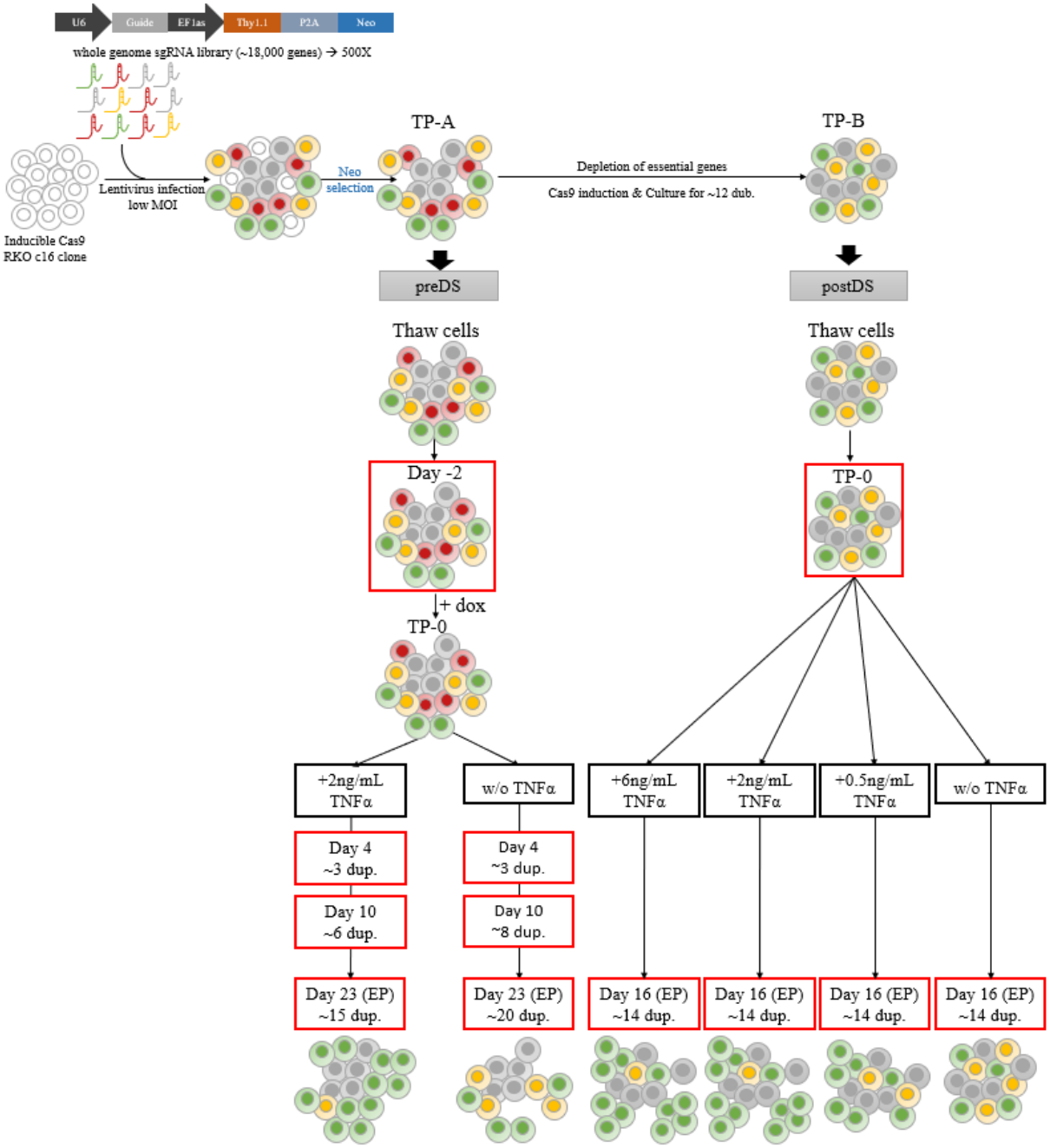

Figure 7: Experimental setup of the performed CRISPR/Cas9 screens
The inducible Cas9 RKO c16 clone was lentivirally transduced with the whole-genome library (U6-sgRNA-EF1as-Thy1.1-P2A-Neo) at 500x representation and at a low MOI. The library contains ~123,000 sgRNAs that target ~20500 genes with ~6 sgRNAs per gene and ~1000 control sgRNAs. Neomycin selection resulted in the depletion of the uninfected cells (white cells). At this time point (TP-A) cells were frozen to later be thawed for a preDOS. Since editing of the cells was not induced yet, this cell population still includes essential genes. To start editing via Cas9 induction, these cells were treated with dox for 18 days. After 12 population doublings cells that express sgRNAs targeting essential genes should have been depleted from the culture. These TP-B samples were cryo-preserved and used as starting point for the postDOS. The different TNFα concentrations screened are shown in black boxes and the red boxes highlight the time points where the sgRNA abundance was analyzed. The yellow cells represent the KO cells which become sensitized towards TNFα treatment, whereas the green cells represent

KO cells which become resistant towards TNFα and hence, enrich upon TNFα treatment. The grey cells are KOs that remain unaffected by TNFα treatment.

Monitoring the cell growth dynamics during the screen by counting the cell numbers at every split, the duplication rate of the different conditions can be depicted in growth curves (Figures 8A & 8B). Results of preDOS and postDOS indicate a similar growth rate inhibition upon treatment with 2 ng/mL TNFα. Even though growth was less effected upon 0.5 ng/mL TNFα treatment compared to the higher dosages, an effect through TNFα-mediated cell death was still detectable. The growth difference between the high and the medium TNFα dosage were similar.

A comparison of the sgRNA abundances between treated vs. non-treated populations at the end point of the screens shows that cells which express the non-targeting control sgRNAs, 1,000 in total (depicted in red), are equally present at both time points (Figure 8C and 8D). In contrast, all six sgRNAs targeting TNFR1 (depicted in yellow) are among the highest enriching sgRNAs, suggesting that TNFR1 KO cells become resistant to TNFα-mediated cell death. These two observations show that the preDOS and postDOS screens were conducted with sufficient coverage of the library and that the modulation of TNFα signaling can be detected using our screening setup.

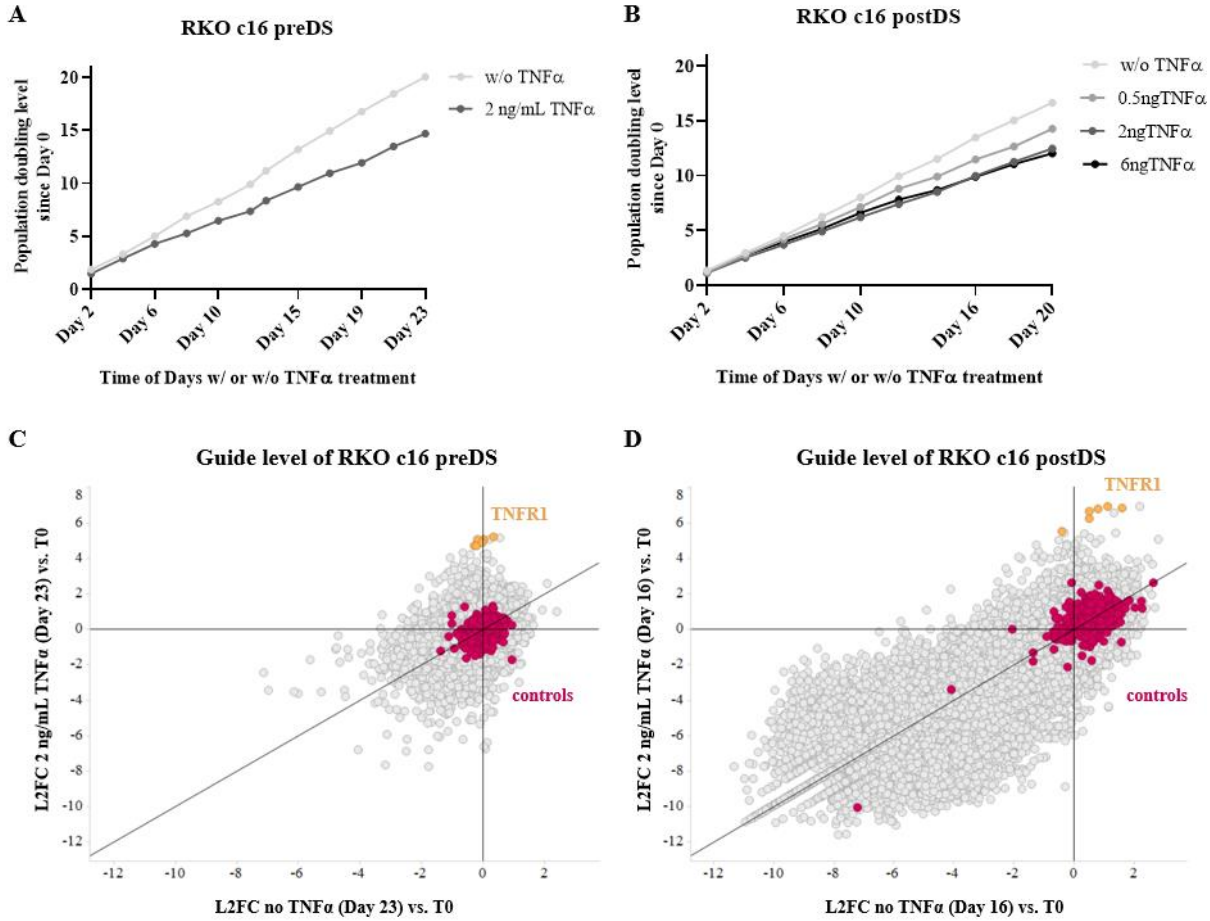

Figure 8: Guide-level based quality control of the performed preDOS and the postDOS screen
Top panel: Line charts depicting the growth curves relative to day 0 of preDOS (A) and postDOS (B), respectively. Bottom panel: Scatter plots depicting the L2FC of the sgRNA between treatment vs. TP-0 and no treatment vs. TP-0 for preDOS (C) and for postDOS (D). Each grey dot represents one sgRNA, the red colored dots represent the control guides and the yellow dots represent the six guides for the TNFR1. The lines depict the horizontal and vertical graph origin and the diagonal.

3.3. Genetic dependencies identified via postDOS

In order to identify genes that modify sensitivity or resistance upon TNFα treatment without any influence by essential genes, a postDOS was performed. Since these cells were already edited and cultured for 12 duplications, all cells containing a KO of an essential genes were depleted from the culture (Figure 7). The comparison of the growth difference between the different TNFα concentrations resulted in the observation that the medium and high dosages were the most informative due to the biggest growth decrease in comparison to the untreated control. Hence, only the sgRNA abundance of the medium and high dosages was analyzed. In comparison to the non-treated control, these two concentrations show a nearly perfect

correlation (Figure 9A). This suggests that the higher dosage might have reached saturation and thus does not lead to an increased effect. In line with this observation, hit identification of the medium and high TNFα screen using effect size and significance cut-offs (Table 21) resulted in highly overlapping gene sets of both, the resistant hits (Figure 9B) and the sensitizing hits (Figure 9C). However, when examining the 6 ng/mL TNFα treated culture around 70 new resistant as well as sensitizing genes can be explored and around 40 are lost.

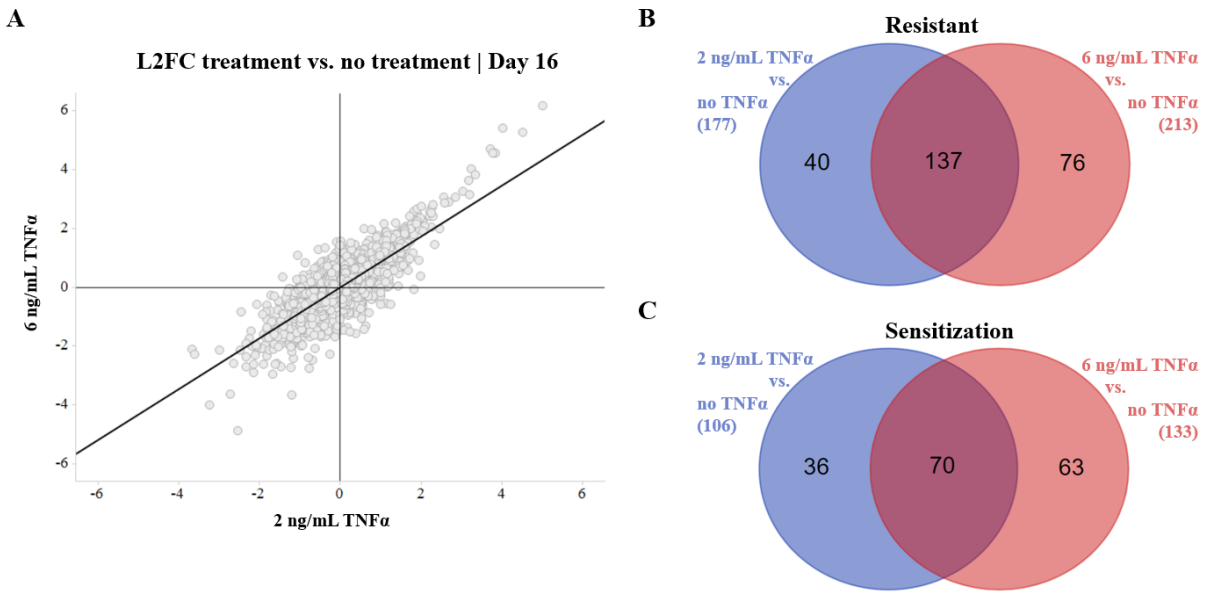

Figure 9: Comparison of 6 ng/mL and 2 ng/mL TNFα treatment
(A) A scatter plot comparing genetic dependcies (gene level) upon 2 ng/ml and 6 ng/ml TNFα treatment in relation to the non-treated control. Only genes which are represented by more than two guides relative to the control population are shown in that plot. (B,C) VENN digramms depicting the overlap of the TNFα treatment resistant hits (B) and the sensitizing hits (C) of the medium dose (2ng/ml; blue) and high dose (6 ng/ml; red) TNFα treated popultions relative to the non-treated popualtion. A gene was considered a hit when it was represented by more than 2 guides. The ratio between good guides and guides (ggratio) was higher or equal to 0.5, its -Log10 p-value was greater or equal to 2.0 and its L2FC was higher or equal to 1.0 for resitant hits and lower or equal to -1.0 for sensitizing hits.

To understand the dependencies of the different signaling modules of the TNFα pathway (Figure 4) in our screen setup, I performed a targeted analysis of selected genes with essential functions in the different branches of TNFα signaling. To this end, I chose the 6 ng/ml TNFα dataset as it displayed superior statistical significance compared to the 2 ng/ml dataset (data not shown). As expected, similar to the guide-level analysis (Figure 8), TNFR1 deficiency is also the top resistant mechanism on the gene level (Figure 10). The results further indicate that neither necroptosis (RIPK3, CYLD and MLKL) nor the intrinsic apoptosis pathway (BCL2L11,

BBC3, BID, BAK1, BAX) play a role in TNFα-mediated cell death or survival of RKO cells as KOs of essential signaling modules do not result in an altered enrichment or depletion in the screen (Figure 10A). However, members of the extrinsic apoptosis pathway, like TRADD, FADD and Caspase 8 demonstrated increased resistance upon gene KO. Surprisingly, and in contrast to common knowledge, loss of members of the NFκB pathway are resulted in enrichment of the KOs. This is in contrast to common knowledge since the NFκB pathway leads to cell survival via transcription factor (TF) activation (Sun and Liu 2011; T. Liu et al. 2017). These include RELA, RIP1, all three members of the IKK complex, the two main LUBAC components HOIP and HOIL-1 as well as TAB1/2 (Figure 10B). Among the top genetic dependencies that sensitize RKO cells to TNFα treatment are NFκB1/2 as well as components of the SCF ubiquitin ligase complex (SKP1/2, RNF7, FBWX2/7, CKS1B), which are important for the activation of NFκB1/2 in the non-canonical pathway. This might suggest that the non-canonical pathway might have different functions compared to the canonical pathway upon TNFα treatment, at least in that specific colon carcinoma cell line clone (Figure 10B).

By conducting the unbiased STRING pathway analysis (Supplemental Table 3-6), several genes that encode histone modifying enzymes are among the genetic dependencies that were identified in the screen (Figure 10C). In particular, several components of the Spt-Ada-Gcn5 acetyltransferase (SAGA) complex exhibit differential dependencies, more specifically of the core structural module of SAGA, the histone acetyltransferase (HAT) module and the deubiquitylation (DUB) module. These include TAF5L and SUPT20H from the core module, KAT2A, TADA3 and TADA2B from the HAT module and USP22 and ATXN7L3 from the DUB module. The specific KO of these genes results in increased resistance to TNFα mediated killing. Beside the HAT module of the SAGA complex three additional HATs are among the significant hits: MRGBP, EPC2 and MEAF6. The KO of each of them leads to sensitization to TNFα mediated killing. In addition, the KO of specific histone deacetylases (HDAC) and their complex components show an overall growth advantage. These include CSNK2A1, ELMSAN1, SIRT6, HDAC1/2 and TET2. However, the KO of two components of the NuRD complex, namely GATAD2A and MTA1, led to an overall growth disadvantage. The NuRD complex is another HDAC complex formed together with HDAC1/2.

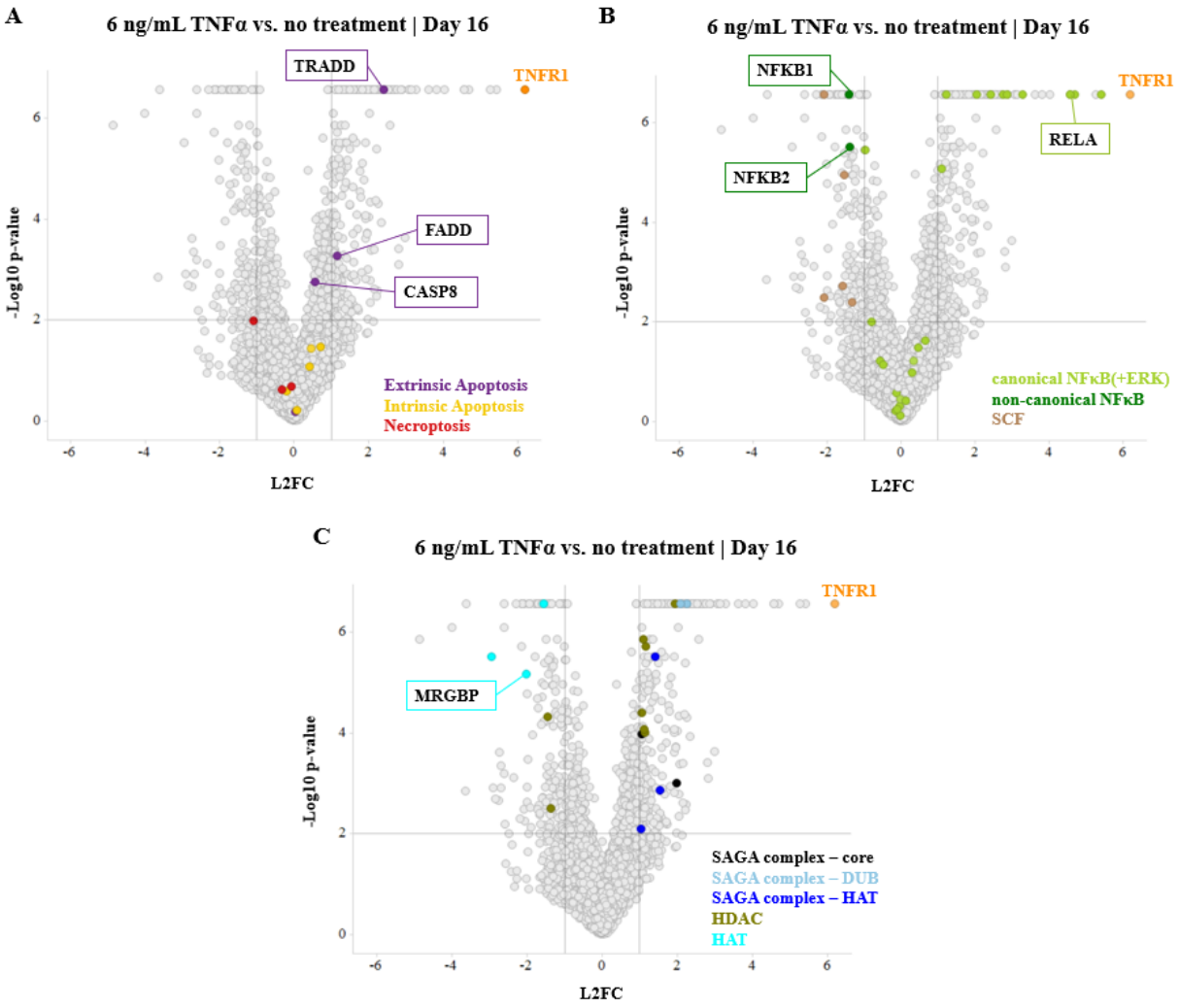

Figure 10: Resistant and sensitizing hits of the postDOS
The volcano plots in this Figure are all the same with different highlighted genes. They depict the comparison of the culture with the high TNFα dosage to the non-treated control according to their L2FC on the x-axis and their -Log10 p-value on the y-axis. It was filtered for genes being represented by more than two guides relative to the control population. The two vertical lines illustrate the L2FC threshold for either a significant resistant or sensitizing hit, whereas the horizontal line illustrates the -Log10 p-value threshold. TNFR1 is highlighted as the top resistant hit in all of them. (A) In the first plot genes belonging to different TNFα killing pathways are highlighted: the extrinsic apoptosis pathway (depicted in purple), to the intrinsic apoptosis pathway (depicted in yellow) and to necroptosis (depicted in red). (B) All genes with a relation to the NFκB pathway are highlighted: the canonical pathway (depicted in light green), the non-canonical pathway (depicted in dark green) and the SCF ubiquitin ligase complex as part of the non-canonical pathway (depicted in brown). (C) This plot shows hits interfering in histone modifications, like the different modules of the SAGA complex (depicted in either black, light-blue or dark blue) and different HDACs (depicted in ocher green) as well as different HATs (depicted in turquoise).

3.4. Genetic dependencies identified via preDOS

3.4.1. Genetic dependencies of essential genes

Many gene products fulfill essential functions to ensure the fitness of a cell (Morgens et al. 2016). Consequently, a cell that harbors a KO of an essential gene will deplete over time in a competitive culture of various KO clones like in a pooled screen. Therefore, to probe the function of such an essential gene towards its role in TNFα mediated fitness, a preDOS screen was performed in which the editing was induced 2 days prior to TNFα treatment. The sgRNA composition of the cell pool, which was cultured either with or without TNFα for 23 days, was sequenced and analyzed (Figure 7). Hits were determined using identical thresholds to the postDOS. Additionally, to focus the analysis on essential genes, threshold filters for a significant depletion in the non-TNFα treated population were used. The analysis of day 23 revealed several essential genes which demonstrated significant TNFα dependencies. However, these might not only indicate a TNFα dependent growth decrease or increase, since a cell population cultured over 23 days becomes susceptible to proliferation disadvantages or advantages. Thus, sequencing of earlier time points with only few rounds of proliferation should allow for the detection of strong effects of TNFα-mediated cell death and less strong effects on reduction of cell proliferation. Another advantage of the earlier time points is that KOs that rapidly deplete from the culture could also be captured. Thus, to avoid capturing proliferation hits and to focus on chances of essential genes, earlier time points, day 4 and day 10, were sequenced. Using identical thresholds as for the late time points, no dependencies that affect TNFα mediated cell death were identified for day 4. By lowering the L2FC threshold value to -0.5 and 0.5, respectively, nine genes whose KO lead to enrichment and five whose KO lead to depletion upon TNFα treatment were found (Figure 12A). Consequently, three population doublings were insufficient to observe a significant guide level difference between the treated sample and the non-treated control. In contrast, eight duplications, achieved at day 10, were sufficient to uncover sensitizing and resistance hits (Figure 12A). An overlap analysis of the identified genetic dependencies shows that most gene KOs result in resistance and only few in sensitization towards TNF-mediated killing (Figure 12B and 11C). The two overlapping sensitization hits are the proliferation and apoptosis adaptor protein 15 (PEA15) and cyclin dependent kinase 6 (CDK6). PEA15 is known as a negative regulator of apoptosis, whereas the

kinase activity of CDK6 is important for the G1 progression and G1/S transition. The two overlapping resistant hits are B-Raf Proto-Oncogene and Integrator Complex Subunit 6 (INTS6). BRAF is a serine-/threonine protein kinase belonging to the RAF family, while INTS6 is a DEAD box protein belonging to the integrator complex.

Next, to functionally group the identified genetic dependencies that cause TNFα mediated cell death or survival, an unbiased protein-protein interaction network and functional enrichment analysis was performed (Supplemental Table 7-10). Therefore, all essential genes which showed a TNFα dependency at all three time points were utilized. This showed that the loss of several proteins important for ubiquitin mediated proteolysis sensitizes towards TNFα-mediated killing. These include members of the cullin-RING ubiquitin ligase complex, namely TCEB1/2, RFWD2 and DET1. Functional groups of genes that make RKO cells more resistant towards TNFα-mediated killing upon KO are related to the mediator complex, to the transcription elongation complex or to the ribosomal translation initiation complex. These include for example the six mediator complex subunits MED12/13/16/19/27/30 or ELP2/3/4/5/6 and IKBKAP which are important for transcriptional elongation.

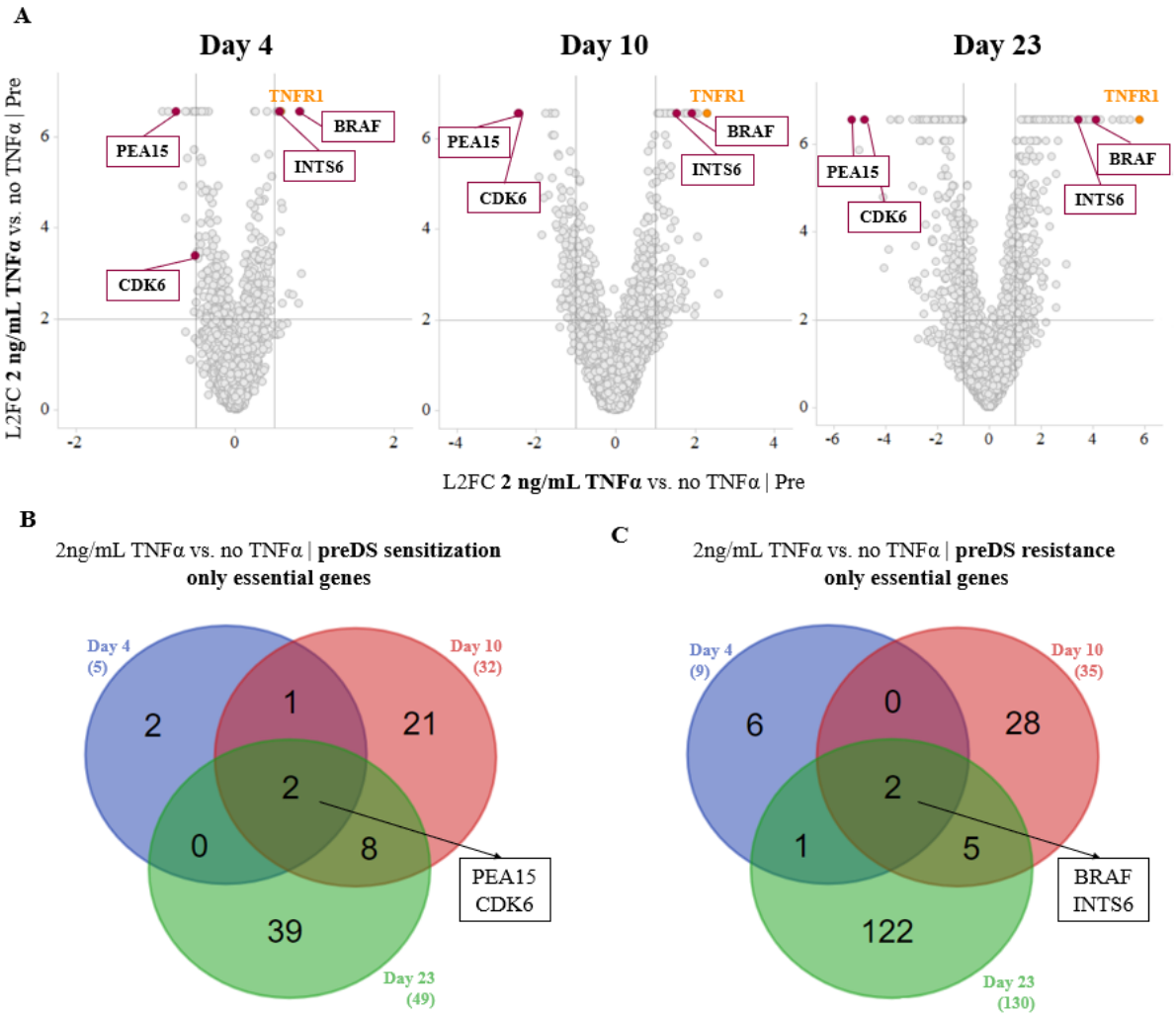

Figure 11: Genetic dependencies of essential genes upon TNFα treatment of cultured cells from preDOS
(A) The volcano plots depict the comparison of the culture with the medium TNFα dosage of the preDOS to the non-treated control according to their L2FC on the x-axis and their -Log10 p-value on the y-axis. It was filtered for genes being represented by more than two guides. The two vertical lines illustrate the L2FC threshold for either a significant resistant or sensitizing hit, whereas the horizontal line illustrates the -Log10 p-value threshold. TNFR1 is highlighted as the top resistant hit in all of them. (B,C) VENN diagrams showing the overlap of genetic dependencies of essential genes mediating sensitization (B) or resistance (C) towards TNFα mediated dropout. The genes from the triple-overlap section are indicated. These four genes are highlighted in purple in panels A and B. The following thresholds were used for hit calling: -Log10 p-value ≥2.0; >two guides per gene; ggratio ≥0.5; L2FC ≥1 for enrichment and ≤-1 for depletion. For day 4 the L2FC threshold was adjusted to 0.5 or -0.5 respectively.

3.4.2. Overlap analysis of the non-essential preDOS

To gain confidence in the hits, the identified genetic dependencies towards TNFα mediated cell death/survival of the preDOS and postDOS were cross compared (Figure 12A and 12B). Genes with essential functions were excluded from the preDOS dataset, because cells expressing sgRNAs against these genes are largely depleted from the postDOS culture. For both, the

sensitization and resistance hits, the groups with by far the largest numbers of co-occurring hits are the late time point samples. However, few genetic dependencies were found at every sampled time point of the screen to affect TNFα mediated cell death.

A STRING analysis of the filtered non-essential preDOS hits (Supplemental Table 11-14) corroborated the role of the histone acetylation (Figure 12C). In addition to the components of the SAGA complex found in the postDOS, several additional members were identified: The core module members TAF6L, TAF12, TADA1 and SUPT20H, the HAT module members TADA3 and CCDC101 and USP22 and ATXN7L3, which belong to the DUB module. Interestingly, loss of TAF13, TAF4 and TAF5, which are members of the TFII complex that interacts with the SAGA interacting complex mediates resistance towards TNFα induced cell death. Similar to the postDOS screen, several HDACs and HATs were identified. Of these, loss of MRGBP resulted in the strongest sensitization towards TNFα mediated killing (Figure 12C).

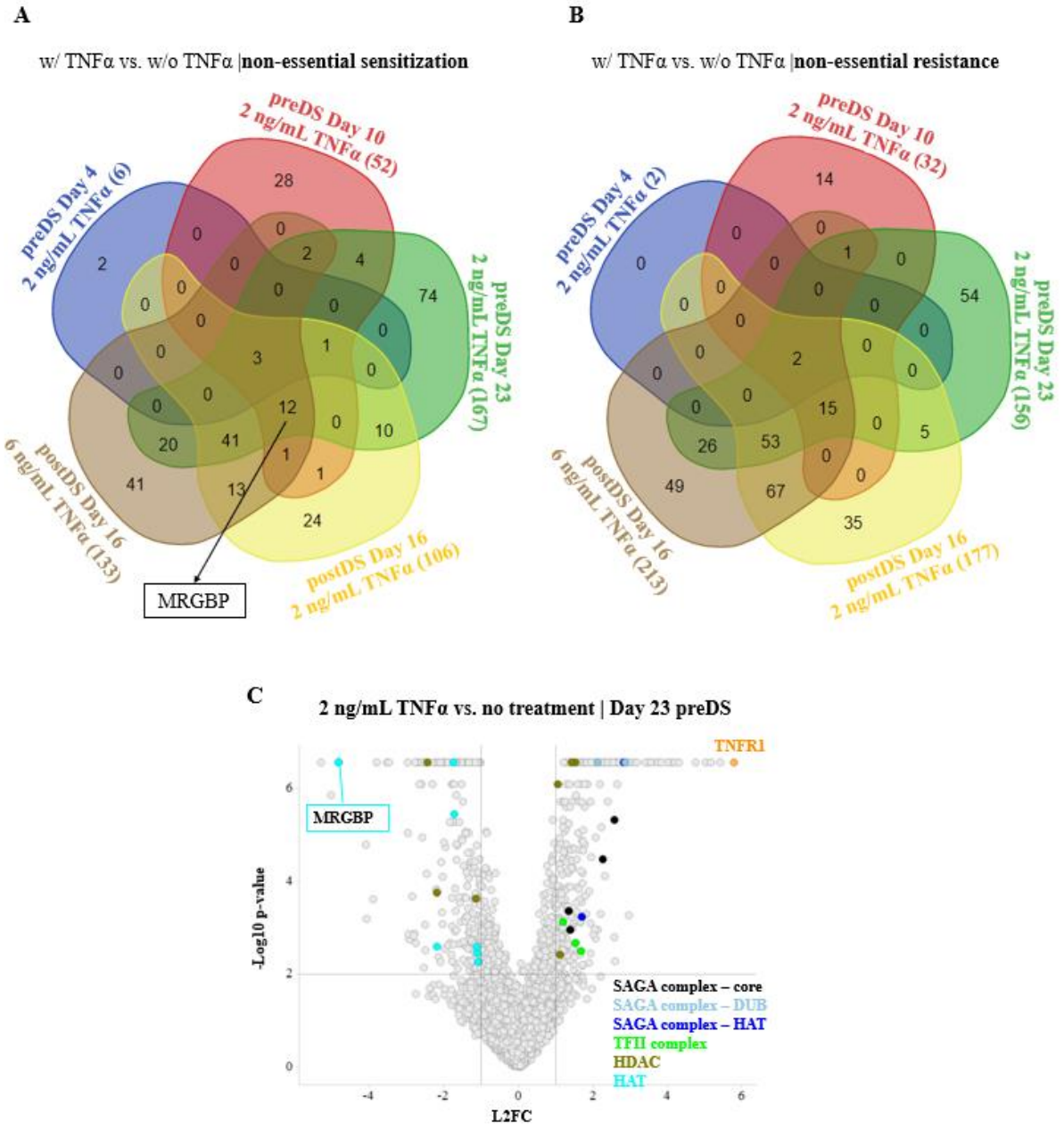

Figure 12: Non-essential sensitizing and resistance hits of preDOS compared to postDOS
(A, B) The VENN diagrams show any overlap between the different sequenced time points of the two different screens for sensitizing hits (C) and for resistant hits (D). For both only non-essential genes which meet the following rules are considered. They need to have a -Log10 p-value greater or equal to 2.0, be represented by more than two guides relative to the control population, have a ggratio greater than or equal to 0.5 and have an L2FC of -1 for sensitization or 1 for resistance. For the sgRNS sequenced on day 4 the L2FC needs to be -0.5 and 0.5, respectively. (C, D) The volcano plots depict all genes which are represented by more than two guides relative to the control population. Highlighting significant genes that belong to any module of the SAGA complex or are a SAGA-unrelated HDAC or HAT (C).

3.5. Single sgRNA validations of sensitizing hits obtained from preDOS and postDOS

To validate the screen results, a single sgRNA competition assay was conducted. I focused on 14 genes whose KOs led to a significant depletion upon TNFα treatment in the preDOS (day 23) and also scored in either the earlier time points of the preDOS, the postDOS or both (Figure 13A and 13B). A sgRNAs expression cassette coupled to a fluorescent reporter was transduced into RKO c16 cells. Two days after the induction of Cas9 expression by Dox, TNFα treatment was started and the proportion of sgRNA expressing to non-infected cells was monitored by FACS over time. As expected, this ratio remained stable over time in cultures expressing AAVS1 control sgRNAs and was not affected by TNFα treatment (Figure 13C). In contrast to this, deletion of the factors that were identified in the TNFα modulator screens resulted in a TNFα dependent growth inhibition of the sgRNA expressing cells. The majority of KO cells exhibited a sensitization towards TNFα comparable to PEA15(1), a positive regulator of TNFα mediated cell death (Greig and Nixon 2014; Exler et al. 2016) (Figure 13D). Upon KO, DUSP5, GTF2I and PBRM1 do not show a clear difference towards TNFα treatment. Interestingly, the KO cells containing one of the two different sgRNAs for MRGBP or PEA15 resulted in differently strong depletion effects. The strongest effect is exhibited by KO cells of either MARGB(2) (Figure 13E) or PIH1D1 with a respective 7 or 5-times enhanced depletion upon TNFα in comparison to the neutral control. CAB39 shows a similar TNFα-dependent growth inhibition of the KO cells compared to the positive regulator PEA15 (Figure 13F). Taken together, this shows that I successfully identified and validated known and novel inhibitors of TNFα-mediated cell death.

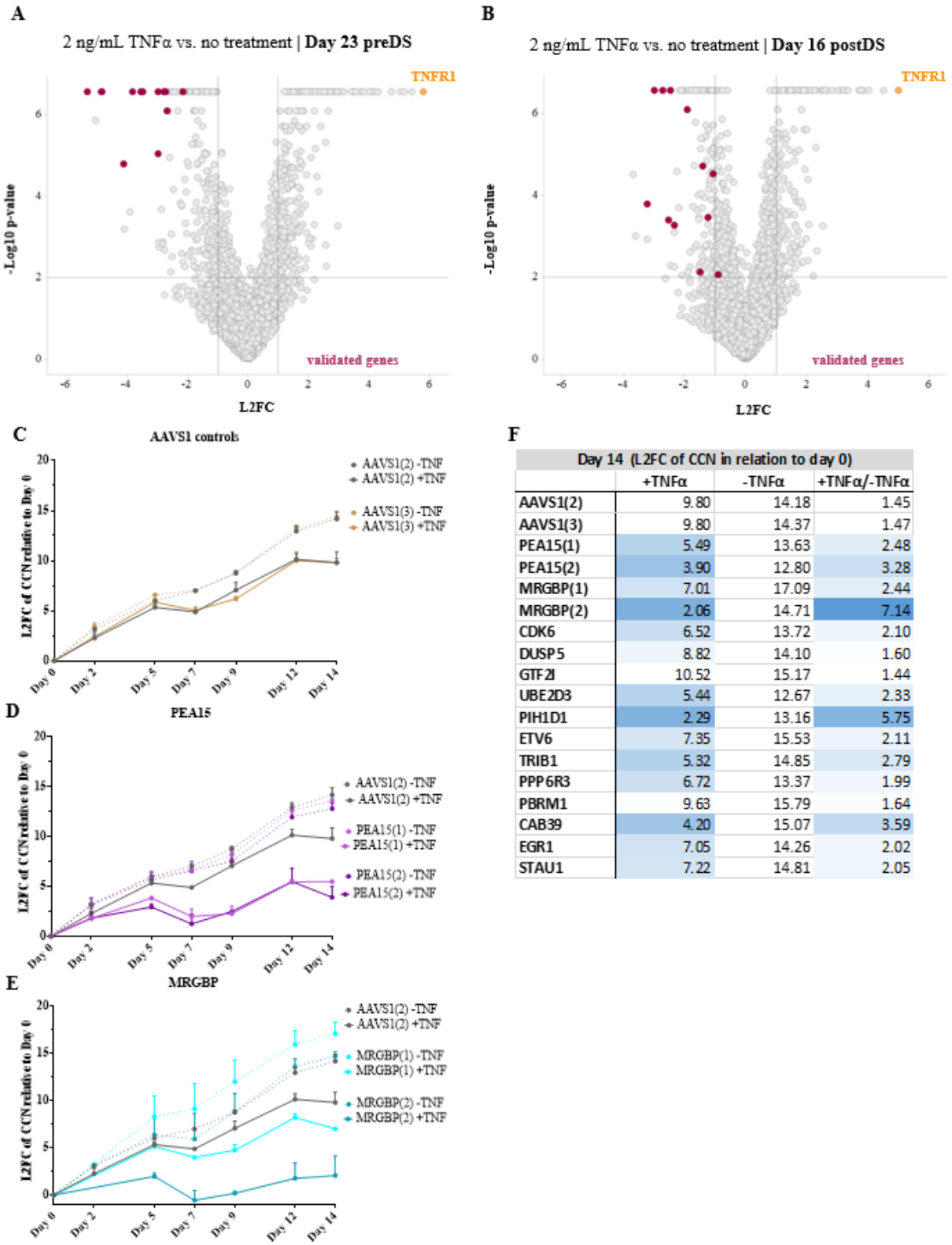

F

Day 14 (L2FC of CCN in relation to day 0)			
	+TNFα	-TNFα	+TNFα/-TNFα
AAVS1(2)	9.80	14.18	1.45
AAVS1(3)	9.80	14.37	1.47
PEA15(1)	5.49	13.63	2.48
PEA15(2)	3.90	12.80	3.28
MRGBP(1)	7.01	17.09	2.44
MRGBP(2)	2.06	14.71	7.14
CDK6	6.52	13.72	2.10
DUSP5	8.82	14.10	1.60
GTF2I	10.52	15.17	1.44
UBE2D3	5.44	12.67	2.33
PIH1D1	2.29	13.16	5.75
ETV6	7.35	15.53	2.11
TRIB1	5.32	14.85	2.79
PPP6R3	6.72	13.37	1.99
PBRM1	9.63	15.79	1.64
CAB39	4.20	15.07	3.59
EGR1	7.05	14.26	2.02
STAU1	7.22	14.81	2.05

Figure 13: Single sgRNA validation of sensitizing hits from preDOS and postDOS
(A, B) The upper volcano plots depict the results of the endpoint from either the preDOS (A) or the postDOS (B) with the L2FC on the x-axis and the -Log10 p-value on the y-axis. Only genes represented by more than two guides

relative to the control population are illustrated. Genes chosen for single sgRNA validation are higlighted in purple. (C) The graph depicts the L2FC of the cumulative cell number related to day 0 of the two control sgRNAs, AAVS1_2 and AAVS1_3. They were both cultured with and without TNFα supplement. (D) The graph shows the results of the single sgRNA validation of five sensitizing hits: PEA15, MRGBP, CDK6, CAB39 and ETV6. Two different sgRNAs were used for PEA15 and MRGBP, respectively. First, the CCN ratio between the treated and untreated culture in relation to day 0 was calculated. In the following, the L2FC of this CCN was normalized to the AAVS1 control.

3.6. Establishment of a human co-culture system to test tumor cell killing via $CD8^+$ T cells

To test whether the TNFα-modulator sensitizes the RKOs towards $CD8^+$ T cell released TNFα, a human co-culture system was established. For this purpose, the HCMV peptide NLV, which is represented by the HLA-A*0201 was chosen. Due to the fact that the RKOs contain a different HLA-type, three different HLA-A*0201 containing constructs were generated. By design, two are engineered to endogenously express the peptide. They contain either the full-length protein pp65 or the NLV peptide linked to an ER signal peptide ensuring proper loading in the ER. The third one solely contains the HLA-A*0201-IRES-IRFP720 sequence, henceforth referred to as empty. This needed to be pulsed with the NLV peptide before usage.
The lenti-virus infection of RKO c20 with the three different HLA-A*0201 containing constructs reached ~80 % infection rate. To compare the HLA-A*0201 infection level per cell, the expression of the construct was monitored through the IRFP720 reporter (Figure 14A). The $IRFP720^+$ cells were FACS sorted and the expression was monitored over time. No silencing of the cassette is detectable over the cultivation period of three weeks. The full-length pp65 containing construct showed the lowest expression levels, which a slightly decrease over time. The low infection rate might be caused by the size of the construct.
For the human co-culture experiment, the HLA-$A*0201^+$ RKOs were mixed in a ratio of 1:1 with human $CD8^+$ T cells. These were either infected with a HCMV-specific TCR or stayed uninfected. The obtained infection rate was 10.6 % of viable cells (data not shown). After 72 h the culture was analyzed by flow cytometry and viable T cells and RKO cells were counted.
An antigen specific killing for the empty and the full-length construct were clearly detectable. However, overexpression of the presenter construct did not result in a T cell dependent killing. Control co-cultures of non-infected $CD8^+$ T cells and target RKO cells showed a slightly decrease in RKO cell number (Figure 14B). This slight decrease might be either due to technical error or donor derived CMV specific $CD8^+$ T cells. Nearly all RKO cells with the empty

construct were killed by $CD8^+$ T cells. Furthermore, the target cell killing correlates with the used NLV concentration. In comparison to the co-culture with non-infected $CD8^+$ T cells, the non-pulsed HLA-A*0201^+ RKOs co-cultured with the infected T cells resulted in a minor decrease (~10 %) in the percentage of RKOs, as depicted in Figure 14B. This might be due to unspecific killing. Altogether, the human co-culture of HLA-A*0201 overexpressing RKO cells and CMV specific $CD8^+$ T cells demonstrated a mostly antigen specific killing efficiency.

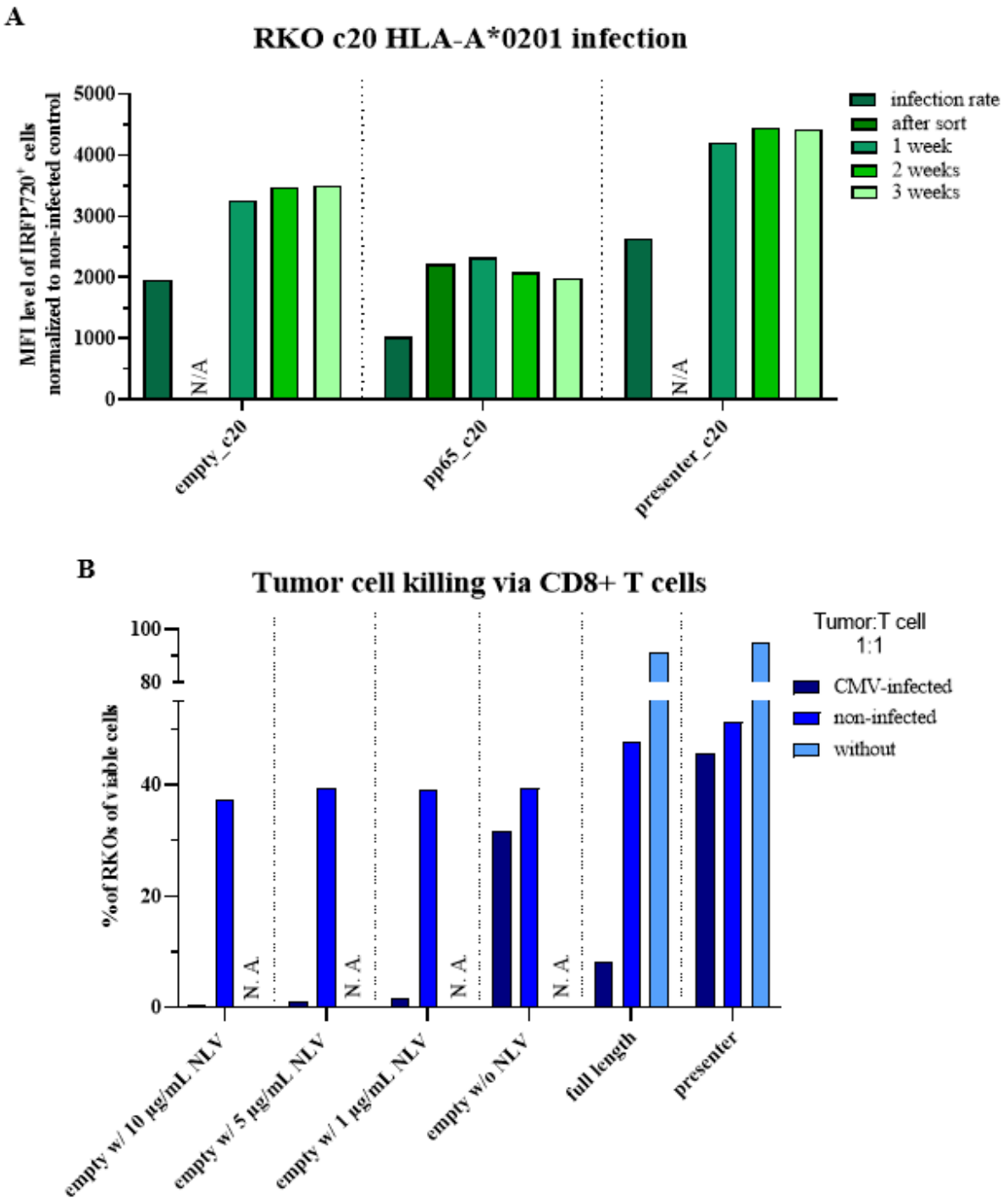

Figure 14: The establishment of a human co-culture system to test the antigen-specific killing efficiency of tumor cells via CD8+ T cells

(A) The MFI levels of HLA-A*0201-IRPF720 containing RKOs normalized to uninfected cells for each of the three constructs is depicted over time. (B) The percentage of viable RKOs after 72 h of co-culture with $CD8^+$ T cells, either HCMV-infected or not-infected, in a 1:1 ratio is depicted.

4. Discussion

The main aim of this thesis was to identify new opportunities for cancer treatment by inducing TNFα-mediated cell death, which together with the IFNγ signaling and antigen presentation is one of the major pathways used for efficient cytotoxic killing of tumor cells (Kearney et al. 2018). However, other studies suggested that TNFα is also involved in tumor promotion and progression. This was demonstrated by the fact that genetically engineered mouse models with a TNFα or TNFR1 KO did not develop cancer (F. Balkwill 2006, 2009). This indicates that TNFα does not only play an important part in immune-mediated cytotoxicity against tumor cells but also in tumor promotion (F. Balkwill 2006, 2009; Waters, Pober, and Bradley 2013). Such pro- and anti-tumorigenic effects of TNFα can result from complex downstream signaling pathways. A complete understanding of the genetic dependencies upon TNFα-mediated signaling pathways in cancer has so far been lacking and has thus created a necessity for further research on the topic. The CRISPR/Cas genome-editing technology together with next generation sequencing technology has enabled me to study such genetic dependencies on a genome-wide level. In this thesis gene-edited colon carcinoma cells were screened for their fitness in presence or absence of TNFα. The results demonstrated that the TNFα signaling pathway might be an interesting target for immune modulatory drugs.

4.1. The experimental CRISPR/Cas9 screen set-up

4.1.1. The effect of different TNFα concentrations on different cell lines

In order to conduct a whole-genome CRISPR/Cas9 screen a suitable TNFα concentration had to be determined at which cell growth is partially inhibited but also allows a high coverage library representation (500x). Since insights into both sensitization and resistant genetic dependencies were of interest, a cell line was sought that has not yet achieved resistance towards TNFα-mediated killing.

Previous research has emphasized a high TNFα serum concentration in colon and pancreas cancer patients as well as in mouse models (Yako et al. 2016; Maier et al. 2010; Karayiannakis et al. 2001; Wenya Li et al. 2017; Zhou and Yuan 2014; F. Balkwill 2006). To state the effect of this TNFα serum concentration, I decided to test the response towards TNFα of one colon carcinoma cell line (RKO) and one pancreas carcinoma cell lines (MIA PaCa-2). Besides

lacking knowledge on their TNFα response, these cell lines were chosen because they were shown to be highly applicable for loss-of-functions CRISPR/Cas9 screens (Zuber lab, unpublished).

While the MIA-PaCa2 BFP2 clone did not show any response upon TNFα treatment, wt RKO cells as well as the clonal cell lines c16 and c20 were susceptible to TNFα treatment. This finding is contradictory to the TNFα-mediated cell survival of other colon cancer cell lines (Zins et al. 2007) and might be explained by cell line specific characteristics. The decision to screen the RKO c16 clone was made due to its similar response to the wt population to ensure that the results did not occur due to clonal differences.

The RKO cells (wt, c16, c20), treated with 10 ng/mL TNFα, revealed a 1.5-2-fold decrease in cell number. In relation to literature, Ha-Ca-T cells also demonstrated a 2-fold decrease upon addition of 10 ng/mL TNFα (Udommethaporn et al. 2016). The concentration used for the CRISPR screen should not affect the overall growth rate to such a degree to maintain the library presentation. An optimal growth reduction of clone c16 was observed at 1 ng/mL TNFα. After correcting for an altered cytokine availability in the large-scale screen culture, I decided to perform the screen with 2 ng/mL TNFα. Additionally, to probe genetic dependencies to low and high dosages of TNFα, the postDOS screen was also conducted with 0.5 ng/ml and 6 ng/ml. The lower concentration resulted in a more diminished tumor growth decrease compared to the two higher concentrations and would consequently lead to less hits. That was the reason why I focused on the two higher concentrations. The medium and the high concentration showed a similar growth inhibition during the screen. In line with this, the observed genetic dependencies under both conditions correlate well. Most of the novel hits received with the higher concentration (~40 %) showed also a respective depleting or enrichment effect with the medium concentration but did not reach the thresholds set for significant hit identification. Thus, the 2 ng/mL TNFα concentration identified the most significant genetic dependencies and is the right choice for conducting a CRISPR screen.

4.1.2. Identification of essential genes influenced by TNFα treatment

The postDOS screen, in which gene editing was induced just prior to TNFα treatment, allowed me to also probe genes essential for the fitness of RKOs for their role in modulating the TNFα response. Essential genes, which upon loss increased the resistance towards TNFα-mediated killing, encoded regulators that are mostly associated with transcription or translation. This

includes members of the mediator complex, which acts as a transcriptional coactivator and interacts with TFs and RNA polymerase II, as well as factors of the ribosomal translation initiation complex. This could be explained by the NFκB dependent expression of pro-apoptotic genes, which also requires the mediator complex for initiation of transcription, while the produced mRNAs need to be translated by ribosomes.

Loss of several essential factors associated with polyubiquitination sensitized RKOs towards TNFα-mediated killing. In the case of TNFα signaling, a key step involving polyubiquitination is the degradation of NFκB inhibitors, resulting in the release of NFκB family members. These can further activate transcription of anti-apoptotic genes. Thus, the KO of important genes for polyubiquitination led to apoptosis due to the absence of anti-apoptotic genes.

4.1.3. Overlap of non-essential hits scoring in the preDOS as well as in the postDOS

A comparison of the non-essential hits of both screens revealed a high overlap of sensitizing as well as resistance causing hits, which resulted in increased confidence of these hits. However, both screens also identified context specific dependencies. A reason therefore could be that the end points of the preDOS and the postDOS differe in the duration of the screen. This would be compatible with the assumption that a prolonged duration would be advantageous to encounter indirect effects on the TNFα signaling pathway. Thus, earlier time points would only encounter direct effects. The high overlap of key identified genes between the earlier time points and the end time points suggest that most of the TNFα modulators have a direct effect and do not deplete or enrich due to proliferative advantages or disadvantages.

4.2. The TNFα-signaling pathways

TNFα signaling results either in cell death or survival, depending on the activated pathway. Cell death is mostly induced by either apoptosis or necroptosis, whereas cell survival is achieved through transcriptional activation of anti-apoptotic genes. To identify which pathways are responsible for TNFα-mediated cell death of the RKOs, a targeted analysis of the different pathway components was conducted.

The focus on central mediator of necroptosis revealed that the loss of neither RIP3, MLKL nor CYLD was significantly affected in their mode of action by TNFα resulting in the theory that necroptosis is not the major cell death mechanism induced by TNFα in RKOs. However, redundancy of factors of the necroptosis pathway cannot be excluded. Additionally,

transcriptome analysis from RKO c16 clone suggested that RIP3 is not expressed (data not shown) supporting the theory that necroptosis is not the major cell death mechanism at least not via RIP3.

Similarly, the loss of members of the intrinsic pathway, (BAK1, BAX, BBC3, BID and BCL2L11) did not affect cell survival upon TNFα treatment. This finding might be explained by the $PIK3CA^{H1047R}$ mutant background of RKO cells, which results in an active protooncogene AKT (Ahmed et al. 2013). AKT inhibits intrinsic apoptosis by activating the translocation of the hexokinase-2 (HK-2) from the cytosol into mitochondria. Located in the mitochondria, HK-2 inhibits the oligomerization of BAX and BAK in the outer mitochondrial membrane. Thus, no pores are created and cytochrome c remains in the mitochondrial intermembrane space (H. Yamaguchi and Wang 2001; Majewski et al. 2004). On the contrary, loss of components of the extrinsic apoptosis pathway, including TRADD, FADD and caspase 8, were found to render the RKO cells resistant towards TNFα treatment. This underlines the importance of the extrinsic apoptosis pathway for TNFα-mediated killing of RKOs. Taken together, these results imply that the binding of TNFα to TNFR1 lead to cell death through the initiation of the extrinsic apoptosis pathway, while the intrinsic apoptosis pathway or necroptosis do not affect TNFα mediated cell death of RKO cells.

Furthermore, several members in the NFκB signaling cascade were found to increase resistance or sensitization towards TNFα mediated cell death upon KO. Enhanced cell growth upon TNFα treatment was seen in cell deficient of TRADD and RIP1 of complex 1, two members of the LUBAC complex, namely HOIL-1 and HOIP, three members of the TAK-complex, namely MAP3K7, TAB1 and TAB2, and all three members of the IKK-complex, namely IKKα, IKKβ and NEMO. Conversely, sensitization towards TNFα mediated cell death was seen upon loss of the NFκB inhibitor NFKBIA and of components of the SCF complex (FBXW7, FBXW2, SKP1, SKP2 and CKS1B). Additionally, three members of the NFκB family were among the top sensitizers or resistance causing genes. NFKB1 or NFKB2 are both activated via the non-canonical pathway and the respective KO led to sensitization towards TNFα-mediated cell death. On the contrary, loss of the third member of the NFκB family, RELA, made cells more resistant to TNFα-mediated cell death.

The NFκB pathway is known for its role in cell survival, e.g. by inducing the expression of anti-apoptotic genes. This is in line with the fact that the activation of the non-canonical

pathway (i.e. NFKB1, NFKB2, SCF) resulted in cell survival upon TNFα infection. On the other hand, the canonical pathway (via RELA) elicited opposite results and induced programmed cell death. A similar role of RELA was shown in the presence of p53 (Ryan et al. 2000; Perkins and Gilmore 2006; Fan et al. 2008). Using an p53-inducible Saos-2 cell line, Ryan et al. (2000) claimed that RELA is necessary for p53 induced programmed cell death. While the anti-apoptotic function of RELA was seen upon TNFα treatment in the absence of p53, a pro-apoptotic function was observed in the presence of p53. The latter parallels the state of wt p53 expressing RKO cells. In addition, the authors claimed that RELA is not activated through phosphorylation of the NFκB inhibitors via the IKK complex, but through S6Kα1 dependent phosphorylation of RELA inhibitors. The phosphorylation of the RELA inhibitor leads to ubiquitination followed by proteasomal degradation. S6Kα1 is either activated via the RAS-RAF-MAPK pathway (Swaika, Crozier, and Joseph 2014; Ryan et al. 2000) or the PIK3CA-mTOR pathway (Chandra Pal et al. 2016). In RKO cells, both pathways are permanently active through the $BRAF^{V600E}$ and the $PIK3CA^{H1047R}$ mutant background. Furthermore, ERK1/2 can be activated via TNFα through the TAK complex (Newton and Dixit 2012) (Figure 15).

Collectively, this model is consistent with the results of our TNFα modulator screen and provides a plausible explanation for the pro-apoptotic role of RELA, the members of the TAK complex, MEK1/2, ERK1/2 and S6Kα1 and the anti-apoptotic role of NFKBIA and PTEN. In our screen setup, p53 activation might be caused by Cas9-induced DNA damage. S6Kα1 is activated by the TAK-complex upon TNFα treatment and can in turn phosphorylate the inhibitor of RELA. Following ubiquitination and proteasomal degradation, activated RELA in combination with p53 can induce the expression of pro-apoptotic genes.

The p53 and NFkB co-dependent model of TNFα mediated cell death is also confirmed in a TNFα modulator screen in p53-mutant MIA PaCa-2 cells. In this screen, the NFκB family members, including RELA, led to the induction of the expression of anti-apoptotic genes. While genes belonging to the RAS-RAF-MAPK pathway showed no effect upon TNFα treatment (Zuber lab, unpublished).

This would imply that every cell containing p53 and active RELA triggers apoptosis which would even include the RKOs cultured without TNFα. However, these cells showed no sign of increased cell death upon activation of p53 due to Cas9 editing. This can be explained due to

the inhibition of p53 via AKT (Abraham and O'Neill 2014) which is constantly active due to the $PIK3CA^{H1047R}$ mutations in RKO cells. Despite the presence of RELA, this results in the inhibition of the pro-apoptotic effect. To release the inhibition of p53 the activation of AKT has to be inhibited. This can be achieved through PTEN which inhibits PI3KCA and thus also the activation of AKT. Additionally, TNFα upregulates PTEN expression via the NFκB pathway (Lee et al. 2007). However, our TNFα modulator screen did not demonstrate an anti-apoptotic effect upon KO of PTEN. Instead, increased sensitization towards TNFα-mediated killing was detected.

Ryan et al. (2000) claimed that the pro-apoptotic function of RELA in combination with p53 is activated by S6Kα1 and not by the IKK complex. However, our TNFα-modulator screen revealed three possible ways, resulting in S6Kα1 activation. As stated above, one possible way is the ERK1/2 activation via the TAK complex. ERK1/2 can also be activated due to the $BRAF^{V600E}$ mutation, which would indicate TNFα independence. This contradicts our TNFα modulator screen, where I did see a TNFα-dependent anti-apoptotic effect upon BRAF KO. In addition, I also did see a pro-apoptotic role of the LUBAC and the IKK complex in the RKO c16. This leads to the assumption that the IKK complex might indeed contribute to the activation of apoptosis via p53 and RELA. If all three pathways contribute to RELA activation, the KO of only one should not lead to a significant effect upon TNFα treatment since the other two would compensate for its absence.

Collectively, the results of the TNFα modulator screen showed that RELA can act as an inducer of programmed cell death in RKO cells. This could be explained by the co-expression of wt p53. However, knowledge on the role of RELA as an inducer of programmed cell death is still lacking and further research needs to validate this genetic dependency.

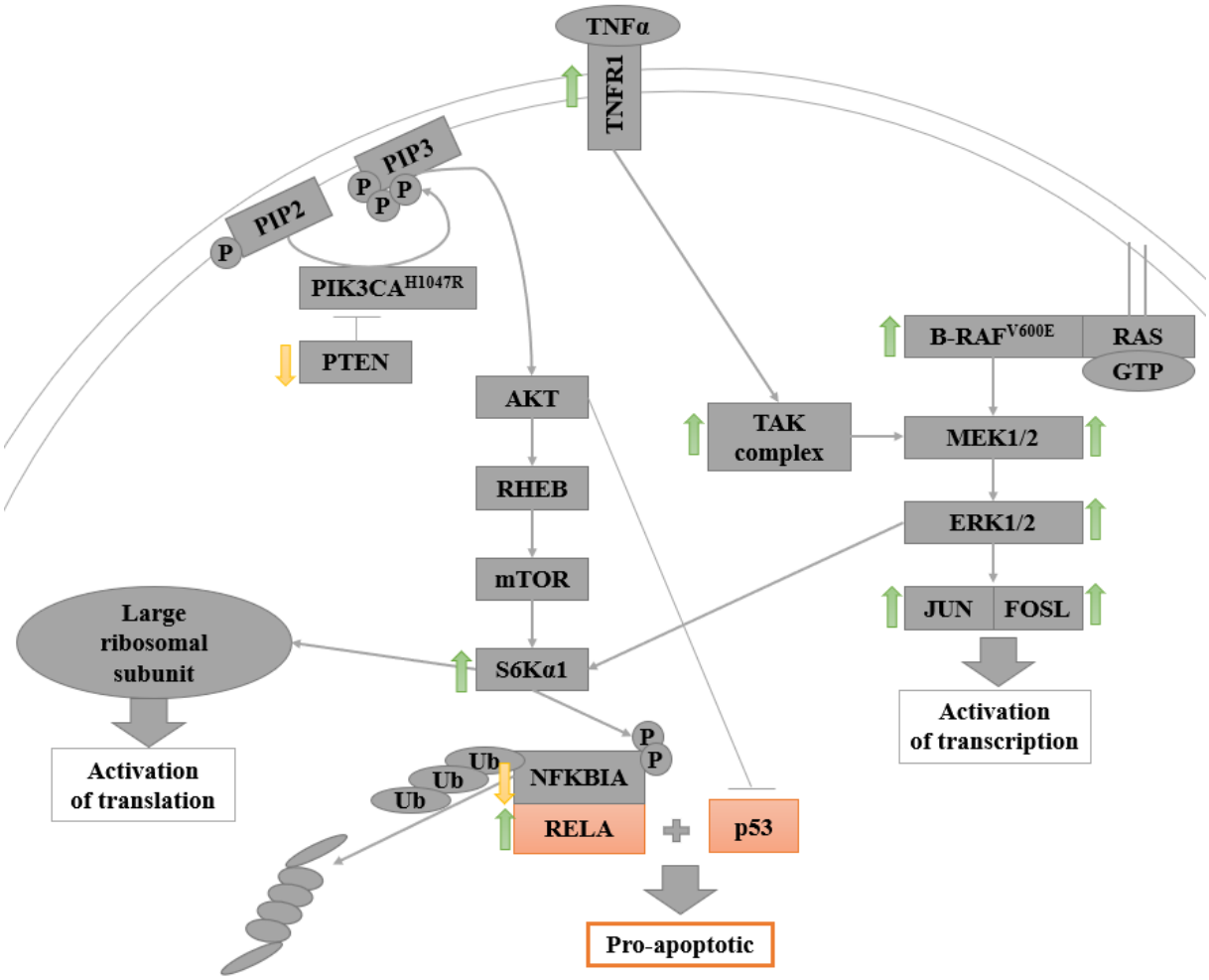

Figure 15: The pro-apoptotic role of RELA in combination with p53
Both, the RAS-RAF-MAPK and the PIKC3A-mTOR pathway, can activate the S6Kα1 kinase, which phosphorylates NFKBIA, the inhibitor of RELA. Next, NFKBIA is ubiquitinated and degraded by the proteasome. Active RELA can induce programmed cell death in combination with p53. The green upward pointing arrows indicate an enrichment upon TNFα treatment of the cells containing the KO of the respective gene in our screen, whereas the yellow downward pointing arrows indicate a depletion.

4.3. Sensitization hits towards TNFα-mediated killing

To select the candidates for the first round of screen validations, a targeted analysis was performed. I selected only those genes, which upon loss resulted in strong sensitization towards TNFα dependent cell death. In total, eleven genes that scored in both, the preDOS and postDOS and three high scoring genes from only the preDOS (PEA15, UBE2D3 and PBRM1) were selected. The validations of all genes confirmed a sensitization towards TNFα-mediated cell death upon KO, except for DUSP5, GTF2I and PBRM1. The KO of MRGBP, CAB39 and

PEA15 exhibited the strongest effect. In the following the effect of these genes will be discussed.

PEA15 has two phosphorylation sites, Ser116 and Ser104. Ser116 can be phosphorylated by AKT, which is continuously activated in RKO cells due to the PIK3CA^{H1047R} mutation. Upon Ser116 phosphorylation the DED domain of PEA15 can bind to FADD and thus inhibit the DISC formation and the extrinsic apoptosis pathway. Additionally, PEA15 inhibits ERK1/2 activity. Only simultaneous phosphorylation at both sites releases PEA15 from ERK1/2 and thereby activates MAPK downstream signaling (Greig and Nixon 2014; Exler et al. 2016). Based on the theory that p53 together with RELA result in cell death, the activation of ERK1/2 leads to cell death. Consequently, the KO of PEA15 sensitized the cells towards TNFα-mediated killing mainly due to a lacking inhibitory effect on the extrinsic apoptotic pathway and partly due to de-repression of ERK signaling.

Another protein also associated with the inhibition of the MAPK pathway is TRIB1 (Kiss-Toth et al. 2004; J. M. Murphy et al. 2015). The TNFα screen suggested that the MAPK pathway is activated upon KO and can lead to cell death in accordance to the theory that p53 together with RELA activate apoptosis.

CDK6 is a cyclin dependent kinase which is important for G1 progression and G1/S transition. In addition, previous research has shown that CDK6 can interact with RELA and thus enhance proper loading of RELA to its chromatin binding sites (Handschick et al. 2014). Our screen demonstrated sensitization towards TNFα-mediated killing upon KO. This can be confirmed under the assumption that RELA induced the expression of anti-apoptotic genes.

Two other genes that influence the NFκB pathway and are among the hits that sensitize towards TNFα mediated cell death are UBE2D3 and PPP6R3. UBE2D3 is an E2 ubiquitin conjugating enzyme, that can result in the ubiquitination of NFKBIA and thereby marks it for proteasomal degradation, followed by release of the NFκB family members (Vuillard, Nicholson, and Hay 1999; Yaron et al. 1998). Consequentially, loss of UBE2D3 might inhibit the NFκB pathway and thus result in extrinsic apoptosis. PPP6R3 is the regulatory subunit of protein phosphatase 6 (PP6). One function of this Ser/Thr phosphatase is the removal of a phosphate group of TAK1 and NFκB inhibitors. This stabilizes the inhibitor of RELA unlike UB3D3. So far, only loss of the phosphatase subunit PPPR1 was shown to result in the

degradation of NFκB inhibitors (Ziembik et al. 2017), while our results suggested a PPP6R3 dependent dephosphorylation of IκBs.

Among the sensitizing hits two transcriptional regulators, EGR1 and ETV6, could be identified. EGR1 was shown to interact with DNA-methyltransferases in gastric cancer (Yang et al. 2019). However, no interaction with NFκB family members has been identified so far. In contrast, ETV6 is suspected to act as a tumor suppressor and is repressed by the epidermal growth factor receptor (EGFR). Until now, ETV6 has not been linked to either TNFα or NFκB. However, loss of ETV6 upregulates EGFR-RAS signaling (Tsai et al. 2018). Thus, there might be a connection between NFκB signaling and ETV6 via the MAPK pathway.

Two hits that sensitized RKOs to TNFα mediated cell death are known to interact with the mTOR pathway. PIH1D1 directly activates mTORC1 (Kamano et al. 2013), whereas CAB39 downregulates mTOR signaling (Y. Kim et al. 2015). No connection between CAB39 and TNFα has been reported so far. However, the knockdown of PIH1D1 in U2SO led to enhanced activation of the extrinsic apoptosis pathway after sensitization with doxorubicin, an apoptosis inducing agent (Inoue et al. 2010). This indicates that PIH1D1 can inhibit the extrinsic apoptosis pathway.

The KO of STAU1 led to sensitization towards TNFα-mediated killing. Ye et al. (2019) claimed that the downregulation of STAU-1 enhanced IFNβ expression upon virus infection. Since TNFα can activate proinflammatory cytokine production like IFNβ, this effect can even be enhanced through the KO of STAU1 due to the fact that IFNβ leads to cell death via anti-proliferative effects (Markowitz 2007).

Altogether, the TNFα modulator screen identified many novel genes resulting in a pro-apoptotic effect upon KO which was confirmed by single sgRNA validation. Most of these novel genes depict a relation to the NFκB pathway.

4.4. Acetylation – an important mechanism with TNFα dependency

The results of our TNFα modulator screen demonstrated that chromatin remodeling plays an important role in dependency to TNFα treatment. A large number of HATs and HDACs were identified. The KO of these HATs, including the validated MRGBP, led to sensitization towards TNFα-mediated cell death. Whereas HDACs showed a more divers effect.

Histone or non-histone protein acetylation and deacetylation are commonly known to regulate the NFκB pathway. Acetylation of histones via HATs results in accessible chromatin and thus enhanced gene expression, whereas deacetylation via HDACs leads to condensed chromatin and to reduced gene expression. Acetylation of a non-histone protein results in increased activation of the protein itself through e.g. enhanced DNA binding of a TF. Non-histone protein acetylation can occur on the IKK complex members and on NFκB family members themselves. Whereas in the case of histone acetylation or histone deacetylation, HATs and HDACs can directly interact with NFκB proteins to regulate transcription.

The NFκB family members that are mostly known for non-histone acetylation/deacetylation are RELA/p65, NFκB1/p50 (the processed form of p105) and NFκB2/p52 as well as its precursor p100 (Calao et al. 2008; Perkins and Gilmore 2006; Fan et al. 2008). In fact, these three NFκB proteins score in our TNFα-modulator screen together with different HATs and HDACs, indicating that an interaction between these might occur.

Deacetylation of an NFκB proteins results in reduced expression of cell survival genes (Ashburner, Westerheide, and Baldwin 2001; Perkins and Gilmore 2006; Kawahara et al. 2009). HDACs that were previously shown to interact with the NFκB proteins are HDAC1/2 and SIRT6. Thus, the KO of these HDACs leads to transcriptional repression of anti-apoptotic genes, which was confirmed by our TNFα modulator screen. In addition, I also detected HDAC associated proteins among our TNFα-dependent resistance causing hits. One example is CSNK2A1, which activates SIRT6 through a specific Ser338 phosphorylation (Bae et al. 2016; Kawahara et al. 2009). Additionally, HDAC specific complex members were detected. Most of them lead to resistance towards TNFα-mediated cell death upon KO, like the SIN3 complex (M. Kim, Lu, and Zhang 2016) and the HDAC1:ELMSAN1 complex (Itoh et al. 2015). The KO of GATA2 and MTA1, members of the NuRD complex, (Basta and Rauchman 2015) resulted in sensitization towards TNFα-mediated killing instead. A possible explanation for this could be that interaction of the NuRD complex with RELA represses the transcription of different genes. In this case, the NuRD complex would repress anti-apoptotic genes, whereas the SIN3 and HDAC1:ELMSAN1 complex would repress pro-apoptotic genes.

CBP, p300, and PCAF are described as the major HATs leading to acetylation of either p65, p50, p52 and p100 and resulting in increased DNA binding and activation of NFκB transactivation (Lanzillotta et al. 2010; Calao et al. 2008). Surprisingly, these HATs do not

show any TNFα dependency upon KO in our TNFα modulator screen. However, I identified several members of the NuA4 HAT complex, also referred to as TIP60, among our sensitization hits. These include EPC2, MEAF6, ING3, YEATS4, BRD8, MRGBP and MORF4L1 (Figure 17). This multi subunit complex acetylates H4 and H2A N-terminal tails (Jacquet et al. 2016; Doyon et al. 2004). Kim et al. (2012) found TIP60 to act as a coactivator for RELA-dependent transcription upon TNFα stimulation. While TNFα induces RELA activation, TIP60 induces open chromatin at RELA recognition sites via H4 and H2A acetylation. After the release of the NFκB inhibitors, RELA is acetylated by p300, which led to the positioning of RELA on its target promoter. This is followed by TIP60 depended inhibition of RELA deacetylation through HDACs, which maintains RELA active (Figure 16). In most cases NFκB family members, including RELA, activate transcription of anti-apoptotic genes and thus lead to cell survival (Sun and Liu 2011). Consequently, loss of any of the TIP60 components should repress RELA-dependent transcription and result in cell death upon TNFα treatment. This theory is in line with the results of our TNFα modulator screen, but in contrast to the previous described induction of the expression of pro-apoptotic genes due to activated RELA in combination with p53. One explanation for this could be that RELA can activate transcription of anti- and pro-apoptotic genes depending on its coactivator.

Kim et al. (2012) described the TRIP60-NFκB model for RELA. It would be interesting to test whether other NFκB family members lead to a similar effect. Additionally, further research on the specific action of the different TIP60 complex members is necessary to fully understand this process.

In our screen seven out of 17 TIP60 members showed a TNFα dependent effect including MRGBP (Figure 17), which results in the strongest sensitization towards TNFα-mediated cell death upon KO. MRGBP stabilizes BRD8 and links MRG15 to the TIP60 complex, which makes it an important component of the TIP60 HAT complex (Cai et al. 2003; Ding et al. 2017, 2018). BRD8 and MRG15, which are both direct interaction partners of MRGBP are also among our depleting hits upon KO. In addition, MRGBP is known to be upregulated in various cancer types, including pancreatic (Ding et al. 2017, 2018) and colorectal cancer (K. Yamaguchi et al. 2010; Kiyoshi Yamaguchi et al. 2011). It was shown to be required for cancer cell proliferation and invasion (Ito et al. 2014; Ding et al. 2017). The proliferative effect may be BRD8 dependent (K. Yamaguchi et al. 2010). Taken together, MRGBP can be

considered as a biomarker for pancreatic and colon cancer lacking in-depth knowledge. This data coupled with the significant TNFα dependent depletion upon loss makes MRGBP an interesting hit for follow up studies to explain why it acts with the strongest dependency of all TIP60 components.

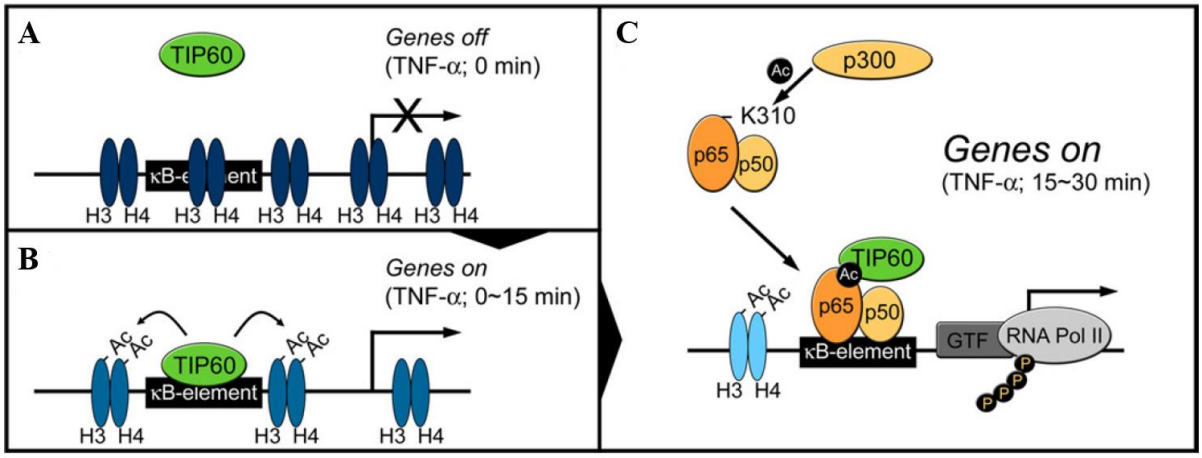

Figure 16: The TIP60/Nu4A HAT NFκB activation pathway (J. W. Kim et al. 2012)
(A-B) The TIP60 complex can open the chromatin at NFκB binding sites via acetylation of H4 and H2A histones. (C) NFκB is activated by acetylation via p300. TIP60 maintains the acetylation to keep NFκB active and subsequently leads to transcription.

Furthermore, TIP60 can interact with the large multiprotein SAGA complex via TRPP. The SAGA complex is involved in transcription initiation, chromatin modification, mRNA export and splicing. It contains 18-20 subunits, which are grouped into different modules based on their activity. The five different modules making up the complex are the core structural module, the TF-binding module, the splicing module, the DUB and the HAT module. Other proteins have also been found to be able to interact with these modules (Helmlinger and Tora 2017). Our TNFα modulator screen identified an enrichment upon loss of several members of the SAGA complex. These include all four members of the HAT-module, two members of the DUB module and five members of the core module. Three members of the TFIID interacting domain and the previously described seven members of the NuA4/TIP60 interacting domain were also identified (Figure 17). Through its acetylation and deubiquitination activity, the SAGA complex together with the TIP60 complex play an important role for chromatin remodeling. TRPP, the interacting protein between SAGA and TIP60, is not influenced by TNFα treatment. An explanation for this could be a TRPP independent recruitment of the HAT complex to

chromatin by NFκB upon TNFα treatment or redundancy by another factor. In contrast to the TIP60 HAT complex, inhibition of the acetylation via the HAT-module of the SAGA complex leads to cell survival under TNFα treatment. This might be explained by the fact that RELA has serval acetylation sites. Whereas some enhance the activity of RELA as a TF, others increase the interaction towards its inhibitors like NFKBIA, resulting in inhibition of RELA and activation of the extrinsic apoptotic pathway (Lanzillotta et al. 2010). This would explain the discrepancy between HATs in regard to their effect upon KO, based on the specific site they acetylate.

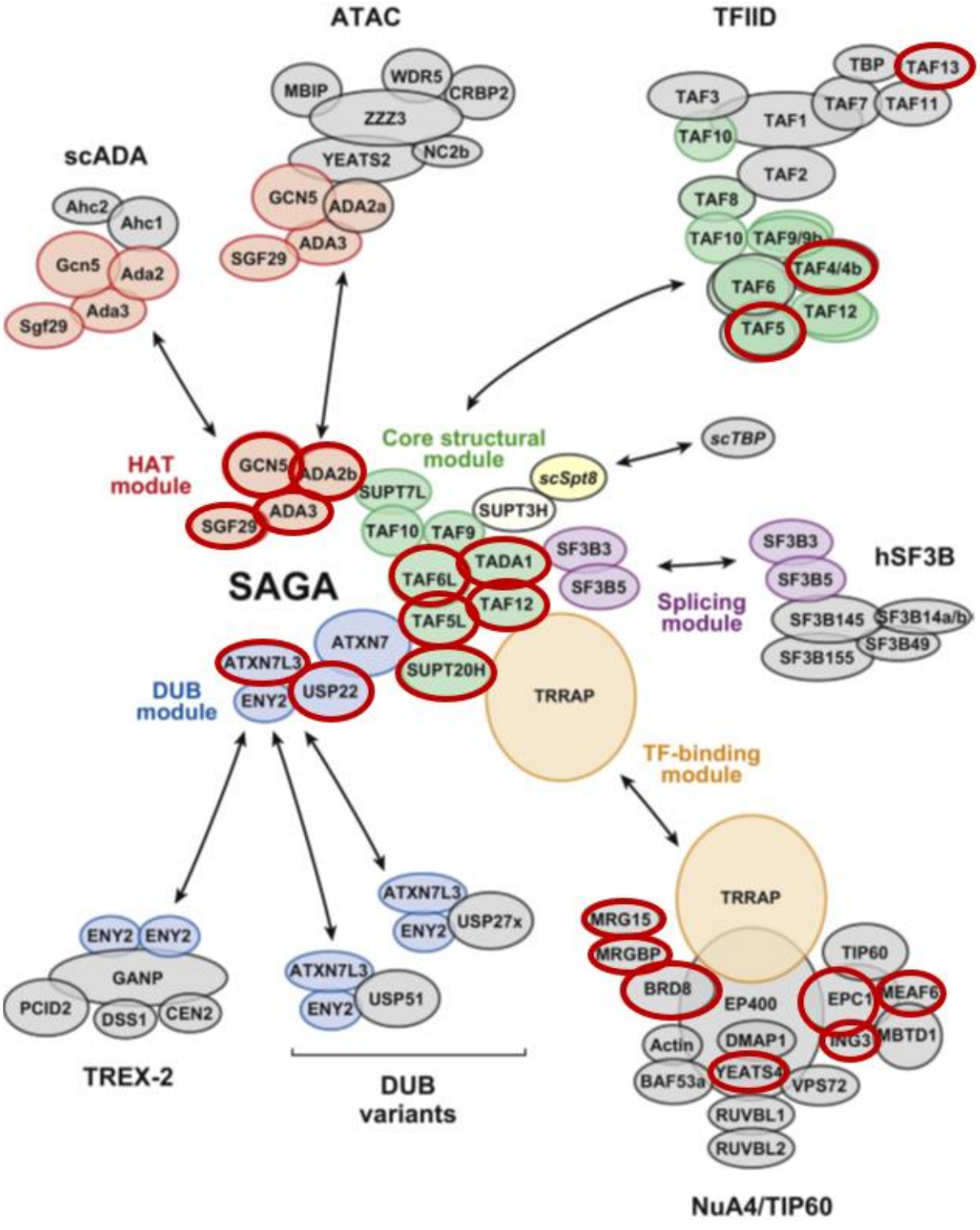

Figure 17: The SAGA complex with its five modules and interacting partners (Helmlinger and Tora 2017) The SAGA complex consists of five modules: the HAT module, the core structural module, the DUB module and the TF-binding module with the interacting NuA4/TIP60. The proteins highlighted in red of the SAGA complex

and TFIID are among the TNFα resistance inducing hits of our TNFα modulator screen, whereas genes encircled in red of the TIP60 complex are among the sensitization hits of our TNFα modulator screen.

4.5. Establishment of a human co-culture system to test tumor cell killing via $CD8^+$ T cells

The human co-culture system was established to test tumor cell killing via $CD8^+$ T cells in an antigen-specific manner.

The co-culture system itself showed efficient killing of RKOs containing the empty or the full-length constructs. However, the RKOs infected with the presenter construct did not show any effect at all, even though they depicted the highest MFI value. A possible reason for this could be that the ER-signal peptide did not efficiently load the HLA-A*0201 with the NLV peptide in the ER. By including the different MFI levels of HLA-A*0201^+ infection, both co-cultures with the RKOs containing either the HLA-A*0201 construct and the full-length p65 or solely the former, similar antigen-specific killing results were observed. For future assays, a ratio with less $CD8^+$ T cells per tumor cell should be used because of the high killing efficiency that almost completely killed the RKOs containing the empty construct.

The NLV concentration of 10 ng/mL used for pulsing is consistent with the concentration mainly recommended by literature (Foster et al. 2004). Again, the concentration should also be viewed in relation to the cell number and not exclusively to the media volume. Due to the high MFI levels and the slight difference between the different NLV concentrations, I would recommend utilizing 10 ng/mL for 1 Mio cells of the NLV peptide to ensure proper peptide loading.

For further experiments I would recommend utilizing the empty construct due to its efficient and specific killing. In this case, the RKOs can be cultured with and without the peptide to have a perfectly controlled experiment. In order to test the effect of different genes, the RKO HLA-A*0201^+ cells can be infected with a single sgRNA KO and utilized for the co-culture with the $CD8^+$ T cells. To be able to distinguish between the killing efficacy, I would recommend measuring first after 24 h and then again after 48 h, as opposed to a 72 h time point. This is because most cells will have been killed at this late time point which makes it impossible to distinguish between the killing efficacy against different KOs.

Altogether, an efficient and antigen-specific human co-culture system to test tumor cell killing via $CD8^+$ T cells was established and can be utilized for further validations.

4.6. Conclusion & Outlook

In summary, the TNFα modulator screen revealed many modifiers that lead to either sensitization or resistance upon KO.

It was possible to validate several of these hits in single sgRNA KO studies in the RKO c16. For further validations, it would be of interest to test if these genes can also show a genetic dependency in different colon cancer cell lines, like the HT-29 and DLD-1. In addition, further research will be conducted by the usage of the successfully established $CD8^+$ tumor killing co-culture system. The aim is to see whether the physiological TNFα produced by the $CD8^+$ T cells themselves shows a difference in the killing effect of single sgRNA tumor KO cells. As a control a TNFR-antibody should be added. Furthermore, a cytokine profiling of the RKO c16 would be interesting to test whether the RKOs can produce TNFα on their own.

Altogether, one of the most revealing findings in the TNFα modulator screen is the different genetic dependencies of the different NFκB family members. A connection was drawn to the p53-RELA-cell death theory and future research should focus on providing proof of this connection. Therefore, the physiological outcome upon TNFα of p53 wt and mutated cell lines needs to be tested. In addition, the contribution, of the IKK complex, the TAK complex and the BRAF and PIK3CA pathway to the p53-RELA-cell death theory should be examined.

The prominent role of acetylation and deacetylation in the NFκB pathway is also quite astonishing, especially the sensitizing effect upon the KO of the MRGBP gene. This protein is of such an high interest due to the fact that it could act as an oncogene, the lack of in-depth knowledge about it and the fact that it is an important player in the TIP60 HAT complex. Therefore, especially MRGB should be considered for further validations, including animal models.

5. Abstract

Besides interferon-γ, tumor necrosis factor-α is one of the key cytokines mediating cytotoxic activity and anti-tumor immunity. However, in certain cancers types resistance to tumor necrosis factor-α mediated killing mechanism were observed that result in rapid cancer progression. Strategies to make cells more sensitive to tumor necrosis factor-α mediated cytotoxicity hold great promise for cancer treatment. On the molecular level, both, sensitization and resistance to tumor necrosis factor-α are incompletely understood.

In recent years, CRISPR/Cas9 loss-of-function screens have proven to be a powerful tool to study biological processes on a genome wide level. The aim is to adapt this technology to identify genetic dependencies that render a human cancer cell line resistant or more sensitive to tumor necrosis factor-α treatment.

For this purpose, the colon carcinoma cell line RKO which is sensitive to tumor necrosis factor-α treatment was utilized. This cell line was adapted for CRISPR screening in the Zuber lab by (i) engineering an inducible Cas9 allele and (ii) infecting with a whole-genome sgRNA library. This enables the induction of Cas9 expression at the starting point of the screen, resulting in gene editing and generation of knockout cells. The comparison of towards tumor necrosis factor-α condition towards the untreated control, enables the identification of genetic dependencies. This knowledge will improve the understanding of the basic mechanisms of resistance and sensitization to tumor necrosis factor -α mediated cytotoxicity and could be exploited to improve cancer immunotherapy strategies.

In addition, a human co-culture system to test killing efficacy of gene-edited tumor cell lines via cytotoxic $CD8^+$ T cells was established and could be used for future validation of these identified genetic dependencies.

6. Zusammenfassung

Neben Interferon-γ ist der Tumornekrosefaktor-α eines der wichtigsten Zytokine, welches auch in der Tumorbekämpfung eine große Rolle spielt. Bei bestimmten Tumoren wurde jedoch eine Resistenz gegen die zytotoxische Aktivität des Tumornekrosefaktor-α beobachtet. Strategien, welche solche Resistenzen aufheben, sind vielversprechend für die Tumortherapie. Auf molekularer Ebene sind Mechanismen, welche zur Sensibilisierung oder Resistenz gegen die cytotoxische Aktivität des Tumornekrosefaktor-α führen bislang weitestgehend unerforscht.

In den letzten Jahren haben sich CRISPR/Cas9 Loss-of-Function Screens als eine vielversprechende Technologie zur Untersuchung biologischer Prozesse auf Genomebene erwiesen. Ziel ist es mithilfe dieser Technologie genetische Abhängigkeiten zu identifizieren, welche eine menschliche Tumorzelllinie resistent oder sensitiver für der Behandlung mit Tumornekrosefaktor-α machen.

Dafür wird eine Darmkrebs-Zelllinie, welche sensitiv zur zytotoxischen Aktivität des Tumornekrosefaktor-α ist, verwendet. Diese Zelllinie wurde im Zuber-Labor für das CRISPR/Cas9-Screening adaptiert, indem sie (i) ein induzierbares Cas9-Konstrukt exprimiert und (2) mit einer sgRNA library infiziert wurde. Dies ermöglicht die Induktion der Cas9 Expression zu Beginn des Screens, was eine Gen-Edition und somit die Entstehung von knockout-Zellen zur Folge hat. Der Vergleich der Tumornekrosefaktor-α behandelten Zellkultur zur unbehandelten Kontrolle ermöglicht es genetische Abhängigkeiten zu identifizieren. Ein besseres Verständnis dieser ermöglicht neue Einblicke in die grundlegenden Mechanismen der Tumorresistenz gegenüber cytotoxischer Aktivität und könnte entscheidend zur Verbesserung der Tumor-Immuntherapien beitragen.

Des weiteren wurde ein humanes Co-Kultur System entwichet, welches die zytotoxische Aktivität von $CD8^+$ T-Zellen gegenüber genveränderten Tumorzellen modelliert. Dieses System kann auch zur Validierung der identifizierten Mechanismen, welche zur Sensibilisierung oder Resistenz gegen die cytotoxische Aktivität des Tumornekrosefaktor-α führen, verwendet werden.

List of abbreviations

APC	antigen presenting cell
AAVS1	adeno-associated virus integration site 1
ANK	ankyrin repeats
BAK	BCL-2 antagonist/killer
BAX	BCL-2-associated X protein
BID	BH3-interacting domain death agonist
BIM	BCL-2-interacting mediator of cell death
BRAF	B-Raf proto-oncogene
CARD	casapses recruiting domain
Cas	CRISPR associated
CCN	cumulative cell number
CDK6	cyclin dependent kinase 6
cIAP1/2	inhibotor of apoptois protein 1/2
CIP	calf-intestinal-phosphatase
CRISPR	clustered regularly interspaced short palindromic repeat
CTL	cytotoxic T lymphocyte
DC	dendritic cell
DD	death domain
DED	death effector domain
DISC	death inducing signalling complex
dox	doxycycline
DUB	deubiquitylation
EB	elution buffer
ECPN	pRRL-U6-filler-improved tracer-EF1a-mCherry-P2A-Neo
FACS	fluorescence activated cell sorting
FADD	Fas associated death domain
GRR	glycin rich region
HAT	histone acetyltransferase
HCMV	human cytomegalovirus
HDAC	histone deacetylases
HDR	homology directed repair
HLA	human leucocyte antigen
HOIL-1	heme-oxidized IRP2 ubiquitin ligase 1
HOIP	HOIL-1 interacting protein
IE1	immediate-early protein 1
IFNγ	interferon γ
IKK	IκB kinase
IKKα/β/γ	inhibibior of NFκB kianse regualtory subuit α/β/γ

IL-7/12/15	interleucine-7/12/15
INTS6	integrator complex subunit 6
ITAM	immunoreceptor tyrosine-based activation motif
KO	knockout
LUBAC	linear ubiquitin assembly complex
MAGeCK	model-based analysis of genome-wide CRISPR/Cas9 knockout
MAP3K7	mitogen-activated protein kianse kinase kinase 7
MEKK3	mitogen activated protein kinase kinase kinase 3
MHC	major histocompatibility complexes
MLKL	mixed lineage kinase domain like
MOI	multiplicity of infection
MOMP	mitochondrial outer membrane permeabilization
mTNF	membrane-bound TNF
mTNFR	membrane-bound TNF receptor
NEMO	IKKγ
NFκB	nuclear factor kappa-light-chain-enhancer of activated B cells
NHEJ	non-homologous end joining
NIK	NFκB-inducing kinase
NK	natural killer
NLV	NLVPMVATV
PAM	protospacer adjacent motiv
PEA15	apoptosis adaptor protein 15
PEI	polyethylenimine
postDOS	post dropout screen
pp65	65kDa phosphoprotein
preDOS	pre dropout screen
PUMA	p53-upregulated modulator of apoptosis
RHD	rel homology domain
RIEP	pRRL-SFFV-rtTA3-IRES-EcoReceptor-PGK-Puro
RIP1/3	receptor interacting kinase 1/3
ROS	reactive oxygen species
SAGA	Spt-Ada-Gcn5 acetyltransferase
sgRNA	single guide RNA
SHARPIN	SHANK-interacting protein like 1
SODD	silencer of the death domain
sTNF	soluble TNF
sTNFR	soluble TNF receptor
TAB1/2/3	TAK1 binding proteins 1/2/3
TACE	TNFα converting enzyme
TAD	transactivation domain

TAK1	tranfoming growth factor beta-activated kinase 1
TAP	transporter associated with antigen processing
tapasin	TAP-associated glycoprotein
TCR	T cell receptor
tet-on	tetracycline-controlled transcriptional regulation system
TF	transcription factor
THD	TNF homology domain
TNFR	TNF receptor
TNFα	TNF homology domain
TP-0/A/B	timepoint 0/A/B
TRADD	TNFR1 associated death domain
TRAF1/2/3	TNFR-associated factor 1/2/3
wt	wild-type
α-RRA	modified robust rank aggregation

References

Abraham, Aswin G., and Eric O'Neill. 2014. "PI3K/Akt-Mediated Regulation of P53 in Cancer." In *Biochemical Society Transactions*. https://doi.org/10.1042/BST20140070.

Ahmed, D., P. W. Eide, I. A. Eilertsen, S. A. Danielsen, M. Eknæs, M. Hektoen, G. E. Lind, and R. A. Lothe. 2013. "Epigenetic and Genetic Features of 24 Colon Cancer Cell Lines." *Oncogenesis*. https://doi.org/10.1038/oncsis.2013.35.

Aksentijevich, Ivona, and Qing Zhou. 2017. "NF-KB Pathway in Autoinflammatory Diseases: Dysregulation of Protein Modifications by Ubiquitin Defines a New Category of Autoinflammatory Diseases." *Frontiers in Immunology*. https://doi.org/10.3389/fimmu.2017.00399.

Andersen, Mads Hald, David Schrama, Per Thor Straten, and Jürgen C. Becker. 2006. "Cytotoxic T Cells." *Journal of Investigative Dermatology*. https://doi.org/10.1038/sj.jid.5700001.

Aregger, Michael, Traver Hart, and Jason Moffat. 2015. " Extensive Mapping of an Innate Immune Network with CRISPR ." *Molecular Systems Biology*. https://doi.org/10.15252/msb.20156373.

Ashburner, B. P., S. D. Westerheide, and A. S. Baldwin. 2001. "The P65 (RelA) Subunit of NF- B Interacts with the Histone Deacetylase (HDAC) Corepressors HDAC1 and HDAC2 To Negatively Regulate Gene Expression." *Molecular and Cellular Biology*. https://doi.org/10.1128/mcb.21.20.7065-7077.2001.

Bae, Jun Sang, See Hyoung Park, Urangoo Jamiyandorj, Kyoung Min Kim, Sang Jae Noh, Jung Ryul Kim, Hye Jeong Park, et al. 2016. "CK2α/CSNK2A1 Phosphorylates SIRT6 and Is Involved in the Progression of Breast Carcinoma and Predicts Shorter Survival of Diagnosed Patients." *American Journal of Pathology*. https://doi.org/10.1016/j.ajpath.2016.08.007.

Balkwill, Frances. 2006. "TNF-α in Promotion and Progression of Cancer." *Cancer and Metastasis Reviews*. https://doi.org/10.1007/s10555-006-9005-3.

Balkwill, Frances. 2009. "Tumour Necrosis Factor and Cancer." *Nature Reviews Cancer*. https://doi.org/10.1038/nrc2628.

Balkwill, Frances R., Audrey Lee, Gary Aldam, Elaine Moodie, J. Alero Thomas, Jan Tavernier, and Walter Fiers. 1986. “Human Tumor Xenografts Treated with Recombinant Human Tumor Necrosis Factor Alone or in Combination with Interferons.” *Cancer Research*.

Barman, Antara, Bornali Deb, and Supriyo Chakraborty. 2019. “A Glance at Genome Editing with CRISPR–Cas9 Technology.” *Current Genetics*. https://doi.org/10.1007/s00294-019-01040-3.

Barrangou, Rodolphe, Christophe Fremaux, Hélène Deveau, Melissa Richards, Patrick Boyaval, Sylvain Moineau, Dennis A. Romero, and Philippe Horvath. 2007. “CRISPR Provides Acquired Resistance against Viruses in Prokaryotes.” *Science*. https://doi.org/10.1126/science.1138140.

Basta, Jeannine, and Michael Rauchman. 2015. “The Nucleosome Remodeling and Deacetylase Complex in Development and Disease.” *Translational Research*. https://doi.org/10.1016/j.trsl.2014.05.003.

Britt, William J., and Suresh Boppana. 2004. “Human Cytomegalovirus Virion Proteins.” *Human Immunology*. https://doi.org/10.1016/j.humimm.2004.02.008.

Brouckaert, Peter G.G., Geert G. Leroux-Roels, Yves Guisez, Jan Tavernier, and Walter Fiers. 1986. “In Vivo Anti-tumour Activity of Recombinant Human and Murine TNF, Alone and in Combination with Murine IFN-γ, on a Syngeneic Murine Melanoma.” *International Journal of Cancer*. https://doi.org/10.1002/ijc.2910380521.

Cabal-Hierro, Lucía, and Pedro S. Lazo. 2012. “Signal Transduction by Tumor Necrosis Factor Receptors.” *Cellular Signalling*. https://doi.org/10.1016/j.cellsig.2012.02.006.

Cai, Yong, Jingji Jin, Chieri Tomomori-Sato, Shigeo Sato, Irina Sorokina, Tari J. Parmely, Ronald C. Conaway, and Joan Weliky Conaway. 2003. “Identification of New Subunits of the Multiprotein Mammalian TRRAP/TIP60-Containing Histone Acetyltransferase Complex.” *Journal of Biological Chemistry*. https://doi.org/10.1074/jbc.C300389200.

Calao, Miriam, Arsène Burny, Vincent Quivy, Ann Dekoninck, and Carine Van Lint. 2008. “A Pervasive Role of Histone Acetyltransferases and Deacetylases in an NF-KB-Signaling Code.” *Trends in Biochemical Sciences*. https://doi.org/10.1016/j.tibs.2008.04.015.

Chandra Pal, Harish, Katherine Marchiony Hunt, Ariana Diamond, Craig A. Elmets, and Farrukh Afaq. 2016. “Phytochemicals for the Management of Melanoma.” *Mini-Reviews in Medicinal Chemistry*. https://doi.org/10.2174/1389557516666160211120157.

Chen, Daniel S., and Ira Mellman. 2013. “Oncology Meets Immunology: The Cancer-Immunity Cycle.” *Immunity* 39 (1): 1–10. https://doi.org/10.1016/J.IMMUNI.2013.07.012.

Cifaldi, Loredana, Franco Locatelli, Emiliano Marasco, Lorenzo Moretta, and Vito Pistoia. 2017. “Boosting Natural Killer Cell-Based Immunotherapy with Anticancer Drugs: A Perspective.” *Trends in Molecular Medicine*. https://doi.org/10.1016/j.molmed.2017.10.002.

Ding, Feng, Shuang Zhang, Shaoyang Gao, Jian Shang, Yanxia Li, Ning Cui, and Qiu Zhao. 2017. “MRGBP as a Potential Biomarker for the Malignancy of Pancreatic Ductal Adenocarcinoma.” *Oncotarget*. https://doi.org/10.18632/oncotarget.19451.

Ding, Feng, Shuang Zhang, Shaoyang Gao, Jian Shang, Yanxia Li, Ning Cui, and Qiu Zhao. 2018. “MiR-137 Functions as a Tumor Suppressor in Pancreatic Cancer by Targeting MRGBP.” *Journal of Cellular Biochemistry*. https://doi.org/10.1002/jcb.26676.

Dixit, Vishva, and Tak W. Mak. 2002. “NF-KB Signaling: Many Roads Lead to Madrid.” *Cell*. https://doi.org/10.1016/S0092-8674(02)01166-2.

Doyon, Y., W. Selleck, W. S. Lane, S. Tan, and J. Cote. 2004. “Structural and Functional Conservation of the NuA4 Histone Acetyltransferase Complex from Yeast to Humans.” *Molecular and Cellular Biology*. https://doi.org/10.1128/mcb.24.5.1884-1896.2004.

Dunn, Gavin P., Allen T. Bruce, Hiroaki Ikeda, Lloyd J. Old, and Robert D. Schreiber. 2002. “Cancer Immunoediting: From Immunosurveillance to Tumor Escape.” *Nature Immunology*. https://doi.org/10.1038/ni1102-991.

Exler, Rachel E., Xiaoxin Guo, Darren Chan, Izhar Livne-Bar, Nevena Vicic, John G. Flanagan, and Jeremy M. Sivak. 2016. “Biomechanical Insult Switches PEA-15 Activity to Uncouple Its Anti-Apoptotic Function and Promote Erk Mediated Tissue Remodeling.” *Experimental Cell Research*. https://doi.org/10.1016/j.yexcr.2015.11.023.

Fadeel, B., A. Ottosson, and S. Pervaiz. 2008. “Big Wheel Keeps on Turning: Apoptosome Regulation and Its Role in Chemoresistance.” *Cell Death and Differentiation*. https://doi.org/10.1038/sj.cdd.4402265.

Fan, Yongjun, Jui Dutta, Nupur Gupta, Gaofeng Fan, and Céline Gélinas. 2008. "Regulation of Programmed Cell Death by NF-KB and Its Role in Tumorigenesis and Therapy." *Advances in Experimental Medicine and Biology*. https://doi.org/10.1007/978-1-4020-6554-5_11.

Fang, Pingping, Cristabelle De Souza, Kay Minn, and Jeremy Chien. 2019. "Genome-Scale CRISPR Knockout Screen Identifies TIGAR as a Modifier of PARP Inhibitor Sensitivity." *Communications Biology*. https://doi.org/10.1038/s42003-019-0580-6.

Feinberg, B., R. Kurzrock, M. Talpaz, M. Blick, S. Saks, and J. U. Gutterman. 1988. "A Phase I Trial of Intravenously-Administered Recombinant Tumor Necrosis Factor-Alpha in Cancer Patients." *Journal of Clinical Oncology*. https://doi.org/10.1200/JCO.1988.6.8.1328.

Festjens, N., T. Vanden Berghe, S. Cornelis, and P. Vandenabeele. 2007. "RIP1, a Kinase on the Crossroads of a Cell's Decision to Live or Die." *Cell Death and Differentiation*. https://doi.org/10.1038/sj.cdd.4402085.

Foster, Aaron E., Kenneth F. Bradstock, Uluhan Sili, Marina Marangolo, Cliona M. Rooney, and David J. Gottlieb. 2004. "A Comparison of Gene Transfer and Antigen-Loaded Dendritic Cells for the Generation of CD4+ and CD8+ Cytomegalovirus-Specific T Cells in HLA-A2+ and HLA-A2- Donors." *Biology of Blood and Marrow Transplantation*. https://doi.org/10.1016/j.bbmt.2004.05.011.

Freeman, Andrew J., Stephin J. Vervoort, Kelly M. Ramsbottom, Madison J. Kelly, Jessica Michie, Lizzy Pijpers, Ricky W. Johnstone, Conor J. Kearney, and Jane Oliaro. 2019. "Natural Killer Cells Suppress T Cell-Associated Tumor Immune Evasion." *Cell Reports*. https://doi.org/10.1016/j.celrep.2019.08.017.

Fritsch, Melanie, Saskia D. Günther, Robin Schwarzer, Marie Christine Albert, Fabian Schorn, J. Paul Werthenbach, Lars M. Schiffmann, et al. 2019. "Caspase-8 Is the Molecular Switch for Apoptosis, Necroptosis and Pyroptosis." *Nature*. https://doi.org/10.1038/s41586-019-1770-6.

Gejman, Ron S., Heather F. Jones, Martin G. Klatt, Aaron Y. Chang, Claire Y. Oh, Smita S. Chandran, Tatiana Korontsvit, et al. 2019. “Identification of the Targets of T Cell Receptor Therapeutic Agents and Cells by Use of a High Throughput Genetic Platform.” *BioRxiv*. https://doi.org/10.1101/267047.

Ghosh, Sankar, and Michael Karin. 2002. “Missing Pieces in the NF-KB Puzzle.” *Cell*. https://doi.org/10.1016/S0092-8674(02)00703-1.

Gradiz, Rui, Henriqueta C. Silva, Lina Carvalho, Maria Filomena Botelho, and Anabela Mota-Pinto. 2016. “MIA PaCa-2 and PANC-1 - Pancreas Ductal Adenocarcinoma Cell Lines with Neuroendocrine Differentiation and Somatostatin Receptors.” *Scientific Reports*. https://doi.org/10.1038/srep21648.

Green, Douglas R., and Fabien Llambi. 2015. “Cell Death Signaling.” *Cold Spring Harbor Perspectives in Biology*. https://doi.org/10.1101/cshperspect.a006080.

Greig, Fiona H., and Graeme F. Nixon. 2014. “Phosphoprotein Enriched in Astrocytes (PEA)-15: A Potential Therapeutic Target in Multiple Disease States.” *Pharmacology and Therapeutics*. https://doi.org/10.1016/j.pharmthera.2014.03.006.

Haas, Tobias L., Christoph H. Emmerich, Björn Gerlach, Anna C. Schmukle, Stefanie M. Cordier, Eva Rieser, Rebecca Feltham, et al. 2009. “Recruitment of the Linear Ubiquitin Chain Assembly Complex Stabilizes the TNF-R1 Signaling Complex and Is Required for TNF-Mediated Gene Induction.” *Molecular Cell*. https://doi.org/10.1016/j.molcel.2009.10.013.

Hanahan, Douglas, and Robert A Weinberg. 2011. “Hallmarks of Cancer: The next Generation.” *Cell* 144 (5): 646–74. https://doi.org/10.1016/j.cell.2011.02.013.

Handschick, Katja, Knut Beuerlein, Liane Jurida, Marek Bartkuhn, Helmut Müller, Johanna Soelch, Axel Weber, et al. 2014. “Cyclin-Dependent Kinase 6 Is a Chromatin-Bound Cofactor for NF-KB-Dependent Gene Expression.” *Molecular Cell* 53 (2): 193–208. https://doi.org/10.1016/J.MOLCEL.2013.12.002.

Helmlinger, Dominique, and László Tora. 2017. “Sharing the SAGA.” *Trends in Biochemical Sciences*. https://doi.org/10.1016/j.tibs.2017.09.001.

Hinterndorfer, Matthias, and Johannes Zuber. 2019. “Functional-Genetic Approaches to Understanding Drug Response and Resistance.” *Current Opinion in Genetics and Development*. https://doi.org/10.1016/j.gde.2019.03.003.

Hu, Wei, and John J. Kavanagh. 2003. “Anticancer Therapy Targeting the Apoptotic Pathway.” *Lancet Oncology*. https://doi.org/10.1016/S1470-2045(03)01277-4.

Inoue, Mika, Makio Saeki, Hiroshi Egusa, Hitoshi Niwa, and Yoshinori Kamisaki. 2010. “PIH1D1, a Subunit of R2TP Complex, Inhibits Doxorubicin-Induced Apoptosis.” *Biochemical and Biophysical Research Communications* 403 (3–4): 340–44. https://doi.org/10.1016/J.BBRC.2010.11.031.

Isaacson, Batya, and Ofer Mandelboim. 2018. “Sweet Killers: NK Cells Need Glycolysis to Kill Tumors.” *Cell Metabolism*. https://doi.org/10.1016/j.cmet.2018.07.008.

Ito, Saya, Takashi Ueda, Akihisa Ueno, Hideo Nakagawa, Hidefumi Taniguchi, Naruhiro Kayukawa, and Tsuneharu Miki. 2014. “A Genetic Screen in Drosophila for Regulators of Human Prostate Cancer Progression.” *Biochemical and Biophysical Research Communications*. https://doi.org/10.1016/j.bbrc.2014.08.015.

Itoh, Toshimasa, Louise Fairall, Frederick W. Muskett, Charles P. Milano, Peter J. Watson, Nadia Arnaudo, Almutasem Saleh, et al. 2015. “Structural and Functional Characterization of a Cell Cycle Associated HDAC1/2 Complex Reveals the Structural Basis for Complex Assembly and Nucleosome Targeting.” *Nucleic Acids Research*. https://doi.org/10.1093/nar/gkv068.

Jackson, Sarah E., Gavin M. Mason, and Mark R. Wills. 2011. “Human Cytomegalovirus Immunity and Immune Evasion.” *Virus Research*. https://doi.org/10.1016/j.virusres.2010.10.031.

Jacquet, Karine, Amélie Fradet-Turcotte, Nikita Avvakumov, Jean Philippe Lambert, Céline Roques, Raj K. Pandita, Eric Paquet, et al. 2016. “The TIP60 Complex Regulates Bivalent Chromatin Recognition by 53BP1 through Direct H4K20me Binding and H2AK15 Acetylation.” *Molecular Cell*. https://doi.org/10.1016/j.molcel.2016.03.031.

Kamano, Yuya, Makio Saeki, Hiroshi Egusa, Yoshito Kakihara, Walid A. Houry, Hirofumi Yatani, and Yoshinori Kamisaki. 2013. “PIH1D1 Interacts with MTOR Complex 1 and Enhances Ribosome RNA Transcription.” *FEBS Letters*. https://doi.org/10.1016/j.febslet.2013.09.001.

Karayiannakis, A. J., K. N. Syrigos, A. Polychronidis, M. Pitiakoudis, A. Bounovas, and K. Simopoulos. 2001. “Serum Levels of Tumor Necrosis Factor-α and Nutritional Status in Pancreatic Cancer Patients.” *Anticancer Research*.

Karin, Michael, and Anning Lin. 2002. “NF-KB at the Crossroads of Life and Death.” *Nature Immunology*. https://doi.org/10.1038/ni0302-221.

Kawahara, Tiara L.A., Eriko Michishita, Adam S. Adler, Mara Damian, Elisabeth Berber, Meihong Lin, Ron A. McCord, et al. 2009. “SIRT6 Links Histone H3 Lysine 9 Deacetylation to NF-KB-Dependent Gene Expression and Organismal Life Span.” *Cell*. https://doi.org/10.1016/j.cell.2008.10.052.

Kearney, Conor J, Stephin J Vervoort, Simon J Hogg, Kelly M Ramsbottom, Andrew J Freeman, Najoua Lalaoui, Lizzy Pijpers, et al. 2018. “Tumor Immune Evasion Arises through Loss of TNF Sensitivity.” *Science Immunology* 3 (23): eaar3451. https://doi.org/10.1126/sciimmunol.aar3451.

Keusekotten, Kirstin, Paul Ronald Elliott, Laura Glockner, Berthe Katrine Fiil, Rune Busk Damgaard, Yogesh Kulathu, Tobias Wauer, et al. 2013. “XOTULIN Antagonizes LUBAC Signaling by Specifically Hydrolyzing Met1-Linked Polyubiquitin.” *Cell*. https://doi.org/10.1016/j.cell.2013.05.014.

Khan, Naeem, Mark Cobbold, Russell Keenan, and Paul A. H. Moss. 2002. “ Comparative Analysis of CD8 + T Cell Responses against Human Cytomegalovirus Proteins Pp65 and Immediate Early 1 Shows Similarities in Precursor Frequency, Oligoclonality, and Phenotype .” *The Journal of Infectious Diseases*. https://doi.org/10.1086/339963.

Khong, Hung T., and Nicholas P. Restifo. 2002. “Natural Selection of Tumor Variants in the Generation of ‘Tumor Escape’ Phenotypes.” *Nature Immunology*. https://doi.org/10.1038/ni1102-999.

Kim, Jung Woong, Sang Min Jang, Chul Hong Kim, Joo Hee An, Eun Jin Kang, and Kyung Hee Choi. 2012. “New Molecular Bridge between RelA/P65 and NF-KB Target Genes via Histone Acetyltransferase TIP60 Cofactor.” *Journal of Biological Chemistry*. https://doi.org/10.1074/jbc.M111.278465.

Kim, Minchul, Falong Lu, and Yi Zhang. 2016. “Loss of HDAC-Mediated Repression and Gain of NF-KB Activation Underlie Cytokine Induction in ARID1A- and PIK3CA-Mutation-Driven Ovarian Cancer.” *Cell Reports*. https://doi.org/10.1016/j.celrep.2016.09.003.

Kim, Yangjin, Gibin Powathil, Hyunji Kang, Dumitru Trucu, Hyeongi Kim, Sean Lawler, and Mark Chaplain. 2015. “Strategies of Eradicating Glioma Cells: A Multi-Scale Mathematical Model with MiR-451-AMPK-MTOR Control.” *PLoS ONE*. https://doi.org/10.1371/journal.pone.0114370.

Kimura, Kiyoji, Tetsuo Taguchi, Ichiro Urushizaki, Ryuzo Ohno, Osahiko Abe, Hisashi Furue, Takao Hattori, et al. 1987. “Phase I Study of Recombinant Human Tumor Necrosis Factor.” *Cancer Chemotherapy and Pharmacology*. https://doi.org/10.1007/BF00570490.

Kiss-Toth, Endre, Stephanie M. Bagstaff, Hye Y. Sung, Veronika Jozsa, Clare Dempsey, Jim C. Caunt, Kevin M. Oxley, et al. 2004. “Human Tribbles, a Protein Family Controlling Mitogen-Activated Protein Kinase Cascades.” *Journal of Biological Chemistry*. https://doi.org/10.1074/jbc.M407732200.

Klenerman, Paul, and Annette Oxenius. 2016. “T Cell Responses to Cytomegalovirus.” *Nature Reviews Immunology*. https://doi.org/10.1038/nri.2016.38.

Lanzillotta, A., I. Sarnico, R. Ingrassia, F. Boroni, C. Branca, M. Benarese, G. Faraco, et al. 2010. “The Acetylation of RelA in Lys310 Dictates the NF-KB-Dependent Response in Post-Ischemic Injury.” *Cell Death and Disease*. https://doi.org/10.1038/cddis.2010.76.

Lawrence, Toby. 2009. “The Nuclear Factor NF-KappaB Pathway in Inflammation.” *Cold Spring Harbor Perspectives in Biology*. https://doi.org/10.1101/cshperspect.a001651.

Lee, Young Rae, Hong Nu Yu, Eun Mi Noh, Hyun Jo Youn, Eun Kyung Song, Myung Kwan Han, Chang Sik Park, et al. 2007. “TNF-α Upregulates PTEN via NF-KB Signaling Pathways in Human Leukemic Cells.” *Experimental and Molecular Medicine*. https://doi.org/10.1038/emm.2007.14.

Li, Wei, Han Xu, Tengfei Xiao, Le Cong, Michael I. Love, Feng Zhang, Rafael A. Irizarry, Jun S. Liu, Myles Brown, and X. Shirley Liu. 2014. “MAGeCK Enables Robust Identification of Essential Genes from Genome-Scale CRISPR/Cas9 Knockout Screens.” *Genome Biology*. https://doi.org/10.1186/s13059-014-0554-4.

Li, Wenya, Jian Xu, Jian Zhao, and Rui Zhang. 2017. “Oxaliplatin and Infliximab Combination Synergizes in Inducing Colon Cancer Regression.” *Medical Science Monitor*. https://doi.org/10.12659/MSM.901880.

Liu, Ting, Lingyun Zhang, Donghyun Joo, and Shao Cong Sun. 2017. “NF-KB Signaling in Inflammation.” *Signal Transduction and Targeted Therapy*. https://doi.org/10.1038/sigtrans.2017.23.

Liu, Zheng Gang. 2005. “Molecular Mechanism of TNF Signaling and Beyond.” *Cell Research*. https://doi.org/10.1038/sj.cr.7290259.

Maier, Harald J., Uta Schmidt-Straßburger, Margit A. Huber, Eva M. Wiedemann, Hartmut Beug, and Thomas Wirth. 2010. “NF-KB Promotes Epithelial-Mesenchymal Transition, Migration and Invasion of Pancreatic Carcinoma Cells.” *Cancer Letters*. https://doi.org/10.1016/j.canlet.2010.03.003.

Majewski, Nathan, Veronique Nogueira, Prashanth Bhaskar, Platina E. Coy, Jennifer E. Skeen, Kathrin Gottlob, Navdeep S. Chandel, Craig B. Thompson, R. Brooks Robey, and Nissim Hay. 2004. “Hexokinase-Mitochondria Interaction Mediated by Akt Is Required to Inhibit Apoptosis in the Presence or Absence of Bax and Bak.” *Molecular Cell*. https://doi.org/10.1016/j.molcel.2004.11.014.

Malissen, Bernard, and Pierre Bongrand. 2015. “Early T Cell Activation: Integrating Biochemical, Structural, and Biophysical Cues.” *Annual Review of Immunology*. https://doi.org/10.1146/annurev-immunol-032414-112158.

Markowitz, Clyde E. 2007. “Interferon-Beta: Mechanism of Action and Dosing Issues.” *Neurology*. https://doi.org/10.1212/01.wnl.0000277703.74115.d2.

Moedl B. 2019. " Probing genetic modifiers of cancer therapeutics using genome-wide CRISPR screens" (Master thesis).

Morgens, David W., Richard M. Deans, Amy Li, and Michael C. Bassik. 2016. “Systematic Comparison of CRISPR/Cas9 and RNAi Screens for Essential Genes.” *Nature Biotechnology*. https://doi.org/10.1038/nbt.3567.

Murphy, James M., Yoshio Nakatani, Sam A. Jamieson, Weiwen Dai, Isabelle S. Lucet, and Peter D. Mace. 2015. “Molecular Mechanism of CCAAT-Enhancer Binding Protein Recruitment by the TRIB1 Pseudokinase.” *Structure*. https://doi.org/10.1016/j.str.2015.08.017.

Murphy, Kenneth, and Casey Weaver. 2017. *Janeway’s Immunbiology. 9th Edition*. *Garland Science*. https://doi.org/10.1007/s13398-014-0173-7.2.

Neefjes, Jacques, Marlieke L.M. Jongsma, Petra Paul, and Oddmund Bakke. 2011. “Towards a Systems Understanding of MHC Class i and MHC Class II Antigen Presentation.” *Nature Reviews Immunology*. https://doi.org/10.1038/nri3084.

Newton, Kim, and Vishva M. Dixit. 2012. “Signaling in Innate Immunity and Inflammation.” *Cold Spring Harbor Perspectives in Biology*. https://doi.org/10.1101/cshperspect.a006049.

Oeckinghaus, Andrea, and Sankar Ghosh. 2009. “The NF-KappaB Family of Transcription Factors and Its Regulation.” *Cold Spring Harbor Perspectives in Biology*. https://doi.org/10.1101/cshperspect.a000034.

Ohainle, Molly, Louisa Helms, Jolien Vermeire, Ferdinand Roesch, Daryl Humes, Ryan Basom, Jeffrey J. Delrow, Julie Overbaugh, and Michael Emerman. 2018. “A Virus-Packageable CRISPR Screen Identifies Host Factors Mediating Interferon Inhibition of HIV.” *ELife*. https://doi.org/10.7554/eLife.39823.

Perkins, N. D., and T. D. Gilmore. 2006. “Good Cop, Bad Cop: The Different Faces of NF-KB.” *Cell Death and Differentiation*. https://doi.org/10.1038/sj.cdd.4401838.

Pickar-Oliver, Adrian, and Charles A. Gersbach. 2019. “The next Generation of CRISPR–Cas Technologies and Applications.” *Nature Reviews Molecular Cell Biology*. https://doi.org/10.1038/s41580-019-0131-5.

Prendergast, G. C. 2008. “Immune Escape as a Fundamental Trait of Cancer: Focus on IDO.” *Oncogene*. https://doi.org/10.1038/onc.2008.35.

Ribeiro, Claudia Mara, Sayonara Rangel Oliveira, Daniela Frizon Alfieri, Tamires Flauzino, Damacio Ramón Kaimen-Maciel, Andréa Name Colado Simão, Michael Maes, and Edna Maria Vissoci Reiche. 2019. “Tumor Necrosis Factor Alpha (TNF-α) and Its Soluble Receptors Are Associated with Disability, Disability Progression and Clinical Forms of Multiple Sclerosis.” *Inflammation Research*. https://doi.org/10.1007/s00011-019-01286-0.

Ryan, K. M., M. K. Ernst, N. R. Rice, and K. H. Vousden. 2000. “Role of NF-KB in P53-Mediated Programmed Cell Death.” *Nature*. https://doi.org/10.1038/35009130.

Singh, Rumani, Anthony Letai, and Kristopher Sarosiek. 2019. “Regulation of Apoptosis in Health and Disease: The Balancing Act of BCL-2 Family Proteins.” *Nature Reviews Molecular Cell Biology*. https://doi.org/10.1038/s41580-018-0089-8.

Stewart, T. J., and S. I. Abrams. 2008. “How Tumours Escape Mass Destruction.” *Oncogene*. https://doi.org/10.1038/onc.2008.268.

Sun, Shao Cong, and Zheng Gang Liu. 2011. “A Special Issue on NF-KB Signaling and Function.” *Cell Research*. https://doi.org/10.1038/cr.2011.1.

Swaika, Abhisek, Jennifer A. Crozier, and Richard W. Joseph. 2014. “Vemurafenib: An Evidence-Based Review of Its Clinical Utility in the Treatment of Metastatic Melanoma.” *Drug Design, Development and Therapy*. https://doi.org/10.2147/DDDT.S31143.

Tsai, Yuan Chin, Tao Zeng, Wassim Abou-Kheir, Hsiu Lien Yeh, Juan Juan Yin, Yi Chao Lee, Wei Yu Chen, and Yen Nien Liu. 2018. “Disruption of ETV6 Leads to TWIST1-Dependent Progression and Resistance to Epidermal Growth Factor Receptor Tyrosine Kinase Inhibitors in Prostate Cancer.” *Molecular Cancer*. https://doi.org/10.1186/s12943-018-0785-1.

Udommethaporn, Sutthirat, Tewin Tencomnao, Eileen M. McGowan, and Viroj Boonyaratanakornkit. 2016. “Assessment of Anti-TNF-α Activities in Keratinocytes Expressing Inducible TNF- α: A Novel Tool for Anti-TNF-α Drug Screening.” *PLoS ONE*. https://doi.org/10.1371/journal.pone.0159151.

Vanamee, Éva S., and Denise L. Faustman. 2018. “Structural Principles of Tumor Necrosis Factor Superfamily Signaling.” *Science Signaling*. https://doi.org/10.1126/scisignal.aao4910.

Vredevoogd, David W., Thomas Kuilman, Maarten A. Ligtenberg, Julia Boshuizen, Kelly E. Stecker, Beaunelle de Bruijn, Oscar Krijgsman, et al. 2019. “Augmenting Immunotherapy Impact by Lowering Tumor TNF Cytotoxicity Threshold.” *Cell*. https://doi.org/10.1016/j.cell.2019.06.014.

Vuillard, Laurent, John Nicholson, and Ronald T. Hay. 1999. “A Complex Containing BTrCP Recruits Ccd34 to Catalyse Ubiquitination of IκBα.” *FEBS Letters*. https://doi.org/10.1016/S0014-5793(99)00895-9.

Wajant, H., K. Pfizenmaier, and P. Scheurich. 2003. “Tumor Necrosis Factor Signaling.” *Cell Death and Differentiation*. https://doi.org/10.1038/sj.cdd.4401189.

Wajant, Harald, and Andreas Beilhack. 2019. “Targeting Regulatory T Cells by Addressing Tumor Necrosis Factor and Its Receptors in Allogeneic Hematopoietic Cell Transplantation and Cancer.” *Frontiers in Immunology*. https://doi.org/10.3389/fimmu.2019.02040.

Waters, John P., Jordan S. Pober, and John R. Bradley. 2013. “Tumour Necrosis Factor and Cancer.” *Journal of Pathology*. https://doi.org/10.1002/path.4188.

Yako, Y., D. Kruger, M. Smith, and M. Brand. 2016. “Cytokines as Biomarkers of Pancreatic Ductal Adenocarcinoma: A Systematic Review.” *HPB*. https://doi.org/10.1016/j.hpb.2016.02.911.

Yamaguchi, Hirohito, and Hong Gang Wang. 2001. “The Protein Kinase PKB/Akt Regulates Cell Survival and Apoptosis by Inhibiting Bax Conformational Change.” *Oncogene*. https://doi.org/10.1038/sj.onc.1204984.

Yamaguchi, K., M. Sakai, T. Shimokawa, Y. Yamada, Y. Nakamura, and Y. Furukawa. 2010. “C20orf20 (MRG-Binding Protein) as a Potential Therapeutic Target for Colorectal Cancer.” *British Journal of Cancer*. https://doi.org/10.1038/sj.bjc.6605500.

Yamaguchi, Kiyoshi, Michihiro Sakai, Joohun Kim, Shin ichiro Tsunesumi, Tomoaki Fujii, Tsuneo Ikenoue, Yoshinao Yamada, et al. 2011. “MRG-Binding Protein Contributes to Colorectal Cancer Development.” *Cancer Science*. https://doi.org/10.1111/j.1349-7006.2011.01971.x.

Yang, Yang, Fei Wu, Jing Zhang, Ruifang Sun, Fang Li, Yulong Li, Su’e Chang, et al. 2019. “EGR1 Interacts with DNMT3L to Inhibit the Transcription of MiR-195 and Plays an Anti-Apoptotic Role in the Development of Gastric Cancer.” *Journal of Cellular and Molecular Medicine*. https://doi.org/10.1111/jcmm.14597.

Yaron, Avraham, Ada Hatzubai, Matti Davis, Iris Lavon, Sharon Amit, Anthony M. Manning, Jens S. Andersen, Matthias Mann, Frank Mercurio, and Yinon Ben-Neriah. 1998. “Identification of the Receptor Component of the IκBα-Ubiquitin Ligase.” *Nature*. https://doi.org/10.1038/25159.

Yi, Fei, Nicholas Frazzette, Anthony C. Cruz, Christopher A. Klebanoff, and Richard M. Siegel. 2018. “Beyond Cell Death: New Functions for TNF Family Cytokines in Autoimmunity and Tumor Immunotherapy.” *Trends in Molecular Medicine*. https://doi.org/10.1016/j.molmed.2018.05.004.

Zhou, Wen, and Junying Yuan. 2014. “Necroptosis in Health and Diseases.” *Seminars in Cell and Developmental Biology*. https://doi.org/10.1016/j.semcdb.2014.07.013.

Ziembik, Magdalena A., Timothy P. Bender, James M. Larner, and David L. Brautigan. 2017. “Functions of Protein Phosphatase-6 in NF-KB Signaling and in Lymphocytes.” *Biochemical Society Transactions*. https://doi.org/10.1042/BST20160169.

Zins, Karin, Dietmar Abraham, Mouldy Sioud, and Seyedhossein Aharinejad. 2007. “Colon Cancer Cell-Derived Tumor Necrosis Factor-α Mediates the Tumor Growth-Promoting Response in Macrophages by up-Regulating the Colony-Stimulating Factor-1 Pathway.” *Cancer Research*. https://doi.org/10.1158/0008-5472.CAN-06-2295.

List of figures

List of tables

Acknowledgment

First of all, I would like to thank Prof. Dr. Johannes Zuber for giving me the opportunity to conduct this project in his group. My project was very interesting and I was able to learn state-of-the-art techniques that not only led to exciting results but also further increased my curiosity and provided me with insights that will accompany me for my entire career as a scientist.

Likewise, I would like to express my gratitude to Univ.- Prof. Dr.med. univ. Veronika Sexl, who assumed the role of the internal supervisor for my master thesis.

Special thanks go to my supervisor Markus Schaefer, PhD, who not only taught me many new techniques and methods in the lab, but also helped me improve my skills in analyzing, presenting and writing up results. Also, thank you for always having an open ear for all my questions and ideas.
Furthermore, I would like to thank Sarah Rieser who also supported me a lot in the lab and to Sebastian Carotta for our fruitful discussions and interesting exchanges.

I really appreciate all the work of our technicians Michaela Fellner and Martina Weißenböck as well as their support with cloning and thank you Kimon Froussios for the bioinformatical analysis.

I would like to express my gratitude to the whole Zuber group for their great support and discussions both inside and outside the lab and for every laugh we shared during this great time.

Lastly, I would like to thank my family, my friends and especially Philip for their support during my master studies and my thesis. Without you this would not have been possible.

Thank you so much to everyone who has contributed to my master thesis!

Supplemental Tables

Supplement Table 1: Top 50 resistant genes (due to preDOS Day 23)

gene	essential in preDOS	RKO c16 [TPM]	preDOS (Day 4)_2ng/mL TNF α vs. no TNF α	preDOS (Day 10)_2ng/mL TNFα vs. no TNFα	preDOS (Day 23)_2ng/mL TNFα vs. no TNFα	postDOS (Day 16)_2ng/mL TNFα vs. no TNFα	postDOS (Day 16)_6ng/mL TNFα vs. no TNFα
TNFRSF1A	no	125.0403	0.57	2.29	5.78	5.00	6.18
CDKN1A	no	227.5958	0.57	1.99	5.42	4.52	5.26
MAPK1	yes	102.2649	0.52	1.80	5.16	3.78	4.57
MAP2K1	yes	184.2099	0.42	1.80	5.03	3.35	3.82
RIPK1	no	42.62223	0.09	1.34	4.74	4.03	5.42
RELA	no	113.0845	0.32	1.39	4.30	3.83	4.57
IKBKG	no	1.601863	0.19	1.32	4.18	3.71	4.70
BRAF	yes	19.24057	0.81	1.91	4.12	2.22	2.41
MAP3K7	no	84.28212	-0.07	0.89	4.01	3.24	4.03
FOSL1	no	340.7961	0.39	1.73	3.99	1.88	2.20
RNF31	no	37.18467	0.16	1.22	3.84	2.00	2.76
DDX6	no	156.4606	0.27	1.17	3.74	3.17	3.61
IKBKB	no	53.97804	0.16	0.90	3.72	3.03	3.27
JUN	yes	550.8196	0.82	2.05	3.56	1.00	1.61
RBCK1	no	58.89022	0.27	1.39	3.56	2.59	2.86
TADA2B	yes	25.86563	0.20	0.79	3.49	1.63	1.53
INTS6	yes	18.96188	0.55	1.53	3.42	3.20	3.14
HIRA	yes	70.08201	0.34	1.20	3.17	2.78	2.98
HNRNPA2	yes	1648.342	0.14	1.03	3.13	2.68	2.88
ETS1	no	255.847	0.40	0.81	3.01	2.27	2.73
MCM7	yes	349.9407	-0.04	0.48	2.96	0.07	#N/A
RPL28	no	211.9848	0.31	1.09	2.94	2.25	2.53
CHUK	no	81.58493	0.21	0.81	2.91	2.25	2.04
TRADD	no	7.727747	0.19	1.23	2.90	2.29	2.41
MAP2K3	yes	130.64	0.20	0.86	2.89	1.37	2.19
ATXN7L3	no	51.62551	0.31	1.17	2.86	2.10	2.09
CCDC101	yes	12.59501	0.20	0.95	2.83	1.13	1.50
RBM4	no	16.69419	0.35	1.41	2.82	1.89	2.67
YBX1	yes	289.3228	0.18	1.29	2.75	1.91	2.49
DYNLL1	yes	374.3549	0.27	0.73	2.73	2.85	3.07
SAMD1	no	46.20247	0.31	1.24	2.71	1.73	1.98
SMG7	yes	79.37962	0.40	0.79	2.68	1.40	1.78
SMARCD1	yes	106.3272	0.29	0.75	2.66	1.27	1.59
AHCYL1	yes	117.8891	0.18	0.68	2.65	-0.06	#N/A
ELP3	yes	37.80272	0.06	0.30	2.60	1.55	1.67
SMG5	yes	95.02545	0.24	0.88	2.59	0.96	#N/A
TAF5L	yes	40.17688	0.08	0.90	2.58	1.53	1.97
TADA1	yes	37.35506	0.17	0.61	2.57	0.95	#N/A
EMC1	yes	60.36918	0.20	0.51	2.56	-0.09	1.53
SON	yes	202.4839	0.28	0.94	2.53	1.60	1.40
TRIM24	no	42.57819	0.24	0.87	2.50	2.21	2.59
TAB2	no	73.62295	0.06	0.70	2.41	1.72	2.42
ELP5	yes	60.94421	-0.08	0.16	2.40	1.23	#N/A
MED16	yes	28.79012	0.15	0.89	2.37	0.00	4.66
ELP6	yes	53.73188	0.04	0.48	2.33	-0.54	1.28
ATMIN	no	27.67327	0.09	0.31	2.32	1.75	2.12
CBFB	no	213.8206	0.25	1.05	2.31	1.98	2.35
SNRPA	yes	139.0061	0.24	0.68	2.28	1.37	1.16
G3BP1	no	431.3775	0.12	0.95	2.28	1.95	2.28
TAF6L	yes	15.49074	0.29	0.83	2.26	0.23	1.35

Supplement Table 2: Top 50 sensitizing genes (due to preDOS Day 23)

gene	essential in preDOS	RKO c16 [TPM]	preDOS (Day 4)_2ng/mL TNF α vs. no TNF α	preDOS (Day 10)_2ng/mL TNFα vs. no TNFα	preDOS (Day 23)_2ng/mL TNFα vs. no TNFα	postDOS (Day 16)_2ng/mL TNFα vs. no TNFα	postDOS (Day 16)_6ng/mL TNFα vs. no TNFα
PEA15	yes	248.5102	-0.75	-2.44	-5.31	-5.74	-2.17
RSBN1	yes	26.13694	#N/A	-0.35	-1.06	-1.51	#N/A
PPA1	yes	365.7618	0.06	-1.07	-5.03	0.00	4.74
CDK6	yes	43.81597	-0.51	-2.47	-4.82	-2.53	-4.86
MEAF6	yes	50.99017	#N/A	-0.47	-1.73	-1.68	-2.96
SZT2	yes	7.71562	#N/A	-0.10	-1.06	#N/A	#N/A
UBE2D3	yes	226.1739	-0.60	-1.88	-4.11	-0.38	-0.01
SETDB1	yes	17.45972	#N/A	-0.43	-2.61	#N/A	-1.29
CHTOP	yes	117.5946	#N/A	-0.71	-1.22	#N/A	-0.92
PSMA5	yes	133.9384	#N/A	-0.60	-4.08	#N/A	0.38
KIAA0907	yes	69.33492	#N/A	-0.35	-1.09	0.00	-0.16
CD1A	yes	0	#N/A	0.06	-1.27	0.30	0.28
COPS4	yes	114.1172	-0.43	-0.89	-3.90	0.36	1.70
ADAMTS4	yes	0	0.05	0.12	-1.05	-0.13	-0.37
UAP1	yes	640.4286	-0.05	-0.59	-1.63	-1.40	-1.44
MPC2	yes	33.90071	-0.11	-0.47	-1.55	-1.28	-1.05
LHX4	yes	1.774496	-0.11	-0.83	-1.34	-1.01	-0.90
PTPN7	yes	103.6547	0.24	0.00	-1.93	-0.85	-0.80
LOC10050	yes	0	-0.29	-0.47	-2.95	0.08	0.12
GIGYF2	yes	56.24535	-0.24	-1.22	-1.45	-0.32	-0.63
PPM1G	yes	552.0395	0.02	-0.77	-1.67	-0.96	-1.07
EPC2	yes	33.44511	0.03	-0.59	-1.75	-1.21	-1.56
CAB39	yes	88.98534	-0.55	-1.62	-2.71	-2.47	-2.14
ATG9A	yes	52.95034	-0.27	-0.67	-2.00	-1.71	-1.31
TUBA4A	yes	81.94365	0.04	0.23	-1.31	-0.71	0.01
EIF4E2	yes	52.12313	-0.15	-0.39	-1.28	-0.64	-0.71
MYEOV2	yes	72.85076	-0.05	-0.57	-1.05	-1.14	-1.80
ING5	yes	16.76147	0.03	-0.55	-1.42	-0.81	-1.61
RASA2	yes	57.30005	-0.23	-0.38	-1.48	-0.76	-0.94
PBRM1	yes	37.1896	-0.17	-1.16	-2.75	-0.90	-0.85
TKT	yes	251.4321	0.02	-0.29	-2.93	-0.49	-1.23
PPP4R2	yes	86.20407	-0.08	-0.50	-1.42	-1.54	-1.51
TBL1XR1	yes	143.3401	-0.13	-0.82	-1.96	-2.06	-2.12
TOP2B	yes	224.8465	-0.19	-0.54	-1.35	-0.54	#N/A
DET1	yes	5.90124	-0.12	-1.39	-2.87	-2.33	-2.70
ARIH2	yes	107.9693	-0.06	-0.50	-1.45	-0.77	-1.02
QRICH1	yes	80.02874	-0.20	-0.88	-2.23	-1.82	-1.40
NPRL2	yes	40.07546	-0.02	-0.28	-1.06	-0.88	-1.36
DHODH	yes	22.33962	-0.05	0.74	-2.83	0.35	2.34
ARF4	yes	403.0794	0.03	-0.35	-1.05	-0.98	-1.34
RNF7	yes	90.30936	-0.14	-0.74	-1.53	-0.69	-1.04
TSC22D2	yes	51.07838	-0.30	-0.48	-1.31	-0.19	-0.39
PDCD10	yes	105.5157	-0.21	-0.54	-1.43	-1.30	-1.54
FAF2	yes	92.69643	-0.18	-1.34	-2.79	0.33	0.70
HTT	yes	33.93154	0.02	-0.44	-1.08	-0.48	-0.22
PDS5A	yes	102.6081	-0.34	-1.27	-2.56	-1.49	-1.54
CNOT6L	yes	30.12207	-0.13	-0.40	-1.65	-0.73	-0.91
FBXW7	yes	31.44349	-0.43	-1.64	-1.54	-1.95	-2.09
ACSL1	yes	82.03579	-0.13	-0.56	-1.18	-0.69	-0.76
WHSC2	yes	43.11465	-0.01	-0.29	-1.17	-1.07	-0.36

Supplement Table 3: Top 30 enriched KEGG pathways among the resistant genes of postdocs (STRING analysis)

#term ID	term description	observed gene count	background gene count	false discovery rate
hsa04668	TNF signaling pathway	17	108	9.67E-11
hsa04620	Toll-like receptor signaling pathway	15	102	2.84E-09
hsa04657	IL-17 signaling pathway	14	92	5.89E-09
hsa05169	Epstein-Barr virus infection	18	194	1.52E-08
hsa04150	mTOR signaling pathway	16	148	1.58E-08
hsa05220	Chronic myeloid leukemia	12	76	4.67E-08
hsa04380	Osteoclast differentiation	14	124	8.76E-08
hsa04010	MAPK signaling pathway	20	293	1.13E-07
hsa04621	NOD-like receptor signaling pathway	15	166	2.99E-07
hsa05160	Hepatitis C	13	131	9.36E-07
hsa05145	Toxoplasmosis	12	109	1.00E-06
hsa04210	Apoptosis	13	135	1.08E-06
hsa05165	Human papillomavirus infection	19	317	1.21E-06
hsa04064	NF-kappa B signaling pathway	11	93	1.47E-06
hsa05142	Chagas disease (American trypanosomiasis)	11	101	2.96E-06
hsa05168	Herpes simplex infection	14	181	3.12E-06
hsa05167	Kaposi's sarcoma-associated herpesvirus infection	14	183	3.33E-06
hsa05203	Viral carcinogenesis	14	183	3.33E-06
hsa05221	Acute myeloid leukemia	9	66	5.53E-06
hsa04622	RIG-I-like receptor signaling pathway	9	70	8.23E-06
hsa05212	Pancreatic cancer	9	74	1.20E-05
hsa04660	T cell receptor signaling pathway	10	99	1.37E-05
hsa04714	Thermogenesis	14	228	2.89E-05
hsa04919	Thyroid hormone signaling pathway	10	115	4.38E-05
hsa04722	Neurotrophin signaling pathway	10	116	4.52E-05
hsa05211	Renal cell carcinoma	8	68	4.83E-05
hsa05140	Leishmaniasis	8	70	5.66E-05
hsa01522	Endocrine resistance	9	95	5.95E-05
hsa04662	B cell receptor signaling pathway	8	71	5.95E-05
hsa05215	Prostate cancer	9	97	6.49E-05

Supplement Table 4: Top 30 enriched cellular components (GO) among the resistant genes of postdocs (STRING analysis)

#term ID	term description	observed gene count	background gene count	false discovery rate
GO:0031981	nuclear lumen	128	4030	5.32E-23
GO:0005654	nucleoplasm	117	3446	5.81E-23
GO:0044428	nuclear part	133	4359	5.81E-23
GO:0070013	intracellular organelle lumen	139	5162	1.91E-19
GO:0005634	nucleus	163	6892	4.87E-19
GO:0043231	intracellular membrane-bounded organelle	204	10365	4.19E-18
GO:0032991	protein-containing complex	129	4792	1.20E-17
GO:0044446	intracellular organelle part	182	8882	9.20E-16
GO:0043227	membrane-bounded organelle	207	11244	1.06E-14
GO:0044424	intracellular part	233	13996	2.38E-14
GO:0005622	intracellular	234	14286	2.04E-13
GO:0043229	intracellular organelle	214	12193	2.66E-13
GO:0044451	nucleoplasm part	45	1073	1.75E-10
GO:1902494	catalytic complex	48	1295	1.87E-09
GO:0005829	cytosol	111	4958	4.39E-09
GO:1990904	ribonucleoprotein complex	34	770	2.24E-08
GO:0005694	chromosome	38	950	2.84E-08
GO:0044427	chromosomal part	33	819	3.20E-07
GO:0036464	cytoplasmic ribonucleoprotein granule	15	191	1.53E-06
GO:0000228	nuclear chromosome	24	514	2.53E-06
GO:0000790	nuclear chromatin	19	333	3.01E-06
GO:0044464	cell part	238	16244	3.01E-06
GO:0070461	SAGA-type complex	7	26	3.01E-06
GO:0005681	spliceosomal complex	14	187	5.57E-06
GO:0044444	cytoplasmic part	161	9377	6.99E-06
GO:0043232	intracellular non-membrane-bounded organelle	86	4005	7.50E-06
GO:0000785	chromatin	22	489	1.12E-05
GO:0016607	nuclear speck	19	381	1.50E-05
GO:0000123	histone acetyltransferase complex	9	76	1.98E-05
GO:0016604	nuclear body	27	742	2.83E-05

Supplement Table 5: Enriched KEGG pathways among the sensitizing genes in the postdocs (STRING analysis)

#term ID	term description	observed gene count	background gene count	false discovery rate
hsa04120	Ubiquitin mediated proteolysis	10	134	6.60E-05
hsa00520	Amino sugar and nucleotide sugar metabolism	5	48	0.0063
hsa05222	Small cell lung cancer	6	92	0.0094
hsa04110	Cell cycle	6	123	0.029
hsa05202	Transcriptional misregulation in cancer	7	169	0.029
hsa05203	Viral carcinogenesis	7	183	0.0302
hsa05166	HTLV-I infection	8	250	0.0356
hsa04217	Necroptosis	6	155	0.0473

Supplement Table 6: Top 30 enriched cellular compartments (GO) among the sensitizing genes of the postdocs (STRING analysis)

#term ID	term description	observed gene count	background gene count	false discovery rate
GO:0031981	nuclear lumen	107	4030	2.67E-30
GO:0005654	nucleoplasm	99	3446	5.70E-30
GO:0044428	nuclear part	109	4359	2.62E-29
GO:0070013	intracellular organelle lumen	111	5162	2.49E-24
GO:0005634	nucleus	125	6892	1.09E-22
GO:0043231	intracellular membrane-bounded organelle	148	10365	5.15E-20
GO:0044446	intracellular organelle part	135	8882	2.42E-18
GO:0043227	membrane-bounded organelle	151	11244	4.75E-18
GO:0044424	intracellular part	162	13996	1.26E-14
GO:0043229	intracellular organelle	152	12193	1.60E-14
GO:0032991	protein-containing complex	87	4792	1.38E-12
GO:0005829	cytosol	86	4958	3.05E-11
GO:1902494	catalytic complex	40	1295	4.12E-11
GO:1990234	transferase complex	29	727	2.23E-10
GO:0044451	nucleoplasm part	31	1073	8.46E-08
GO:0044464	cell part	164	16244	2.05E-07
GO:0005694	chromosome	28	950	3.06E-07
GO:0044427	chromosomal part	25	819	9.77E-07
GO:0016607	nuclear speck	16	381	5.14E-06
GO:0000785	chromatin	18	489	5.70E-06
GO:0005737	cytoplasm	126	11238	4.33E-05
GO:0000228	nuclear chromosome	17	514	4.62E-05
GO:0044454	nuclear chromosome part	16	480	7.99E-05
GO:0000790	nuclear chromatin	13	333	0.00012
GO:0000151	ubiquitin ligase complex	12	285	0.00013
GO:0016604	nuclear body	19	742	0.00036
GO:0070603	SWI/SNF superfamily-type complex	6	67	0.00045
GO:0019005	SCF ubiquitin ligase complex	5	47	0.00094
GO:0043232	intracellular non-membrane-bounded organelle	56	4005	0.00098

Supplement Table 7: Enriched KEGG pathways among the essential resistant genes of the preDOS (STRING analysis)

#term ID	term description	observed gene count	background gene count	false discovery rate
hsa04919	Thyroid hormone signaling pathway	11	115	1.51E-06
hsa03022	Basal transcription factors	6	44	0.00032
hsa03040	Spliceosome	8	130	0.0012
hsa04122	Sulfur relay system	3	8	0.004
hsa03015	mRNA surveillance pathway	6	89	0.0051
hsa04714	Thermogenesis	9	228	0.0051
hsa05168	Herpes simplex infection	8	181	0.0051
hsa04150	mTOR signaling pathway	7	148	0.0072

Supplement Table 8: Top 30 enriched cellular compartments (GO) among the essential resistant genes of the preDOS (STRING analysis)

#term ID	term description	observed gene count	background gene count	false discovery rate
GO:0031981	nuclear lumen	102	4030	4.70E-28
GO:0044428	nuclear part	106	4359	4.70E-28
GO:0005654	nucleoplasm	93	3446	1.00E-26
GO:0070013	intracellular organelle lumen	111	5162	5.92E-26
GO:0043231	intracellular membrane-bounded organelle	150	10365	7.91E-25
GO:0005634	nucleus	123	6892	3.19E-23
GO:0032991	protein-containing complex	103	4792	3.19E-23
GO:0043227	membrane-bounded organelle	153	11244	3.95E-23
GO:0044446	intracellular organelle part	138	8882	6.24E-23
GO:0044422	organelle part	139	9111	1.76E-22
GO:0043229	intracellular organelle	153	12193	1.84E-18
GO:0044424	intracellular part	158	13996	5.78E-15
GO:1990904	ribonucleoprotein complex	32	770	3.20E-12
GO:0044451	nucleoplasm part	37	1073	6.61E-12
GO:0070461	SAGA-type complex	10	26	6.61E-12
GO:0030914	STAGA complex	7	13	4.04E-09
GO:0033588	Elongator holoenzyme complex	6	6	6.02E-09
GO:0005681	spliceosomal complex	14	187	3.07E-08
GO:0043232	intracellular non-membrane-bounded organelle	67	4005	5.45E-08
GO:1902494	catalytic complex	33	1295	1.98E-07
GO:0044464	cell part	159	16244	3.92E-07
GO:0016591	RNA polymerase II, holoenzyme	10	103	5.44E-07
GO:0044427	chromosomal part	24	819	1.97E-06
GO:0005694	chromosome	26	950	1.99E-06
GO:0005730	nucleolus	25	926	4.08E-06
GO:0033276	transcription factor TFTC complex	5	15	6.53E-06
GO:0016592	mediator complex	6	34	1.11E-05
GO:0005829	cytosol	70	4958	1.30E-05
GO:0044798	nuclear transcription factor complex	10	166	2.56E-05
GO:0090575	RNA polymerase II transcription factor complex	9	139	4.69E-05

Supplement Table 9: Enriched KEGG pathways among the essential sensitizing genes of the preDOS (STRING analysis)

#term ID	term description	observed gene count	background gene count	false discovery rate
hsa04120	Ubiquitin mediated proteolysis	6	134	0.001

Supplement Table 10: Top 30 enriched cellular compartments (GO) among the essential sensitizing genes of the preDOS (STRING analysis)

#term ID	term description	observed gene count	background gene count	false discovery rate
GO:0044428	nuclear part	49	4359	5.94E-14
GO:0005634	nucleus	59	6892	9.86E-14
GO:0005654	nucleoplasm	42	3446	1.58E-12
GO:0031981	nuclear lumen	45	4030	1.58E-12
GO:0070013	intracellular organelle lumen	47	5162	4.15E-10
GO:0043231	intracellular membrane-bounded organelle	64	10365	3.24E-09
GO:0005829	cytosol	42	4958	1.22E-07
GO:0044446	intracellular organelle part	57	8882	1.67E-07
GO:0032991	protein-containing complex	40	4792	4.74E-07
GO:0044451	nucleoplasm part	18	1073	1.25E-06
GO:0016363	nuclear matrix	7	106	4.16E-06
GO:0044424	intracellular part	68	13996	1.92E-05
GO:1902494	catalytic complex	17	1295	6.07E-05
GO:0000346	transcription export complex	3	10	0.0002
GO:1990234	transferase complex	11	727	0.0011
GO:0016604	nuclear body	11	742	0.0012
GO:0016607	nuclear speck	8	381	0.0012
GO:0097346	INO80-type complex	3	23	0.0015
GO:0036452	ESCRT complex	3	27	0.0022
GO:0000445	THO complex part of transcription export complex	2	6	0.0044
GO:0044444	cytoplasmic part	49	9377	0.005
GO:0072357	PTW/PP1 phosphatase complex	2	7	0.005
GO:0034098	VCP-NPL4-UFD1 AAA ATPase complex	2	8	0.0061
GO:0005694	chromosome	11	950	0.0072
GO:0070449	elongin complex	2	9	0.0072
GO:0000812	Swr1 complex	2	10	0.0081
GO:0044427	chromosomal part	10	819	0.0081
GO:0000815	ESCRT III complex	2	11	0.0091
GO:0031464	Cul4A-RING E3 ubiquitin ligase complex	2	11	0.0091
GO:0008023	transcription elongation factor complex	3	52	0.0092

Supplement Table 11: Enriched KEGG pathways among the non-essential resistant genes of the preDOS (STRING analysis)

#term ID	term description	observed gene count	background gene count	false discovery rate
hsa00520	Amino sugar and nucleotide sugar metabolism	5	48	0.0288
hsa05202	Transcriptional misregulation in cancer	8	169	0.0331
hsa05203	Viral carcinogenesis	8	183	0.0364
hsa04010	MAPK signaling pathway	10	293	0.0391

Supplement Table 12: Top 30 enriched cellular compartments (GO) among the non-essential resistant genes of the preDOS (STRING analysis)

#term ID	term description	observed gene count	background gene count	false discovery rate
GO:0031981	nuclear lumen	107	4030	6.29E-22
GO:0005654	nucleoplasm	98	3446	9.29E-22
GO:0044428	nuclear part	109	4359	7.24E-21
GO:0005634	nucleus	137	6892	9.55E-20
GO:0070013	intracellular organelle lumen	110	5162	8.72E-16
GO:0044424	intracellular part	188	13996	1.28E-14
GO:0043231	intracellular membrane-bounded organelle	160	10365	4.17E-14
GO:0043227	membrane-bounded organelle	166	11244	2.45E-13
GO:0043229	intracellular organelle	171	12193	6.42E-12
GO:0044446	intracellular organelle part	140	8882	4.01E-11
GO:0005829	cytosol	90	4958	3.19E-08
GO:0032991	protein-containing complex	88	4792	3.19E-08
GO:1902494	catalytic complex	36	1295	1.11E-06
GO:0000785	chromatin	21	489	1.13E-06
GO:0005694	chromosome	30	950	1.13E-06
GO:0044451	nucleoplasm part	32	1073	1.27E-06
GO:0000790	nuclear chromatin	17	333	1.92E-06
GO:0044464	cell part	189	16244	6.06E-06
GO:0044427	chromosomal part	26	819	7.05E-06
GO:0000228	nuclear chromosome	20	514	7.93E-06
GO:1990234	transferase complex	24	727	9.32E-06
GO:0016607	nuclear speck	16	381	4.15E-05
GO:0035267	NuA4 histone acetyltransferase complex	5	18	4.15E-05
GO:0044454	nuclear chromosome part	18	480	4.15E-05
GO:1902562	H4 histone acetyltransferase complex	6	34	4.15E-05
GO:0016604	nuclear body	22	742	0.00012
GO:0000123	histone acetyltransferase complex	7	76	0.00025
GO:0043232	intracellular non-membrane-bounded organelle	66	4005	0.00026
GO:0000151	ubiquitin ligase complex	12	285	0.00054
GO:0000118	histone deacetylase complex	6	60	0.00055

Supplement Table 13: Top 30 enriched KEGG pathways among the non-essential sensitizing genes of the preDOS (STRING analysis)

#term ID	term description	observed gene count	background gene count	false discovery rate
hsa04668	TNF signaling pathway	14	108	6.14E-10
hsa04657	IL-17 signaling pathway	13	92	7.05E-10
hsa04620	Toll-like receptor signaling pathway	12	102	2.14E-08
hsa05169	Epstein-Barr virus infection	15	194	2.19E-08
hsa04621	NOD-like receptor signaling pathway	14	166	2.38E-08
hsa04064	NF-kappa B signaling pathway	11	93	5.70E-08
hsa04622	RIG-I-like receptor signaling pathway	10	70	5.70E-08
hsa05145	Toxoplasmosis	11	109	1.98E-07
hsa04380	Osteoclast differentiation	11	124	6.06E-07
hsa05142	Chagas disease (American trypanosomiasis)	10	101	9.15E-07
hsa05160	Hepatitis C	11	131	9.15E-07
hsa04210	Apoptosis	11	135	1.02E-06
hsa04010	MAPK signaling pathway	15	293	1.27E-06
hsa05168	Herpes simplex infection	12	181	1.81E-06
hsa05167	Kaposi's sarcoma-associated herpesvirus infection	12	183	1.89E-06
hsa05220	Chronic myeloid leukemia	8	76	8.64E-06
hsa05165	Human papillomavirus infection	14	317	1.46E-05
hsa05418	Fluid shear stress and atherosclerosis	9	133	4.75E-05
hsa05203	Viral carcinogenesis	10	183	7.92E-05
hsa05166	HTLV-I infection	11	250	0.00018
hsa05131	Shigellosis	6	63	0.00029
hsa04660	T cell receptor signaling pathway	7	99	0.00035
hsa05221	Acute myeloid leukemia	6	66	0.00035
hsa04659	Th17 cell differentiation	7	102	0.00039
hsa04920	Adipocytokine signaling pathway	6	69	0.00039
hsa05140	Leishmaniasis	6	70	0.0004
hsa05161	Hepatitis B	8	142	0.0004
hsa05200	Pathways in cancer	15	515	0.00045
hsa05212	Pancreatic cancer	6	74	0.00049
hsa04658	Th1 and Th2 cell differentiation	6	88	0.0012

Supplement Table 14: Top 30 enriched cellular compartments (GO) among the non-essential sensitizing genes of the preDOS (STRING analysis)

#term ID	term description	observed gene count	background gene count	false discovery rate
GO:0005654	nucleoplasm	72	3446	3.29E-11
GO:0031981	nuclear lumen	79	4030	3.29E-11
GO:0044428	nuclear part	80	4359	2.47E-10
GO:0005634	nucleus	105	6892	3.80E-10
GO:0070013	intracellular organelle lumen	85	5162	6.70E-09
GO:0043231	intracellular membrane-bounded organelle	129	10365	7.22E-08
GO:0043227	membrane-bounded organelle	135	11244	1.43E-07
GO:0044424	intracellular part	153	13996	5.15E-07
GO:0043229	intracellular organelle	140	12193	9.32E-07
GO:0032991	protein-containing complex	75	4792	9.78E-07
GO:0005622	intracellular	154	14286	1.10E-06
GO:0043226	organelle	141	12432	1.53E-06
GO:0005829	cytosol	75	4958	3.45E-06
GO:0044446	intracellular organelle part	111	8882	6.26E-06
GO:0031264	death-inducing signaling complex	4	9	8.29E-05
GO:0044451	nucleoplasm part	25	1073	0.00019
GO:0010494	cytoplasmic stress granule	6	51	0.0002
GO:0036464	cytoplasmic ribonucleoprotein granule	10	191	0.0002
GO:0000124	SAGA complex	4	14	0.00028
GO:0031248	protein acetyltransferase complex	7	85	0.00028
GO:1902494	catalytic complex	27	1295	0.00042
GO:0000790	nuclear chromatin	12	333	0.00074
GO:0097342	ripoptosome	3	6	0.00075
GO:0008385	IkappaB kinase complex	3	7	0.001
GO:0000123	histone acetyltransferase complex	6	76	0.0011
GO:0044444	cytoplasmic part	107	9377	0.0012
GO:0005694	chromosome	21	950	0.0013
GO:0044464	cell part	159	16244	0.0014
GO:0000785	chromatin	14	489	0.0015
GO:1905368	peptidase complex	6	87	0.0017

Supplement Table 15: gBlocks

HLA-A*0201	TCACTCGGCGCGCCAGTCCTCCGACAGACTGAGTCGGCCGGTG GATCTACCGGTCCACCATGGCGGTAATGGCTCCACGAACACTG GTCCTGTTGCTGAGTGGGGCGCTGGCTTTGACCCAAACCTGGG CCGGCTCACATAGCATGCGGTACTTCTTCACTTCAGTGTCACGA CCAGGACGAGGTGAGCCTCGCTTTATAGCCGTTGGGTACGTGG ATGACACTCAGTTTGTACGCTTCGATTCAGACGCAGCTAGCCA AAGGATGGAGCCCAGGGCGCCCTGGATAGAACAGGAGGGGCC GGAATACTGGGACGGTGAGACGAGAAAGGTTAAGGCCCACTC TCAGACACATCGAGTTGACTTGGGTACACTCCGAGGATACTAT AATCAATCCGAGGCCGGGAGCCACACAGTCCAGCGGATGTACG GGTGTGACGTGGGGTCAGACTGGAGATTCTTGCGCGGCTATCA CCAATACGCATACGATGGAAAAGACTATATCGCACTCAAAGAG GACCTCAGATCTTGGACAGCAGCTGATATGGCAGCGCAAACTA CGAAACATAAGTGGGAGGCAGCCCATGTCGCAGAACAGCTGC GGGCCTACCTCGAGGGCACTTGTGTTGAGTGGTTGCGGAGGTA CCTGGAAAACGGTAAGGAGACGCTCCAGCGAACTGATGCCCCA AAAACTCATATGACACATCATGCTGTGTCTGACCATGAGGCTA CACTTCGATGTTGGGCATTGAGTTTTTATCCGGCAGAAATAACC TTGACGTGGCAGAGAGATGGAGAAGACCAGACACAAGATACA GAACTCGTGGAGACTAGACCTGCCGGTGACGGGACCTTTCAGA AATGGGCGGCTGTAGTCGTTCCAAGTGGACAGGAGCAACGATA TACTTGTCATGTGCAGCACGAAGGGCTCCCCAAACCACTCACC CTGCGATGGGAACCTTCCAGTCAGCCCACGATCCCGATAGTTG GTATCATCGCCGGGTTGGTGTTGTTTGGCGCTGTGATCACTGGA GCCGTCGTTGCCGCAGTTATGTGGCGGCGGAAATCTTCTGATA GAAAAGGAGGCAGTTATAGTCAAGCTGCCTCAAGTGATAGCGC CCAAGGCAGCGACGTTTCACTCACTGCGTGCAAAGTGTGACTA AGTAAGGATCCGCGGCCGCAC

pp65	GGCTCAGGTGCCACCAACTTCAGCTTGTTGAAACAGGCTGGGG ATGTAGAGGAAAACCCCGGTCCCATGGAATCAAGAGGCAGGA GGTGTCCGGAAATGATTTCTGTGCTTGGACCAATTTCAGGGCA CGTTCTTAAAGCCGTTTTTTCACGGGGCGATACTCCTGTACTGC CTCACGAGACTAGGCTCCTGCAAACGGGTATACATGTTCGCGT ATCACAACCGAGCCTTATTTTGGTGAGTCAATACACTCCCGATA GTACACCGTGTCATCGCGGCGACAATCAGCTGCAGGTGCAACA TACATACTTCACCGGGTCTGAGGTTGAGAATGTATCTGTGAAT GTGCATAATCCCACGGGTCGCTCAATATGTCCCTCACAGGAAC CAATGTCAATTTATGTCTATGCACTGCCACTCAAGATGTTGAAT ATACCCAGCATCAATGTACACCACTACCCCAGCGCCGCAGAGC GCAAACATAGACACCTGCCAGTGGCTGATGCAGTAATTCATGC TTCAGGAAAGCAGATGTGGCAGGCCCGGTTGACGGTGTCTGGG CTGGCATGGACCCGGCAGCAAAATCAGTGGAAAGAGCCTGAT GTGTATTATACATCAGCCTTCGTATTTCCCACAAAAGACGTAGC TCTCCGCCATGTGGTTTGCGCCCACGAACTGGTTTGTAGCATGG AAAACACCCGCGCTACGAAGATGCAAGTCATTGGCGACCAATA CGTAAAAGTATATCTCGAGAGTTTTTGCGAAGATGTGCCCTCC GGCAAGCTCTTCATGCACGTTACCCTGGGCAGCGACGTTGAGG AGGATCTCACGATGACACGAAATCCGCAACCATTTATGCGCCC CCATGAACGCAATGGGTTCACAGTGCTTTGCCCTAAGAATATG ATAATTAAGCCTGGGAAGATTTCACACATAATGCTCGATGTGG CTTTTACCTCACACGAGCACTTCGGACTCCTGTGTCCGAAGTCT ATTCCCGGTCTGAGCATCTCCGGGAACCTGCTCATGAACGGGC AACAGATCTTTCTCGAAGTGCAGGCAATTAGGGAGACAGTGGA ACTCCGACAGTATGACCCAGTTGCCGCCTTGTTCTTTTTTGATA TTGATTTGCTGCTTCAAAGGGGTCCCCAATATTCCGAGCACCCT ACGTTTACGAGCCAGTATAGAATACAAGGTAAACTGGAATATA GACACACGTGGGACAGACATGATGAAGGAGCAGCTCAAGGTG ATGACGATGTCTGGACTTCCGGGTCCGATAGTGATGAGGAACT GGTCACGACAGAGCGAAAGACACCGAGAGTAACCGGTGGCGG

	CGCAATGGCATCCGCTAGCACAAGTGCAGGTCGGAAACGGAA AAGCGCTTCTTCAGCAACTGCTTGCACAGCGGGTGTAATGACA CGAGGGAGATTGAAGGCTGAATCCACCGTTGCCCCAGAAGAA GACACAGATGAGGATTCTGATAATGAGATTCACAATCCAGCCG TGTTTACTTGGCCGCCGTGGCAGGCAGGGATTCTTGCCCGCAA CCTTGTCCCGATGGTAGCCACGGTACAGGGCCAAAATCTGAAG TATCAGGAATTTTTTTGGGACGCCAATGATATATATAGGATATT CGCGGAACTCGAGGGGGTGTGGCAGCCAGCGGCCCAGCCGAA GAGGAGGCGGCATCGACAGGACGCACTGCCAGGACCATGTAT AGCCAGCACACCGAAGAAACATCGGGGATGA
ER-NLV	GGCTCAGGTGCCACCAACTTCAGCTTGTTGAAACAGGCTGGGG ATGTAGAGGAAAACCCCGGTCCCATGCCTAATCATCAGTCCGG GTCACCTACCGGCAGTTCAGACCTGCTCCTTGATGGCAAGAAA CAACGAGCCCATCTGGCGCTGAGGAGAAAACGGCGACGGGAA ATGCGCAAGATTAACCGAAAGGTGAGAAGAATGAATCTCGCA CCCATTAAAGAAAAAACAGCCTGGCAGCACCTGCAAGCTCTGA TCTTCGAGGCGGAAGAAGTGTTGAAGACTTCTCAAACTCCACA GACCTCCCTCACGCTGTTTCTAGCACTCTTGGCCGTATTGGCCC CGCCACCTGTGAGCGGGAACCTGGTGCCCATGGTGGCCACCGT GTAA